

Rochester Institute of Technology

**RIT Scholar Works**

---

Theses

---

9-1-1987

**Deuterium isotope effects on in vitro dealkylation of  
1,1-dimethylhydrazine and 1,1-dimethylnitrosamine via hepatic  
enzymes**

Robert Sloane

Follow this and additional works at: <https://scholarworks.rit.edu/theses>

---

**Recommended Citation**

Sloane, Robert, "Deuterium isotope effects on in vitro dealkylation of 1,1-dimethylhydrazine and 1,1-dimethylnitrosamine via hepatic enzymes" (1987). Thesis. Rochester Institute of Technology.  
Accessed from

This Thesis is brought to you for free and open access by RIT Scholar Works. It has been accepted for inclusion in Theses by an authorized administrator of RIT Scholar Works. For more information, please contact [ritscholarworks@rit.edu](mailto:ritscholarworks@rit.edu).

DEUTERIUM ISOTOPE EFFECTS ON IN VITRO  
DEALKYLATION OF 1,1-DIMETHYLHYDRAZINE AND  
1,1-DIMETHYLNITROSAMINE VIA HEPATIC ENZYMES

Robert Sloane

SEPTEMBER 1987

THESIS  
SUBMITTED IN PARTIAL FULFILLMENT OF THE  
REQUIREMENTS FOR THE DEGREE OF MASTER OF SCIENCE

APPROVED Francis L. Scott

PROJECT ADVISOR

Gerald Takacs

STAFF CHAIRMAN

Name Illegible

LIBRARY

ROCHESTER INSTITUTE OF TECHNOLOGY  
ROCHESTER, NEW YORK 14623  
DEPARTMENT OF CHEMISTRY

Title of Thesis.... Deuterium Isotope Effects on in vitro Dealkylation of  
1,1-Dimethylhydrazine and 1,1-Dimethylnitrosamine via  
Hepatic Enzymes.

I, Robert Sloane, Hereby grant permission to the Wallace Memorial Library,  
of Rochester Institute of Technology, to reproduce my thesis in whole or in  
part. Any reproduction will not be for commercial use of profit.

DEUTERIUM ISOTOPE EFFECTS ON IN VITRO  
DEALKYLATION OF 1,1-DIMETHYLHYDRAZINE AND  
1,1-DIMETHYLNITROSAMINE VIA HEPATIC ENZYMES

## ACKNOWLEDGMENTS

## ACKNOWLEDGEMENTS

I would like to thank Dr. F. L. Scott for his efforts in completing this project. My deepest gratitude goes to the faculty and staff of the Rochester Institute of Technology Chemistry Department, especially Drs. Gerald Takacs, Kay Turner, Terry Morrill and Jerry Adduci for their compassion and direction.

A special thanks goes to Dr. Russell A. Prough of the Biochemistry Department at the State University Health and Science Center of Texas at Dallas and Dr. Christian Reinhardt of the Rochester Institute of Technology Chemistry Department. Their direction was fundamental in the completion of this project. Along with my Texas thank you goes a deep appreciation for having an opportunity to work with the likes of Dr. Steven Moloney, Scott Cummings, Sherman Ross, and Will French.

I would also like to thank the following people for their help in performing various instrumental analysis:

Boris for his  $^1\text{H}$ -nmr work, the instrumentation staff at the University of Rochester Chemistry Department and Dr. Steven (Mongo) Moloney at the State University Health and Science Center of Texas at Dallas for their work in mass spectrometry and Mr. David Tyminski for his gas chromatography help. I would also like to thank Mr. David (The Deer Killer) Marchner for his help in graphic design of some of the Figures in the thesis.

Finally, I would like to thank my wife, Karen for patiently holding our lives and family together during the preparation of this thesis.

**To: Karen D. Sloane**

## TABLE OF CONTENTS

I	ACKNOWLEDGEMENTS.....	
II	LIST OF TABLES.....	1
III	LIST OF FIGURES.....	2
IV	RESEARCH OBJECTIVE.....	5
V	ABSTRACT.....	8
VI	INTRODUCTION.....	13
	CYTOCHROME P-450 PROFILE.....	14
	Background.....	14
	Catalytic Operation.....	16
	Drug Oxidation Pathways.....	24
	Cytochrome P-450 Induction.....	29
	Cytochrome P-450 Spectral Properties.....	31
	Inhibition and Metabolite-Complexes.....	33
	FLAVIN-CONTAINING MONOOXYGENASE PROFILE.....	38
	Background.....	38
	Induction and Inhibition Studies.....	39
	Catalytic Operation of the Enzyme.....	41



CHEMISTRY OF HYDRAZINES.....	45
General Properties.....	45
Reactions Involving 1,1-Dimethylhydrazine.....	47
METABOLISM OF HYDRAZINES.....	52
CHEMISTRY OF NITROSAMINES.....	58
General Properties.....	58
Reactions Involving Nitrosamines.....	59
METABOLISM OF NITROSAMINES.....	64
General Properties.....	64
Metabolic Mechanism.....	64
KINETIC ISOTOPE EFFECTS.....	69
Deuterium Labelled Compounds.....	69
Elimination Reactions and Isotope Effects.....	72

## VII EXPERIMENTAL

CHEMISTRY.....	78
Deuteration of 1,1-Dimethylnitrosamine.....	78
Nitrosamine Reduction to Hydrazine.....	81
METABOLIC STUDIES:.....	88
Cytochrome P-450.....	88
Microsomal Flavin-Containing Monooxygenase.....	93

## VIII RESULTS AND DISCUSSION

CHEMICAL STUDIES.....	99
Deuteration of 1,1-Dimethylnitrosamine.....	99
Mechanism and Reaction.....	99
Purity and Proof of Structure.....	100
Reduction of Nitrosamine to Hydrazine.....	114
Mechanism and Reaction.....	114
Purity and Proof of Structure.....	115
Summary.....	133
Miscellaneous.....	133
METABOLISM STUDIES.....	134
Cytochrome P-450 Oxidation of Substrates.....	134
Formation of Spectral-Complex.....	134
Kinetic Studies.....	137
Nitrosamine-Enzyme Binding Studies.....	141
Flavin-Containing Monooxygenase Studies.....	143
General.....	143
Enzyme Kinetics.....	146
Experimental Design.....	148
Enzyme Activity and Concentration.....	148
Initial Rates Results.....	151
Theoretical Isotope Effect on $V_{max}$ .....	158
Experimental Isotope Effect on $V_{max}$ .....	159
Theoretical Isotope Effect on $V_{max}/K_m$ .....	159
Experimental Isotope Effect on $V_{max}/K_m$ .....	160

## VIII RESULTS AND DISCUSSION (cont.)

### METABOLISM STUDIES

#### Flavin-Containing Monooxygenase Studies

	Theoretical Isotope Effect on $k_{cat}/K_m$ .....	160
	Experimental Isotope Effect on $k_{cat}/K_m$ .....	161
	Kinetic Summary.....	162
	Theoretical Analysis of Transition States.....	163
	Steric Effects on Reactants.....	164
	Experimental Results on Chemical Oxidation Products....	165
	Experimental Results on Metabolic Oxidation Products...	165
IX	EXPERIMENTAL RESULTS SUMMARY.....	167
X	GLOSSARY OF TERMS.....	169
XI	REFERENCES.....	171

## GLOSSARY OF TABLES

Table 1:	Typical N-O stretching frequencies. (Silverstein <u>et. al.</u> , 1981)(51).....	59
Table 2:	Sample and reference cell conditions for monitoring active protein content and initial rates of NADPH oxidation by the mixed-function monooxygenase enzyme.....	96
Table 3:	Infrared spectra typical of 1,1-dimethylnitrosamine (51).....	109
Table 4:	Common fragments and possible structures from Figures 31-33 .....	118
Table 5:	Hydrazine derivatives and their ability to form the 438 nm-complex.....	140
Table 6:	Experimental Results: Initial rates for the calculation of the flavin-containing monooxygenase enzyme's active protein content.....	96
Table 7:	Michaelis-Menten parameters for selected hydrazine compounds and the flavin-containing monooxygenase (Hines, (27)).....	154
Table 8:	Experimental Results: Rates of NADPH oxidation by the flavin-containing monooxygenase enzyme using 1,1-dimethylhydrazine-d <sub>6</sub> and 1,1-dimethylhydrazine as substrate. A. - <u>without</u> n-octylamine in the buffer B. - <u>with</u> n-octylamine in the buffer.....	152 & 153
Table 9:	Experimental Results: Lineweaver-Burk plot data.....	155
Table 10:	Experimental Results: Michaelis-Menten parameters and observed isotope effects for 1,1-dimethylhydrazine and 1,1-dimethylhydrazine-d <sub>6</sub> and the flavin-containing monooxygenase.....	156

## GLOSSARY OF FIGURES

Figure 1:	Difference absorption spectrum of the ferrous-carbonyl-complex of cytochrome P-450.....	15
Figure 2:	Nicotinamide adenine dinucleotide NAD <sup>+</sup> , and its phosphorylated form NADP <sup>+</sup> .....	17
Figure 3:	The molecular structure of (A) FAD and (B) FMN.....	17
Figure 4:	Mechanism of substrate oxidation by the cytochrome P-450 dependent monooxygenase.....	19
Figure 5:	A. Type I binding spectra. B. Type II binding spectra.....	20
Figure 6:	Functional reactions for microsomal drug oxidation.....	24
Figure 7:	Possible organic mechanisms for microsomal drug oxidation.....	25
Figure 8:	Carbene (A) and oxene (B) insertion reactions.....	26
Figure 9:	Carbene (C) and oxene (D) addition reactions.....	26
Figure 10:	Aromatic attack by carbene (E) and oxene (F) reactions.....	27
Figure 11:	Oxene mechanism involving an N-dealkylation reaction.....	28
Figure 12:	Difference binding spectra of ferrous-cytochrome P-450 substrate. ....	36
Figure 13:	Possible reactivity sites in amine oxidation.....	38
Figure 14:	Tertiary (A) and secondary (B) amine oxidation.....	40
Figure 15:	The chemical and proposed mechanism for the the flavin-containing monooxygenase directed metabolism of 1,1-dimethylhydrazine .....	57
Figure 16:	Nitrosation of a tertiary amine.....	60
Figure 17:	Possible reaction sites of nitrosamines.....	61
Figure 18:	Relative acidity of alpha protons as determined by the conformational effect of deuterium exchange on a conformationally biased system.....	62
Figure 19:	A generally accepted scheme of 1,1-dimethyl-nitrosamine microsomal directed metabolism.....	65

Figure 20:	Repetitive scanning of cytochrome P-450 ferrous-NO optical difference spectra generated by the addition of NO gas bubbled into microsomal suspensions containing cytochrome P-450 and cytochrome P-450 reductase.....	68
Figure 21:	Zero-point vibrational energy as the source of kinetic deuterium isotope effects.....	71
Figure 22:	a. Hepatic metabolism of caffeine to theobromine b. Hepatic metabolism of 1-methyl-d <sub>3</sub> -caffeine to theophylline.....	75
Figure 23:	a. Mass spectrum of 1,1-dimethylnitrosamine. b. Mass spectrum of 1,1-dimethylnitrosamine from the literature.....	102
Figure 24:	Mass spectrum of 1,1-dimethylnitrosamine-d <sub>6</sub> .....	103
Figure 26:	<sup>1</sup> H-nmr spectrum of 1,1-dimethylnitrosamine.....	106
Figure 27:	<sup>1</sup> H-nmr spectrum of exchanged nitrosamine (1,1-dimethylnitrosamine-d <sub>6</sub> ).....	107
Figure 28:	The IR spectrum of 1,1-dimethylnitrosamine, neat (Source: Aldrich).....	111
Figure 29:	The IR spectrum of exchanged material. (1,1-dimethylnitrosamine-d <sub>6</sub> ), neat (Source: experimental result).....	112
Figure 30:	The IR spectrum of 1,1-dimethylnitrosamine.....	113
Figure 31:	Mass spectrum of 1,1-dimethylhydrazine-oxalate salt.....	119
Figure 32:	Mass spectrum of the reduction product (1,1-dimethylhydrazine-d <sub>6</sub> -oxalate salt).....	120
Figure 33:	Mass spectrum of 1,1-dimethylhydrazine, neat, liquid.....	121
Figure 34:	Infrared spectrum of 1,1-dimethylhydrazine, neat, liquid.....	124
Figure 35:	Infrared spectrum of 1,1-dimethylhydrazine-oxalate salt (KBr pellet).....	125
Figure 36:	Infrared spectrum of (1,1-dimethylhydrazine-d <sub>6</sub> -oxalate salt) (KBr pellet).....	126
Figure 37:	<sup>1</sup> H-nmr spectrum of oxalic acid, diluted in DMSO-d <sub>6</sub> , TMS reference.....	129

Figure 38:	a. $^1\text{H}$ -nmr spectrum of 1,1-dimethylhydrazine, liquid, b. $^1\text{H}$ -nmr spectrum of 1,1-dimethylhydrazine, liquid, from the literature.....	130
Figure 39:	$^1\text{H}$ -nmr spectrum of 1,1-dimethylhydrazine-oxalate salt. diluted in $\text{D}_2\text{O}$ , oxalate reference.....	131
Figure 40:	$^1\text{H}$ -nmr spectrum of reduction product (1,1-dimethylhydrazine- $\text{d}_6$ -oxalate salt),.....	132
Figure 41:	Difference absorption spectra of the N-amino-piperidine metabolite-hemoprotein-complex.....	135
Figure 42:	The difference absorbance binding spectra exhibited by cytochrome P-450 in the presence of hydrazine substrate and NADPH.....	136
Figure 43:	A&B. The increase in absorbance difference between 438 and 510 nm for 1,1-dimethylhydrazine as substrate.....	139
Figure 44:	A generally accepted scheme of 1,1-dimethylnitrosamine microsomal directed metabolism.....	144
Figure 45:	Kinetic analysis of the N-oxidation of 1,1-dimethylhydrazine by the flavin-containing monooxygenase.....	145
Figure 46:	Kinetic analysis of the N-oxidation of 1,1-dimethylhydrazine and its deuterated analog by the flavin-containing monooxygenase.....	157

## RESEARCH OBJECTIVE



## RESEARCH OBJECTIVE

The liver is the main site of xenobiotic metabolism. Such metabolism is genetically controlled and fundamentally involves either changing a foreign material into a more suitable form for the body's use or changing it to some form that would facilitate its elimination from the body. For the most part this transformation of materials produces harmless waste products for the body's elimination. However, there are classes of hazardous compounds that undergo metabolic change which result in products more injurious than the starting material. Two of these compound classes are the N,N-alkylhydrazines and N,N-alkylnitrosamines.

Both 1,1-dimethylhydrazine and 1,1-dimethylnitrosamine play a large and diverse role in today's market place. Derivatives of 1,1-dimethylhydrazine can be found in rocket fuel, boiler water oxygen scavenger systems and fertilizers. 1,1-Dimethylnitrosamine is believed to be the in vivo oxidation product of nitrite and nitrate metabolism as well as an undesirable by-product of the manufacturing of rubber baby bottle nipples.

Both materials are highly toxic and are listed by the Occupational Safety and Health Agency (OSHA), the U.S. Food and Drug Administration (FDA) and the Environmental Protection Agency (EPA) as being a cancer suspect agent. Both materials also require metabolic activation to elicit their pathological effects.

Prough in 1980 clearly established that hepatic cytochrome P-450 forms an abortive complex with a metabolite of 1,1-dimethylhydrazine and that the microsomal flavin-containing enzyme, identified and characterized by Zeigler in 1964, rapidly metabolizes 1,1-dimethylhydrazine to its monomethylhydrazine and formaldehyde. However, 1,1-dimethylhydrazine's exact biological site and mechanism of pathological activation is not well documented.

Under aerobic conditions, 1,1-dimethylnitrosamine has been shown to undergo cytochrome P-450 dependent alpha-hydroxylation as its first step in becoming a DNA alkylating agent. During periods of oxygen deprivation it is theorized that cytochrome P-450 dependent reduction of the nitrosamine to its corresponding hydrazine may occur.

This study was initiated to investigate the effects of deuterium labelling of both 1,1-dimethylhydrazine and 1,1-dimethylnitrosamine on their rate of cytochrome P-450 and monooxygenase directed metabolism. Both materials will be subjected to enzymatic oxidation under aerobic and anerobic conditions in the presence of nicotinamide adenine dinucleotide phosphate, reduced form (NADPH) or sodium dithionite.

It is believed that by examining the kinetic and spectral information resulting from this study we may gain insight to the mechanism by which these compounds exert their toxic and oncological effects.

## **ABSTRACT**

### ABSTRACT

Boiling 1,1-dimethylnitrosamine or unsymmetrical dimethylnitrosamine several times with 25% NaOD in D<sub>2</sub>O promoted the complete exchange of the nitrosamine's alpha protons for deuterium.

The deuterated nitrosamine was reduced by LiAlH<sub>4</sub> in anhydrous diethyl ether to the corresponding 1,1-dimethylhydrazine-d<sub>6</sub>. An in-process production of the oxalate salt was necessary due to the air sensitivity of the free base hydrazine.

After recrystallization from absolute ethanol and extensive drying, the oxalate salt was evaluated for purity by mixed melting point, high performance liquid chromatography and thin layer chromatography. When protonated hydrazine-oxalate salt (mp=146 °C) was mixed with a sample of the exchanged hydrazine salt there was no melting point depression. Several chromatographic procedures were used to investigate the presence of impurities in the sample. Each process revealed only the presence of the free base hydrazine and oxalic acid.

Complete deuterium exchange was characterized by mass spectrometry and <sup>1</sup>H-nmr. The mass spectrum of the 1,1-dimethylhydrazine-d<sub>6</sub> had a molecular ion peak at mass 66 relative to the protonated free base hydrazine and the protonated hydrazine-oxalate salt whose molecular ion peak was at mass 60.

The subsequent  $^1\text{H}$ -nmr spectra of both the protonated and deuterated hydrazine-oxalate salts, when dissolved in  $\text{D}_2\text{O}$ , exhibited peaks specific for the two protons on the oxalic acid but only the protonated form had two additional absorbance peaks due to the two sets of alpha methyl protons.

Using difference absorbance spectroscopy, the interaction of both protonated and deuterated 1,1-dimethylhydrazine with microsomal cytochrome P-450 was examined. As enzyme substrates, both hydrazines exhibited identical difference absorbance spectra when added to suspensions of rat liver microsomes. Also, the resulting difference absorbance spectra were similar to many nitrogenous ligands to cytochrome P-450.

With the addition of NADPH, the enzyme suspension containing the hydrazine, formed a time and oxygen dependent microsomal hemoprotein spectral-complex. Both hydrazines formed a spectral-complex that exhibited a Soret absorbance maximum at 438 nm with alpha and beta absorbance bands at 575 and 547 nm. Upon standing the suspensions were depleted of oxygen thus causing a bathochromic shift of the Soret absorbance to give a second complex with a maximum absorbance at 449 nm. Upon subsequent oxygenation of the suspension the 438 nm absorbance was re-established which is consistent for ferric to ferrous transition of the hemoprotein. Both the protonated and deuterated form of the hydrazine formed the 438 nm-complex suggesting that the presence of deuterium had little effect on the mechanism of substrate reduction.  $V_{\text{max}}$  for both substrates was so great however, that kinetic evaluation of the reaction mechanism could not be done.

Normally, 1,1-dimethylnitrosamine exhibits a type I difference binding spectra when added to rat liver microsomal suspensions. However, this was not observed for either the protonated or the deuterated form of the nitrosamine. Further changes in the reaction environment failed to yield the type I binding spectra or a 438 nm-complex.

Inverse kinetic isotope effects on  $V_{max}$  and  $V_{max}/K_m$  were observed when 1,1-dimethylhydrazine- $d_6$ , instead of 1,1-dimethylhydrazine, was added to purified liver microsomal flavin-containing monooxygenase, the Zeigler enzyme. Isotope effects on  $V_{max_H}/V_{max_D}$ ,  $V^D/V$  were 0.76 without the presence of n-octylamine and 0.82 when n-octylamine was present in the reaction mixture. Isotope effects on  $V_{max}/K_m$ ,  $V^D/K$  were 0.36 without the presence of n-octylamine and 0.55 when n-octylamine was present in the reaction mixture. The inverse isotope effect was observed relative to the protonated substrate when each were added, as substrate, to the purified enzyme and in the presence of NADPH. n-Octylamine, known to increase the rate of Ziegler enzyme reaction, had little effect on the magnitude of the inverse kinetic effect.

Possible explanations for this inverse kinetic effect may be due to the deuterium affecting the binding rate of substrate to enzyme.

Examination of the acid quenched reaction products revealed the presence of monomethylhydrazine.

The formation of the monomethylhydrazine supports the findings by Prough, (11). Prough found the enzyme promoted the formation of a 1,1-dimethyl-diazeno intermediate, possibly from the dehydration of an N-hydroxy-metabolite. Under acid conditions, this tautomerization of the diazeno via an azo-intermediate to a methylhydrazine and then on to the monomethylhydrazine is favored over a possible bimolecular reaction involving the diazeno which would promote the formation of a corresponding tetramethyltetrazene.

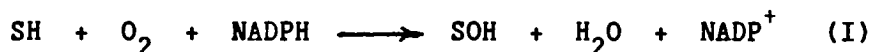
## **INTRODUCTION**



## CYTOCHROME P-450

### BACKGROUND:

Cytochrome P-450 is a terminal oxidase enzyme (hemeprotein in nature) that performs as a monooxygenase in the endoplasmic reticulum of most mammalian cells. It is called a monooxygenase because it acts on its substrate with molecular oxygen, introducing one oxygen atom into the substrate's structure concomitantly with the reduction of the second oxygen atom to water. In other words, the substrate gets oxidized to a more hydrophilic form while half of molecular oxygen gets reduced to water (I).



This reaction requires the presence of NADPH and molecular oxygen.

Cytochrome P-450 was the subject of a review by Estabrook in 1971 (1). This review noted that the enzyme system's photochemical ability to form Soret absorbances\* at 450 nm following its exposure to CO but subsequent to treatment with dithionite (Figure 1) was one of its earliest outstanding features recognized. Sato and Omuro in 1964 (2,3) further characterized the enzyme as a membrane-bound hemoprotein. It's heme center and surrounding protein are responsible for the enzyme's unique spectral absorbance properties.

\*\*\*\*\*

\* - Terms asterisked are defined in the glossary.

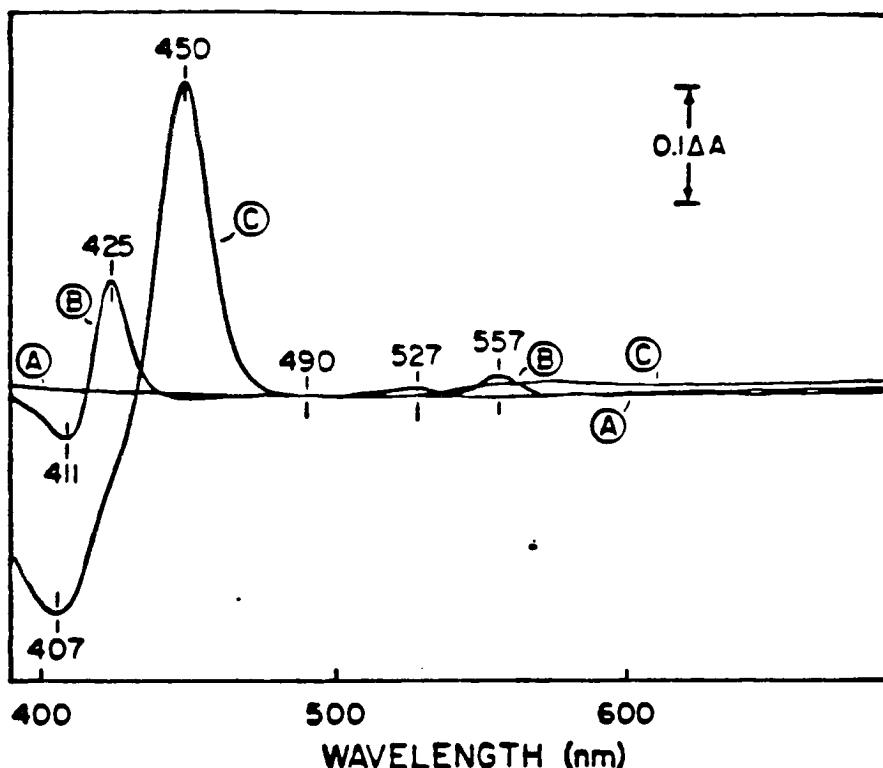


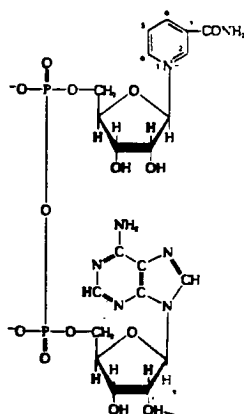
Figure 1: Difference absorption spectrum of the ferrous carbonyl complex of cytochrome P-450. Microsomes prepared from phenobarbital pretreated animals were suspended in 50 mM potassium phosphate buffer (ph 7.6) with 0.1 mM EDTA to a final concentration of 1.0 mg protein per ml. The suspension was split into reference and sample cuvettes and a base line of equal light was recorded (A). Cytochrome  $b_5$  was reduced in the sample cuvette by the addition of 0.01 mM NADH. An equal volume of buffer was added to the reference cuvette and after mixing, the reduced minus oxidized cytochrome  $b_5$  spectrum was recorded (B). The sample cuvette was bubbled briefly with CO and then 5 to 10 grains of sodium dithionite was added to both reference and sample cuvettes. After thorough mixing by inversion, the sample cuvette was rebubbled with CO for 30 sec and the ferrous cytochrome P-450 carbonyl complex minus ferrous cytochrome P-450 difference spectrum recorded (C). Reprinted from Hines (1980) (27).

Cytochrome P-450's role in metabolism was elucidated by Estabrook and co-workers in 1963 (4). They along with Cooper and co-workers (5) discovered cytochrome P-450's role in drug hydroxylation and oxidative dealkylations. Cytochrome P-450 plays a key role in pharmacology and toxicology as a result of its transforming a large number of lipophilic xenobiotics. Such reactions may result in the deactivation of some substrates but also may transform others into compounds potentially more hazardous and toxic than the original substrate.

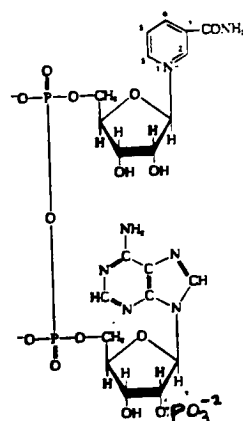
The earliest source of the cytochrome P-450 monooxygenase was from the liver. Subsequent investigations that followed Estabrook's initial work established that the enzyme was ubiquitous throughout the body with a large majority of the membrane bound material found in microsomal preps from the lung, kidney and liver (Masters et al., 1980)(6). Other sites where the enzyme was found include the mitochondria of steroid producing organs and glands (Harding et al., 1964)(7) and the microsomes of some bacteria (Sato 1978)(8).

#### PROPERTIES AND BIOCHEMISTRY: CYTOCHROME P-450 CATALYTIC OPERATION:

Precursors: The functionality of the cytochrome system relies on the presence of pyridine containing compounds, nicotinamide adenine dinucleotide  $\text{NAD}^+$ , and/or its phosphorylated form  $\text{NADP}^+$  (Figure 2). These compounds play the role of hydrogen transfer agents via a hydride transfer mechanism .



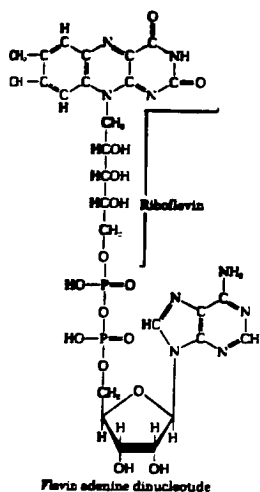
A



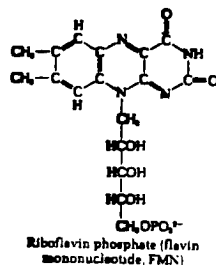
B

Figure 2: Nicotinamide adenine dinucleotide  $\text{NAD}^+$  (A), and its phosphorylated form  $\text{NADP}^+$  (B).

The cytochrome systems have endogenous cofactors called the flavinprotein reductase system which acts as a series of electron relaying biomolecules. This flavoprotein system provides the electrons for the two one-electron reductions shown in equation I. The reductase system contains two moles of flavin in the form of one mole of flavin adenosine dinucleotide (FAD) and one mole of flavin adenosine mononucleotide (FMN) for each mole of enzyme (Masters *et al.*, 1965)(9). Figure 3 shows the molecular structures of FAD and FMN (FMN: nucleotide not shown).



A



B

Figure 3: The molecular structure of (A) FAD and (B) FMN.

Both moieties are capable of accepting two electrons with the FMN moiety responsible for two one-electron reductions (Peterson et al., 1977)(10) in the cytochrome P-450 dependent monooxygenase reaction cycle.

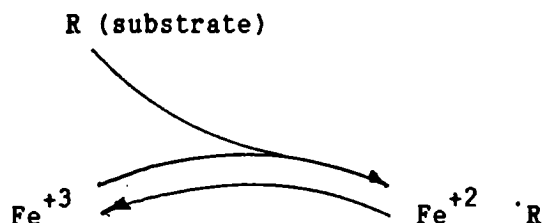
The final acceptance of the electrons that the pyridine and flavin moieties provide is done by the heme center of the cytochrome system. The iron center undergoes a reversible change ( $\text{Fe}^{+2} \rightleftharpoons \text{Fe}^{+3}$ ) during its catalytic operation. The heme center is complexed in a hexavalent (octahedral) form bound to four nitrogens from pyrrole rings with its geometry allowing (or requiring) two additional ligands to achieve the octahedral state.

The catalytic cycle: The overall cycle by which this system operates is shown in Figure 4. This process will be broken down step by step with each step discussed.

The initial step (step 1) is the substrate binding to the enzyme. In the absence of substrate the heme center of the cytochrome is in a low spin\* hexacoordinated form. This is characterized by the enzyme's uv spectrum exhibiting (a Soret maximum absorbance) peak at 418 nm.

---

Step 1: Substrate interaction.



\* see Glossary.

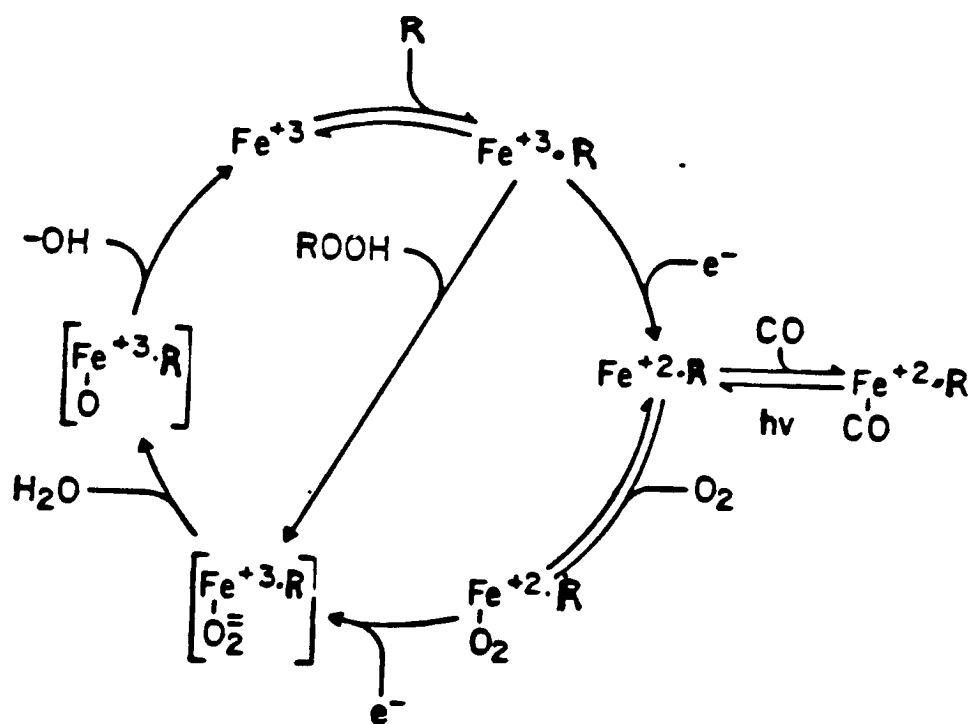


Figure 4: Mechanism of substrate oxidation by the cytochrome P-450 dependent monooxygenase. (Prough et.al., 1981)(11).

The presence of the substrate causes a perturbation in the electron cloud about the heme center. The substrate is complexed as a heme ligand leaving a single electron in the iron creating a paramagnetic heme center. This change in the iron complex may be characterized by an absorbance spectrum with maximum absorbance at or about 390 nm. This shift is attributed to the heme iron's electron configuration changing from low to high spin form\*.

The resulting spectral data obtained from the complex formed is a function of the nature of the substrate. Of the various methods of monitoring monooxygenase activity, measuring the cytochrome's spectral properties offers the most useful information because cytochrome P-450's spectral characteristics change as a direct result of its substrate interactions.

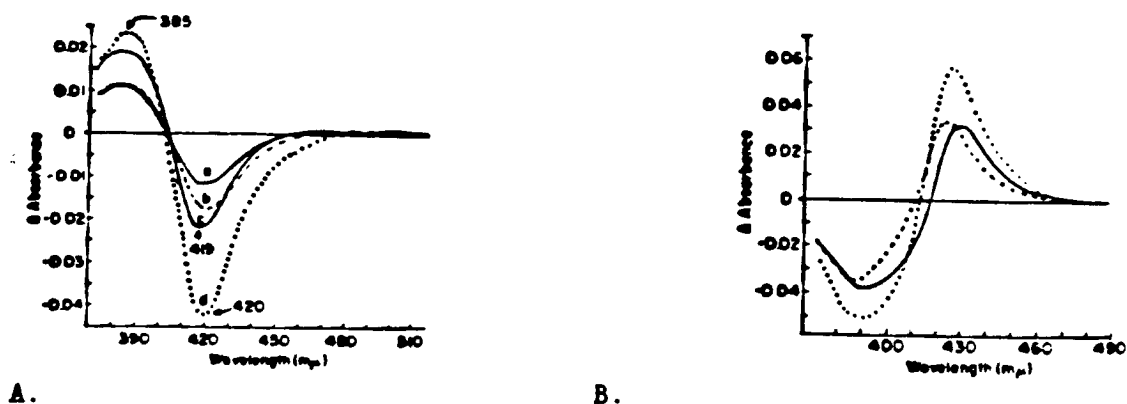


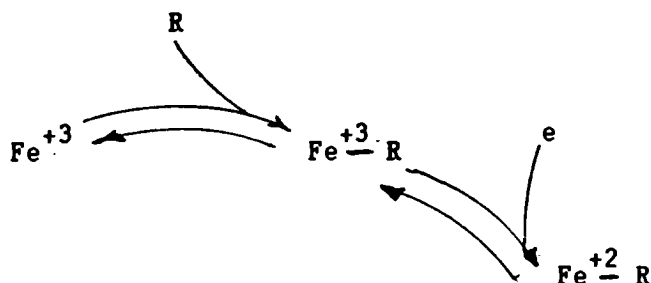
Figure 5: A. Type I binding spectral changes. B. Type II binding spectral changes.

Cytochrome P-450 belongs to a group of heme proteins which when reduced form complexes with substrates that exhibit spectral absorbances that are characterized by two basic types of UV spectral changes. A type I spectral change is characterized by an absorbance maximum at a longer wavelength than the heme center exhibited in the absence of NADPH or substrate (Mitani and Horie, 1969)(12). A type II spectral change exhibits a maximum absorbance at a shorter wavelength than the heme center exhibited in the absence of NADPH or substrate (Jeffcoate and Gaylor, 1969)(13). Type I binding spectral changes arise from a complex whose heme center is changing from low spin to high spin. The converse is true with type II binding where spectral changes arise from high spin to low spin conversions.

In step 2 of the cycle, the enzyme-substrate-complex gets reduced with the heme center going from ferric ( $\text{Fe}^{+3}$ ) to ferrous ( $\text{Fe}^{+2}$ ) cytochrome.

---

Step 2: Reduction of the cytochrome P-450 substrate-complex.



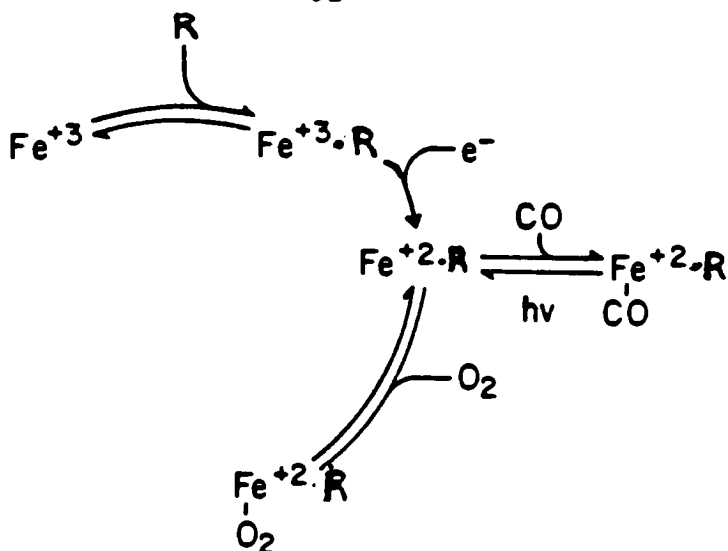

---

Step 3: [As has been noted, In the presence of carbon monoxide a CO-substrate-complex forms that has a characteristic absorbance peak at 450 nm.] However, presently molecular oxygen is the ligand involved resulting in an  $\text{O}_2$ -substrate-complex. (Estabrook et al., 1963)(4).



---

Step 3: Reaction with oxygen.

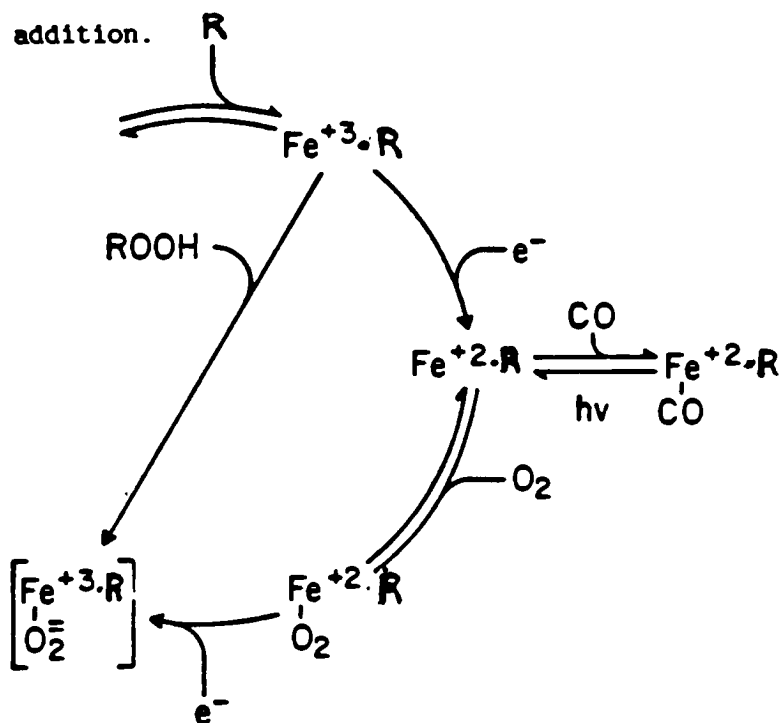



---

Acceptance of another electron at this stage causes the iron center to shift from the ferrous to the ferric form creating an electron rich oxygen molecule. At this point several reactions may occur to circumvent the cycle and produce hydrogen peroxide and other products. These pathways are outside present discussion.

---

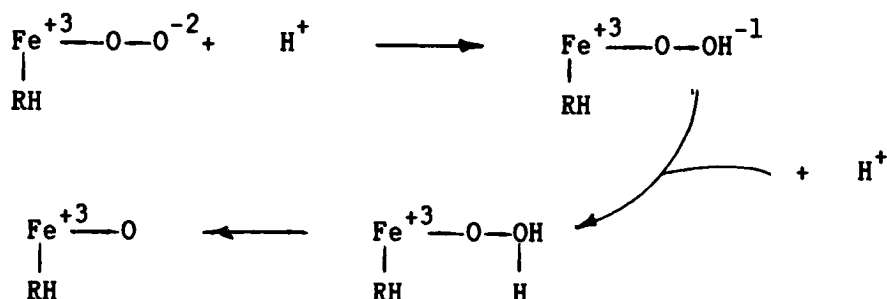
Step 4: Second electron addition.



With the substrate and oxygen both complexed and sufficient electrons available the next key step is cleavage of the O-O bond.

---

Step 5: Oxygen activation.



Thus by a series of proton additions the O-O bond is encouraged to cleave resulting in an iron-substrate oxene complex.

This next step is the point of the entire exercise. In it the reactive oxygen species attacks the substrate. While this will be discussed in detail shortly for now it can be represented as:

---

Step 6: Oxene-substrate interaction.



After the substrate-oxygen interaction has taken place (step 6), then the product of that reaction leaves the enzyme free to begin the cycle again (Figure 4).

Details about these steps have been acquired using an ethyl isocyanide substrate. This gave an oxidized enzyme-substrate-complex with a binding spectrum showing a Soret maximum band at 455 nm. The stoichiometry of the reaction indicated that the complex was formed by the enzyme first binding the isocyanide moiety to the ferric heme center. This site was later characterized as the catalytic site (Ullrich and Schnabel, 1973)(14). The oxidized complex is destabilized by the new ligand thus, facilitating the reduction of the heme center to the ferrous state by the acceptance of an electron. The reduced enzyme-substrate-complex exhibits a spectral absorbance maximum at 455 nm. The reduction is followed by a slow conformational change within the enzyme that eventually results in an absorbance spectrum with a maximum at 433 nm. The shift to the 433 nm form makes the complex susceptible to oxygen interaction.

#### DRUG OXIDATION PATHWAYS AND MICROSOMAL ENZYMES OF THE LIVER:

Microsomal drug oxidation may involve functional changes of the following kind; N-dealkylations, O-dealkylations, hydrocarbon oxidation, aromatic hydroxylation and oxidative deamination. These reactions are summarized in Figure 6. All involve the incorporation of an oxygen atom into a substrate by the breaking of a substrate's hydrogen bond.

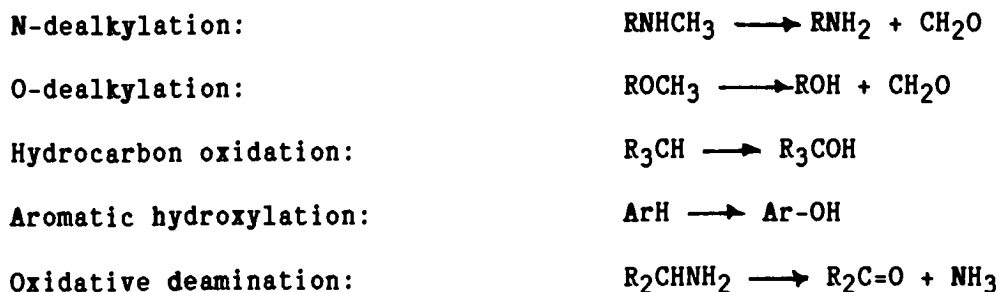


Figure 6: Functional changes achieved by microsomal drug oxidation.

The breaking of a covalent hydrogen bond X:H may proceed, classically, by one of three pathways. First, the bond homogeneously breaks so that each atom retains one of its electrons (Figure 7A). This is a free radical pathway. Second, if X is more electronegative than hydrogen then the bond may break heterogeneously with X retaining both the electrons (becoming an anion) and the hydrogen leaving as a proton (Figure 7B). This, of course, is readily seen in examples of O--H bond breaking. Third, the X:H bond may break with hydrogen retaining both electrons (becoming a hydride ion), leaving behind X as the cation  $X^+$  (Figure 7C). Where X:H is a carbon-hydrogen bond then these pathways represent free-radical pathways, carbanion formation and carbonium involvement respectively.

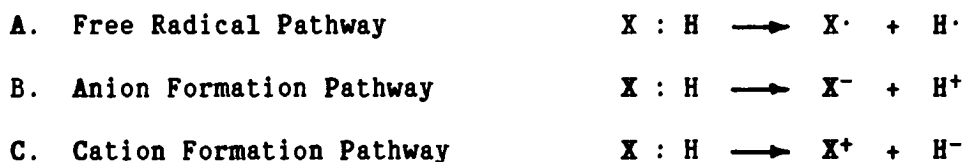


Figure 7: Modes of hydrogen bond breaking.

There is evidence that certain cytochrome P-450 mediated reactions can involve one of these various pathways: e.g. carbanion formation in reactions with fluorene and free radicals involved in halogenated hydrocarbon metabolism.

However it became apparent in the early 1960's that there may be another mechanism for the incorporation of oxygen into a microsomal mediated oxidation reactions (Hamilton 1964)(15). This other mechanism required the presence of an electrophilic oxygen species, which by analogy with carbon chemistry where carbons lacking two electrons are called carbenes, this species is called an oxene.

This oxygen atom with six valence electrons is stabilized by complexing with the iron atom involved.

Similarities between oxene and carbene behavior is seen in insertion reactions, aromatic attack and additions.

Insertion reactions with carbenes result in the carbene species inserting itself between unactivated alkane carbon hydrogen bonds forming products that retain their original optical configuration (A). Oxenes exhibit similar insertions in their hydroxylation of hydrocarbons (B).

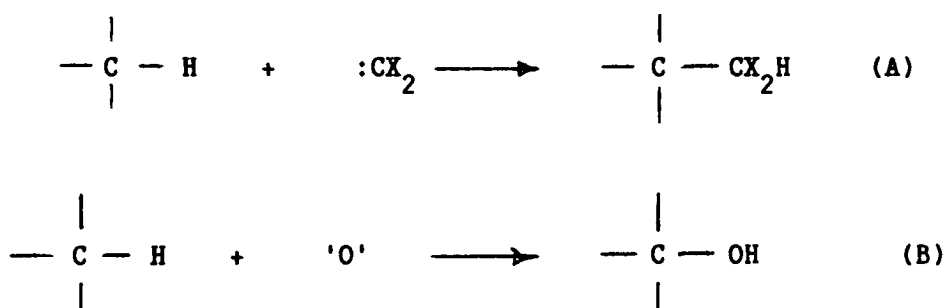


Figure 8: Carbene (A) and oxene (B) insertion reactions.

Addition reactions with carbenes give cyclopropanes (C). oxenes give epoxides (D)

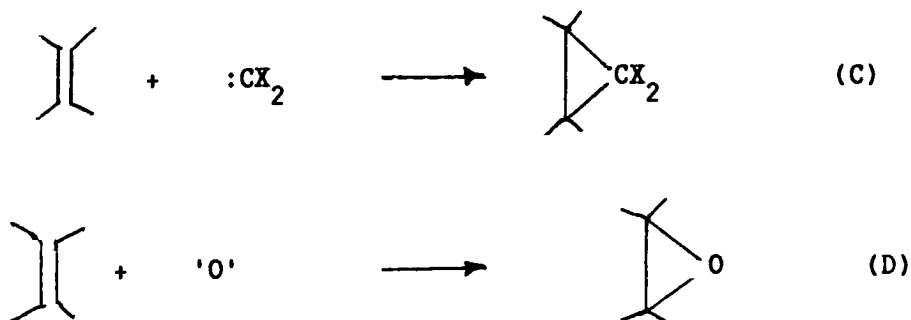


Figure 9: Carbene (C) and oxene (D) addition reactions.

Aromatic attack by carbenes give alkylbenzenes and bridged products (E). Oxenes can convert aromatic compounds to areneoxides that may be in equilibrium with oxepines (F).

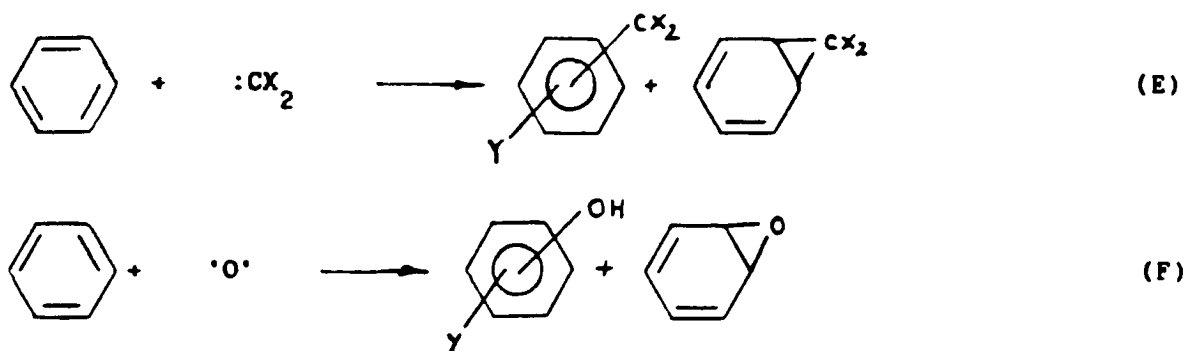


Figure 10: Aromatic attack by carbene (E) and oxene (F) reactions.

With amine N-dealkylation one can write the following oxene pathway for the cytochrome P-450 reaction: (Figure 11)

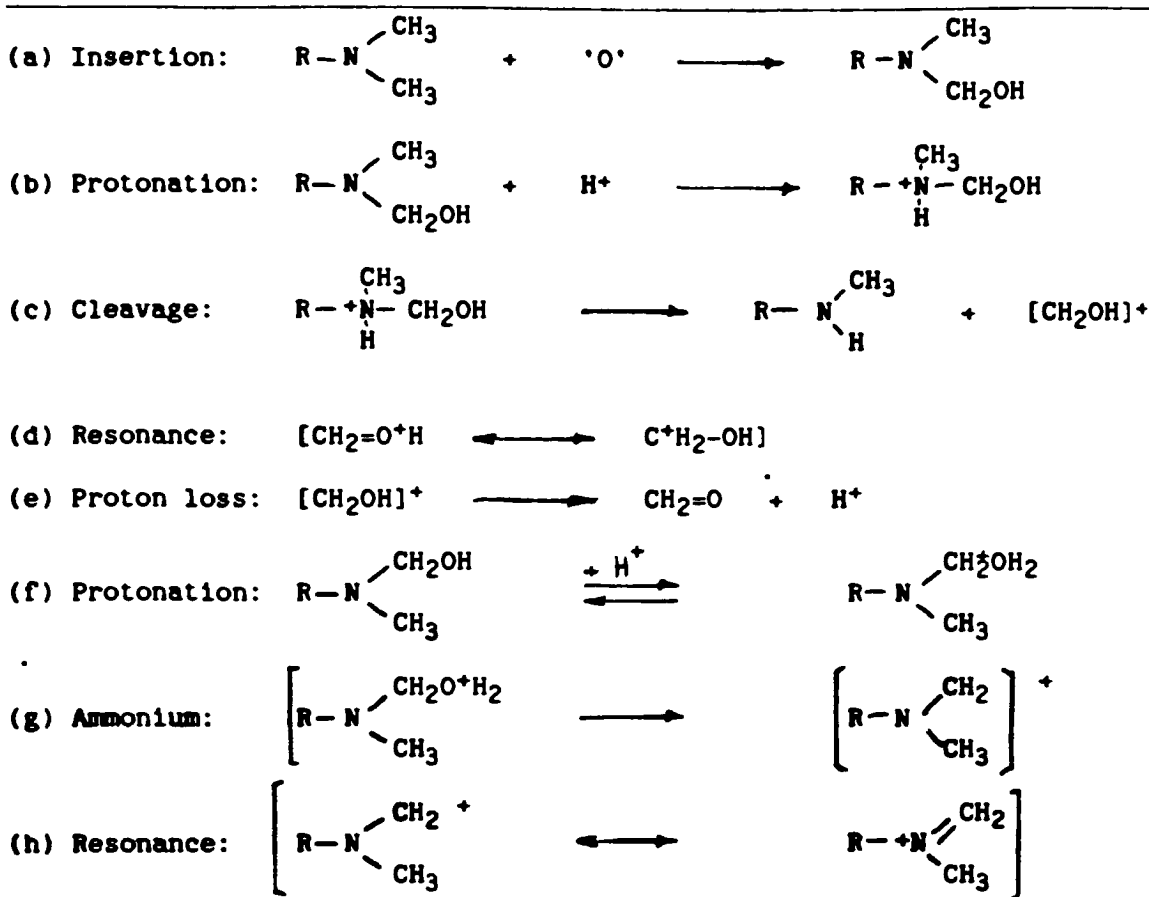


Figure 11: Oxene mechanism involving an N-dealkylation reaction.

The mechanism in Figure 11a involves first an oxene insertion to give a carbinolamine. Protonation then occurs at the nitrogen atom (step b). The resulting ammonium salt can then be cleaved to form the hydroxymethyl carbonium ion and the dealkylated amine (step c). The resonance stabilized ion in (d) rapidly loses a proton, to give formaldehyde in step e. Conceptually, that is the major pathway for the dealkylation step. Steps f and g cover what may happen if the oxygen in step e is protonated. Step h illustrates the resonance structure of the product in step g.

## CYTOCHROME P-450 INDUCTION:

Microsomal drug oxidation activity was found to be induced by the administration of specific compounds to test animals that were used to supply the microsomes. It has been shown (Ernester & Orrenius, 1965)(16) that the amount of cytochrome P-450 in the liver is increased as a result of such in vivo pretreatment. Pretreatment of test animals often involves the intraperitoneal (i.p.) injection of the inducing substance into the animal over a period of 3 or 4 days, followed by a 24 hour starvation period prior to sacrifice. After this period of time the amount of cytochrome P-450 induced is maximized. So long as the inducing agent is present in the liver cells it enhances the rate of synthesis of the heme as well as of the protein moiety by causing an increase in messenger-RNA formation in the nucleus (Remmer 1970)(17).

Some specific inducers of cytochrome P-450 are phenobarbital and other barbiturates. Other aromatic hydrocarbons such as 3-methylcholanthrene may be used to induce the formation of another form of cytochrome type monooxygenase, cytochrome P-448.

Just as it is possible to increase the amount of cytochrome P-450 so is it possible to produce various kinds of cytochrome P-450s. Elucidation of multiple forms of cytochrome P-450 indicates that the enzyme has wide application yet remains site and substrate specific (Wiebil et al., 1971)(18). Ultimately the form of cytochrome and the amount present in animals are a function of sex, age, drug pre-treatment, species and strain.

Sources of enzyme are kept constant during an experiment to achieve reproducibility. It has been shown that using cytochrome P-450 from two different sites of the same animal (i.e. liver and lung) resulted in different catalytic reaction rates.



Speculation has it that each organ, by virtue of its own metabolic position, requires specific substrates with their own unique activation sites.

Methods of documenting the existence of multiple forms of the enzyme include atomic absorption analysis of the protein back bone, sedimentation rate studies of purified enzyme (molecular weights), chromatography, catalytic activity, antigenic properties and chemical-light absorbance difference spectra.

#### SPECTRAL PROPERTIES OF CYTOCHROME P-450:

Optical properties of cytochrome P-450 were first observed by comparing the turbidity of microsomal samples treated with hydrogen peroxide to samples without peroxide. By balancing the turbidities of the two solutions the absolute spectrums of high and low spin forms of cytochrome P-450 can be observed.

As purification techniques improved so did the resultant absorbance spectra. Induction experiments using a known cytochrome P-450 inducer and substrate provided evidence for the existence of multiple forms of cytochrome P-450. Balanced turbidity tests run with microsome suspensions from animals pretreated with the proper inducing agent (either 3-methylcholanthrene or phenobarbital), a reductase preservative, NADPH, substrate, and oxygen revealed that phenobarbital pretreatment induces an enzyme system that exhibits low spin spectra and 3-methylcholanthrene pretreatment induces a form of enzyme that exhibits high spin type spectra. As noted earlier, purification techniques had developed enough to prove that various species of enzymes exist in the microsome each having its own requirements for a reductase systems.

As the technique of purification progressed, the isolation of the enzyme from its surroundings proved that in many cases material once thought of as impurities were actually necessary for the enzyme to function properly. One instance of this is that the purification of cytochrome P-450 from a lipid moiety that is attached to it resulted in complete loss of enzyme catalytic activity. Because of this, it was unnecessary (and undesirable ) to completely purify cytochrome P-450.

Instead of drastic or tedious efforts to purify an enzyme, it was found that suspensions of microsome material taken from phenobarbital-pretreated animals would yield a useful and intact enzyme system (Lowry et al., 1951)(19).

In the cytochrome oxidative cycle, it was mentioned that a unique enzyme substrate binding complex could be observed when suspensions of microsomes from phenobarbital-pretreated animals, were mixed with carbon monoxide, reduced (by sodium dithionite) and analysed by difference spectroscopy. The unique binding spectrum had a Soret absorbance peak at 450 nm with no  $\alpha^*$  or  $\beta^*$  peaks. This is unusual in that hemoproteins tend to have  $\alpha$  and  $\beta$  absorbances and Soret absorbances at lower wavelengths.

Other substrates that form unique binding spectra with dithionite reduced cytochrome P-450 are the alkyl isocyanides. At a neutral pH, when ethyl isocyanide was added to dithionite reduced aerobic microsomal suspensions, the difference binding spectra observed was a Soret maximum absorbance peak at 430 nm with  $\alpha$  and  $\beta$  peaks at 560 and 530 nm, respectively (Omura & Sato, 1964)(2).

Spectral observations made on reduced cytochrome P-450 indicate an enzyme sensitivity to the suspension's pH, ionic strength, and substrate's alkyl chain length. These results indicated that changing the pH of the microsomal solution showed that two distinct forms of cytochrome exist, each in equilibrium to the other. The two forms vary inversely in their absorbance peak ratios with absorbance maxima at 430 nm and 455 nm respectively. Both are competitively inhibited by carbon monoxide and both have equal affinities for specific substrates (Imai & Sato 1966)(20). Which form predominates depends on pH, ionic strength (Imai and Sato 1967)(21) and alkyl chain length of substrate (Ichikawa and Yamano 1968)(22). Further work on binding spectra resulted in the finding that only lipophilic ligands cause heme proteins to exhibit these equilibrium forms (Imai and Sato 1967) (20).

Nishibayashi in 1966 (23) observed the binding spectra by difference spectroscopy of oxidized cytochrome P-450 bound to an isocyanide compound. His group observed a binding spectrum with a Soret absorbance at 434 nm and alpha and beta peaks at 590 nm and 553 nm respectively. Cytochrome P-450 was found to be a unique cytochrome in that its binding spectrum was insensitive to changing pH or ionic strength. The dissociation constant for various substrates was however sensitive to alkyl chain length. The dissociation constant of the substrates tended to decrease as the number of alkyl groups on the bound substrate increased. The results from such observations is that the heme center must be surrounded by a strong hydrophobic group when in the oxidized form. Following the formation of the substrate-oxidized enzyme complex, the ferric heme center is reduced to a ferrous type center. This reduction is observed by a change in absorbance spectrum with the maximum absorbance band shifting from 434 nm to 455 nm.

The reduced form of the complex then undergoes a slow conformational change to a final form that is susceptible to oxygen attachment. This experiment offers a method for following the cytochrome P-450 oxidation cycle using absorbance spectra.

Narasimhulu et al., 1963 (23) were the first to observe a substrate induced difference absorbance spectra. They originally used various steroids from adrenocortical microsome preparations but inadvertently left out the reducing equivalents (NADPH or sodium dithionite). The difference spectrum had a peak at 390 nm followed by an absorbance minimum (trough) at 420. What they obtained was a suspension whose spectral character was dependent on the size, type and relative concentration of substrate. In doing the same type of experiment using nitrogen containing substrates and reduced cytochrome P-450, difference spectrum exhibited an absorbance peak at 430 nm but the absorbance minimum (trough) had shifted from a relatively high wavelength to the lower wavelength of 390 nm (Schenkman et al., 1967)(24) (Remmer et al., 1967)(25). Thus type I or type II spectral changes are determined by the nature of the substrate.

#### ENZYME INHIBITION AND CYTOCHROME P-450 METABOLITE-COMPLEXES:

Some enzymes are specific for one particular substrate and catalyze one particular reaction. Enzymes like cytochrome P-450 however, have a range of substrates with which they can react. This wide range means any substrate is likely to impede the metabolism of another. As was noted in the catalytic cycle of cytochrome P-450 normally the substrate's affinity for the oxidized form of the enzyme is greater than the reaction product's affinity for the reduced form of the enzyme.

However with certain specific substrates the products that form during the cytochrome P-450 directed reaction go on to complex with the reduced enzyme. These resulting complexes are often inhibitory in nature to the function of the enzyme. The type of inhibitory complex that forms depends on the substrate, resulting product, and the sites at which they bind on the enzyme.

Inhibition of the enzyme's function can result from substrate-competition or by other means. In cytochrome systems the substrate's binding site might be the heme center and/or the lipophilic protein back bone resulting in a complex that would exhibit a unique difference absorbance spectrum. The protein portion of the enzyme is recognized as possessing the activation site because of the role it plays in facilitating the heme centers conformational changes during enzymatic reactions (complex formation). There are several compounds that are metabolized by cytochrome P-450 whose metabolites form inhibitory complexes. Should the metabolite be lipophilic and show a high affinity for the activation site on the protein the end result is an inhibitory metabolite-enzyme complex.

Such binding at the enzyme's activation site yields reaction rate kinetics indicative of competitive inhibition. Formation of this type of inhibitory complex competes with the formation of other enzyme-substrate-complexes. This is exemplified when perfluorinated hydrocarbons inhibit cytochrome P-450's hydroxylation reactions (Ullrich and Schnabel, 1973)(14).

As stated earlier, the cytochrome P-450's heme center directs the actual oxygen insertion into a substrate. This heme center is considered the catalytic site because of the role iron plays. Substrates binding to the catalytic site of cytochrome P-450 yield binding spectra and reaction kinetics indicative of non-competitive type enzyme inhibition.

Cytochrome P-450 gets its name from this type of reaction when carbon monoxide complexes with the heme center and displaces oxygen.

Inhibitory complexes involving both the activation and catalytic sites of the enzyme result in the most potent type of inhibition. Such interaction is produced through the concerted effort of a substrate (or metabolite) that possesses both a lipophilic hydrocarbon group and an electron donating group. Cytochrome metabolism of metyrapone, 1-phenylimidazole and n-octylamine exhibits this type of inhibition. Each substrate has an electron donating center originating from the two lone pair electrons on a nitrogen atom.

One mechanism of inhibition was mapped using piperonyl butoxide, NADPH,  $O_2$ , and hepatic microsomal suspension prepared from phenobarbital pretreated Sprague-Dawley rats. A key metabolite reacted with heme center and formed a stable ferrous-cytochrome P-450 complex with spectral binding characteristics similar to ferrous-cytochrome P-450-isocyanide complexes (see Figure 12).

Another example of inhibitory binding spectra is that of the metabolite of safrole and cytochrome P-450 (Mansuey et al., 1979)(26). Here however, the resulting binding spectra exhibited was similar to ferric cytochrome P-450-isocyanide complexes. Mansuey went on to speculate that initially carbene formation occurred and this then bound to the enzyme deactivating it.

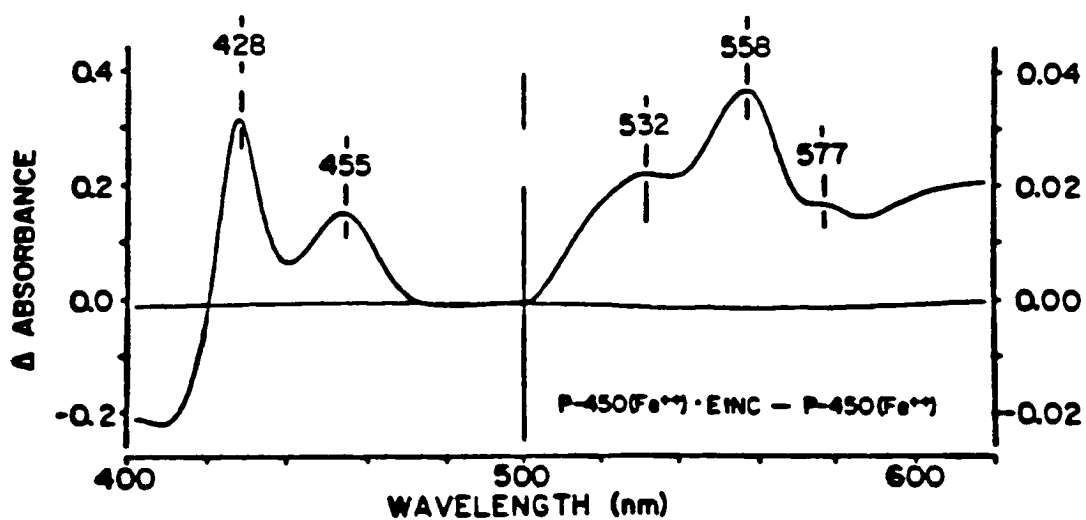


Figure 12: Difference binding spectra of the isocyanide complex of ferrous-cytochrome P-450. (Hines, 1980)(27).

The similarity of carbene chemistry to nitrene chemistry refocused attention on nitrogenous compound group metabolism and the involvement of cytochrome P-450. Using benzophetamine as substrate to cytochrome P-450 the binding spectra exhibited had a Soret peak at 456 nm. The exact metabolite is not presently known (Werringloer & Estabrook, 1978)(28). (Mansuey et al., 1976, 1977)(29,30) but nitrene involvement is indeed possible.



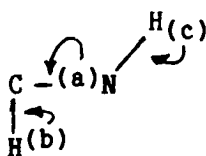
## MICROSOMAL FLAVIN-CONTAINING MONOOXYGENASE:

### THE ZIEGLER ENZYME

#### BACKGROUND:

Amine metabolism can be accomplished at three sites, the nitrogen atom (a). at one of the side chain carbons (b), and/or one of the hydrogen atoms (c).

---



---

Figure 13: Possible reactivity sites in amine oxidation.

Two enzyme systems responsible for N oxidation are amine oxidase and cytochrome P-450. The work done by Hines (1980) (27) indicate that 1,1-dimethylhydrazine is not metabolized by the cytochrome system instead it forms an abortive substrate-enzyme complex when oxygen and NADPH are present. Hines concluded that the flavin-containing monooxygenase system was directly responsible for 1,1-dimethylhydrazine's hepatic metabolism.

The role of the flavin-containing monooxygenase in hepatic amine oxidation was first investigated by Baker in 1962 (31). Ziegler noted Baker's work and went on to investigate a similar enzyme system that was found particularly active in elderly sow's liver microsomes. Because of this work, Ziegler in 1964 (32) characterized and finally isolated the enzyme that Baker had described earlier.

The description Ziegler gave of this enzyme was that it was dependent on oxygen and NADPH. It oxidized 1,1-dimethylaniline, DMA at the same rate and level of oxygen consumption as Baker's enzyme.

In 1969 Ziegler et al., (33) published their work giving a clear description of the purification process and characterized the enzyme's capabilities.

The Ziegler enzyme is a microsomally bound monooxygenase whose activity depends on the presence of NADPH and oxygen. Although the enzyme has been found in livers, lung, and kidney of all mammals and other vertebrates, researchers found that pig hepatocytes were supplied with a more than adequate amount of the material. The enzyme was also found in all other parts of the body except muscle tissue.

Aerobically, the isolated enzyme consumes 90-110 nmoles of NADPH/min/ng of protein at 30 °C. N,N-Dimethylaniline, DMA was used as the standard substrate in all of the following cited monooxygenase activity studies. In 1972 Ziegler and Mitchell provided data that the enzymes optimal pH was 8.4 (for enzyme activity during the presence of both NADPH and the substrate DMA) and is subject to denaturation at temperatures above 30°C.. Under optimal conditions enzyme oxidation of DMA occurs at least 10 times faster than NADPH oxidation. In all studies using the monooxygenase and NADPH, a minute amount of peroxide was produced (which may be a result of the action of endogenous catalase). Hydrogen peroxide given off during the catalysis of amine oxidation is dependent upon the presence of oxygen.

#### INDUCTION/INHIBITION OF THE ZIEGLER ENZYME:

Inducer/inhibitor studies conducted showed that the cytochrome P-450 inhibitor, SKF-525A (diethylaminoethyl-2,2-diphenylvalerate-HCl), and its inducer, phenobarbital, had no effect on the Ziegler enzyme catalyzed oxidation of DMA. Although attempts to induce this enzyme through direct xenobiotic pretreatment have failed, induction via natural inducers such as hormones (prednisolone in rats) have had some success (Ziegler, 1980)(34).

The microsomal amine monooxygenase has broad substrate specificity and catalyzes the N oxidation of tertiary and secondary amines to their respective amine oxides (A) and hydroxylamines (B).

---

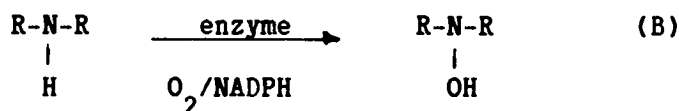
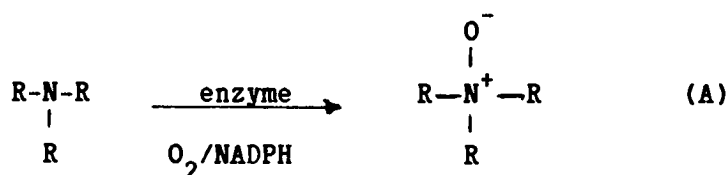


Figure 14: Tertiary (A) and secondary (B) amine oxidation.

Hydrazines undergo N-oxidation (Prough, 1973)(35), and thiocarbamides, thioamides, and sulfides undergo S oxidation (Poulsen et al., 1974)(36) when metabolized by this monooxygenase system.

Amine oxidation products are a result of enzymatic action at the nitrogen atom. Primary amines are not oxidized by the Ziegler enzyme but do participate in the oxidation of other amines by acting at the enzyme's activation site (Ziegler & Mitchell, 1972)(37). The reaction rate of oxidation increases significantly when the primary amine is present relative to reactions without the primary amine.

Large alkyl groups near the nitrogen enhances the amine's rate of oxidation.

Amines with polar groups attached to or near the nitrogen are not oxidized by the enzyme.

The stoichiometry of the enzyme reaction requires that 1 mole of  $\text{NADP}^+$  be present for each mole of substrate oxidized. As indicated above primary amines do not act as substrates however, they do act as activators for the enzyme. The oxidation rate of DMA can be doubled by adding 1mM of n-octylamine to the reaction media (Prough et al., 1981)(11). The presence of the n-octylamine does not effect the binding of the substrate but increases the overall reaction's velocity. Other activators are phenethylamine, amphetamine, and mescaline. Aniline and cadaverine are ineffective in enhancing the enzymes action.

Materials that act as metabolic inhibitors such as SKF-525A, carbon monoxide, cyanide, and azide all failed to inhibit the enzyme's DMA monooxygenase activity. 1, -(1-naphthyl)-2-thiourea (NTU) proved to be effective in specifically inhibiting the Ziegler monooxygenase enzyme's action on DMA. Because of NTU's affinity for the flavin-containing monooxygenase it can be used to differentiate the flavin-containing monooxygenase from other microsomal enzymes that may be present in a matrix.

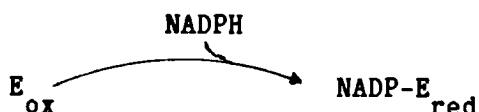
#### CATALYTIC OPERATION OF THE ENZYME:

The enzyme's catalytic behavior may be characterized by its ter-bi\* order kinetics resulting in the one electron oxidation of substrate exemplified in Figure 15.

This model is justified by the order in which the enzyme reacts with NADPH,  $O_2$ , then the substrate. In the first stage the enzyme must be reduced by forming a complex with NADPH.

---

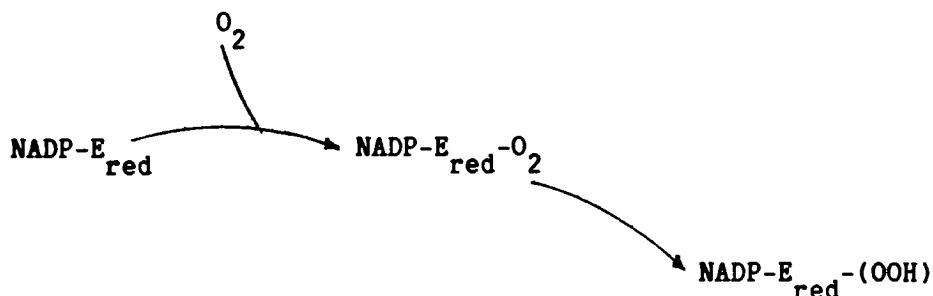
Enzyme reduction:



This reduced form of the enzyme accepts molecular oxygen that rapidly forms the NADP-peroxyflavin intermediate. The formation of a NADP-peroxyflavin intermediate is required before metabolism of the substrate can occur.

---

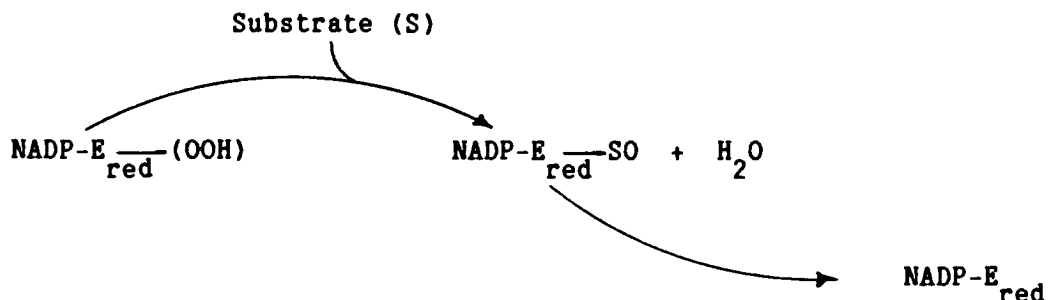
NADP-Peroxyflavin intermediate formation:



Following this the substrate then forms a complex with the intermediate resulting in an unstable ternary complex. At this point the peroxide degenerates to water and oxidized product. The specific mechanism for the oxygen insertion has not been elucidated. Possible mechanisms were discussed in the previous section.

---

Substrate oxidation:



---

The complex is stabilized by the loss of the oxidized pyridine nucleotide moiety. If there is no substrate, the peroxyflavin-complex slowly decays and hydrogen peroxide is slowly formed. However, under the same conditions and in the presence of substrate, hydrogen peroxide is rapidly released and the unstable binary-complex (NADP-enzyme) decomposes to oxidized enzyme and NADP. (Paulsen and Ziegler, 1979)(38).

Under anerobic conditions, the enzyme supports two electron transport between NADPH and substrates that are specific for two electron oxidation. This type of process is seen in the metabolism of certain types of dyes. The substrate that accepts two electrons is metabolized faster than substrates that accept only one electron. Examples of such reactions involve dichlorophenolindophenol and ferricyanide, respectively (27).

Under anerobic conditions, two electron substrate metabolism is not inhibited by the presence of substrates that are normally metabolized under aerobic conditions. However, when oxygen is introduced to an anerobic suspension, the anerobic process will shut down in favor of aerobic oxidation.

Aerobic metabolism (and its primary status) indicates the enzyme's regulation mechanism operates by requiring the presence of oxygen and not the presence of a substrate. It also shows that oxygen is in direct competition with other two electron carriers (Paulsen and Ziegler, 1979)(38).

Spectrophotometric analysis coupled with enzyme specific substrates revealed that any hydrogen peroxide produced was caused by a small amount of endogenous catalase. Spectrophotometric analysis of enzyme complexes specific for monooxygenase , NADPH, cytochrome c reductase and diaphorase indicated that none of these were present (Paulsen et al., 1979)(38) when the soluble form of the enzyme was analyzed for purity. The enzyme structure did show a small amount of lipid structure, which was responsible for a small endogenous NADPH oxidation observed in spectral studies that use the enzyme. However, this lipid material could not be removed without the subsequent loss of enzyme activity.

## CHEMISTRY OF HYDRAZINES

### GENERAL PROPERTIES:

Emil Fischer in 1875 was the first to correctly identify and name hydrazine. While Curtius isolated derivatives of hydrazine in 1887 the actual isolation of hydrazine itself had to wait for another twenty years. In 1907 Raschig was given the credit of having been the first person to isolate the actual compound. He did this by reacting ammonia with sodium hypochlorite in an oxidation reaction that yielded hydrazine in saline. This reaction is now called the Raschig reaction (39).

Hydrazine itself is a colorless liquid at room temperature and shares many physical characteristics similar to water. It boils at  $113^{\circ}\text{C}$  and freezes at  $2^{\circ}\text{C}$ . Like the amine family from which it originates hydrazine acts as a strong base having a  $\text{pK}_a$  of 7.95 ( $25^{\circ}\text{C}$ ). It is strongly hygroscopic and fumes in moist room air. It is isoelectronic with hydroxylamine and hydrogen peroxide. As one might expect, hydrazine shares redox properties with both of these compounds also.

The nomenclature used here will identify alkyl and aryl substituted hydrazines by using hydrazine as a suffix and locating the substituents by numbering the two nitrogens N1 and N2.

Another method used to label substituted hydrazines involves the symmetry of substitution. 1,1-Disubstituted hydrazines could just as easily be named unsymmetrical disubstituted hydrazines. The advantage of using symmetry is that abbreviations easily denotes the proper compound. i.e. unsymmetrical disubstituted hydrazine can be abbreviated as UDSH.

Hydrazine and its derivatives may be viewed as two amine groups linked by an N-N bond.



Each amine group has its substituents (or hydrogens) and lone electron pairs in a tetrahedral geometry ( $sp^3$  hybridized nitrogen). The geometry along the N-N bond is similar to the geometry of ethane along its C-C bond. Rotation about these bonds will result in the molecule assuming the most stable conformation. Hydrazine may be considered an azoethane or a nitrogen analog of ethane. The lone pair of electrons on each nitrogen directs the molecule to adopt an orthogonal conformation. An eclipsed electron conformation would cost too much in the way of energy. It has been calculated that the energy difference between the orthogonal and the eclipsed form is  $\Delta G$  of  $96 \text{ KJ mol}^{-1}$ .

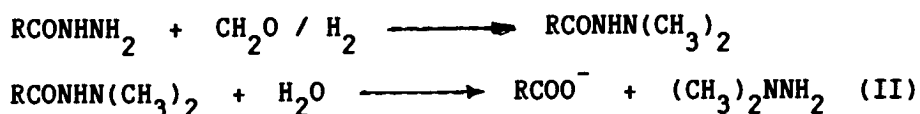
Like carbon compounds, nitrogen compounds change their conformation when the nitrogen substituents require charge delocalization. A carbonium ion stabilized by charge delocalization to an amine group causes the nitrogen to take some of the positive charge off the carbonium ion. The loss of carbonium character is balanced by the formation of an  $sp^2$  hybridized ammonium ion (iminium ion), or  $R_1R_2N^+=CX_2$ . The nitrogen adopts  $sp^2$  hybridization and the whole molecule becomes linear, similar to alkene chemistry. This change in conformation during delocalization can and has been mapped out using  $^1\text{H}$ -nmr. The substituents may also offer resistance to conformational change by retarding rotation about the nitrogen-nitrogen bond. Rotational hinderence is also reinforced by the repulsive force between the lone pair electrons.

Most of the alkyl and arylhydrazines are liquids at room temperature and share the characteristic ammonia-like odor of the parent compound. Chemical characteristics of substituted hydrazines include a decrease in basicity as the number of alkyl substituents increases and as the alkyl chain length increases.

Substituents alter the chemistry of hydrazine derivatives through inductive and resonance effects. Resonance effects by delocalization in phenylhydrazine lowers its basicity. To illustrate this, hydrazine has a pKa of 7.95 and phenylhydrazine a pKa of 5.27. The alkylated forms of hydrazine act as proton acceptors and under particular reaction conditions also act as nucleophiles in substitution reactions. Because of their nucleophilic properties, alkylated hydrazines are used for derivative forming reactions with alkylating agents and compounds possessing carbonyl groups.

#### REACTIONS OF 1,1-DISUBSTITUTED HYDRAZINES:

Preparation of 1,1-disubstituted hydrazines - Preparation is done by reducing the corresponding nitrosamine to its respective hydrazine using sodium borohydride or lithium aluminum hydride as reducing agent. Another route to 1,1-disubstituted hydrazines is by the Raschig Method using a disubstituted amine instead of ammonia. There is also a catalytic method that utilizes reductive alkylation of a hydrazide with formaldehyde and hydrogen (II).



Salt Formation - While fuming in moist air and hygroscopic tendencies are properties of hydrazine itself, its substituted derivatives retain these qualities as well. These properties are often undesirable especially when trying to isolate the derivatives. Hydrazine and its derivatives form salts with a variety of anionic species. On standing, hydrazine forms the carbamic acid by reaction with atmospheric carbon dioxide.

McBride and Kruse in 1957 (40) used a variety of anions to derivatize the end products of this substituted hydrazine reaction (III).

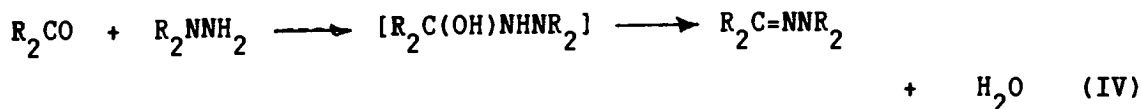


Heat Stability - Dialkyl hydrazines are generally heat stable and can be distilled without decomposition. Aryl hydrazines however are not heat stable and decompose at a slow rate when heated. The principal reaction involving diaryl hydrazines is dismutation, that is one-half of the compound is oxidized and the other half is reduced. Reduction of the one-half usually involves cleaving the N-N bond in the hydrazine resulting in the formation of the corresponding amine.

Nitrosation - 1,1-Dialkylhydrazines react with nitrous acid to form nitrous oxide and the corresponding secondary amine. Chlorides of sulfuric acid and phosphorous acids, both organic and inorganic, react with the hydrazine in much the same way that other acylating agents work.

Hydrazone Formation - One mole of hydrazone and a mole of water are formed as a result of a carbonyl-containing compound combining with a substituted hydrazine. The use of this reaction is common place because of the highly characteristic hydrazone derivatives used to identify the presence of a carbonyl group in unknown compounds. The reaction mechanism consists of a two-stage process, addition then dehydration.

The rate-determining step depends on each of the compound's structures and reaction conditions (IV).



Oxidation - 1,2-Dialkylhydrazines undergo oxidation resulting in the corresponding azo compounds. 1,1-dialkylhydrazines however form an array of oxidation products whose formation depends on a number of factors. The simplest oxidative process is at the N-N bond resulting in the formation of the secondary amine and nitrogen. Fehlings solution, ferric chloride, or a permanganate solution can be used to accomplish this type of oxidation.

Oxidation reactions that result in removal of the two hydrogens at N2 yield the charge separated species diimides (McBride and Kruse 1957)(40).



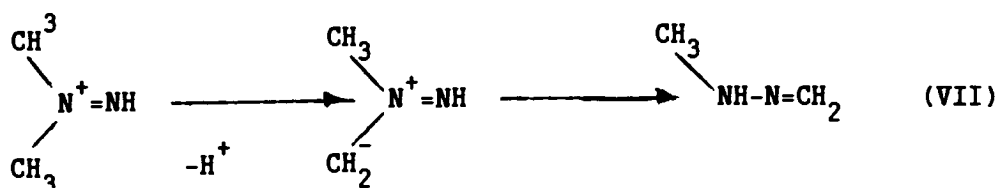
Diimides may form by the hydrazine first losing a hydrogen from N2 to get the acid stabilized 1,1-dialkyldiazenium ion.



The diazenium ion is further oxidized in weakly acidic solutions to the corresponding diimide.

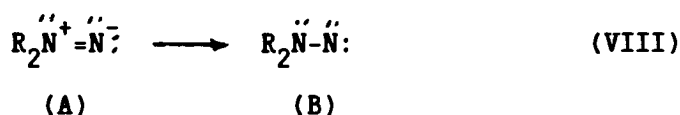
Further oxidation of the diazenium ion under alkaline conditions may proceed by losing another N2 hydrogen and rearranging to form a hydrazone.

Using 1,1-dimethyldiazinium as an example:



The hydrazone may be further oxidized to other products. Upon hydrolysis, hydrazones may fragment to the corresponding aldehyde and monosubstituted hydrazine.

Again, literature is not always consistent in the naming of diimides. P.A.S. Smith (39) uses the term diimide, McBride and Kruse (1957)(40), and David Lemal (41) uses diazene for the charge separated form (A) and aminonitrene for the uncharged form (B).

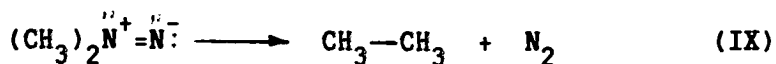


Diimides are most stable in acidic solutions and rapidly dimerize to the tetrazene form when the solution is neutralized under atmospheric conditions and in polar solvents. Diimides also form acid-stable salts called azamines.

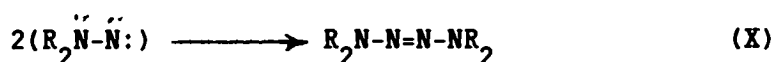
Diimide stabilization is similar to carbene chemistry in that the alkyl groups stabilize and delocalize the charge separation. Bulky alkyl, allyl, and aryl groups when attached to the diimide stabilize the charge separation.

Diimide formation is also enhanced by the presence of substituents at the alpha carbon that tend to stabilize radical formation or charge separation in the intermediate and in polar solvents. Non-polar solutions support diimide fragmentation with subsequent nitrogen gas formation. The simplest example is seen in the reduction of 1,1-dimethylnitrosamine producing azamines in the presence of dithionite (IX).

In diethyl ether the diimine's charges are not stabilized well by the methyl groups or the solvent and the reaction forms nitrogen gas and ethane.



What one actually isolates during an oxidation reaction depends on the amount of oxidant used, the nature of the oxidant and the reaction conditions (McBride and Bens, 1958) (42). Tetrazenes formed are usually a result of azamines reacting with excess or unreacted hydrazine (VIII) under acid conditions. .



## METABOLISM OF HYDRAZINES

The metabolism of hydrazines (or indeed any other substrates) involves at least two broad aspects - the products of the metabolic process and the "metabolic book-keeping" i.e. the extent to which these products are formed (and perhaps the rates at which they are produced).

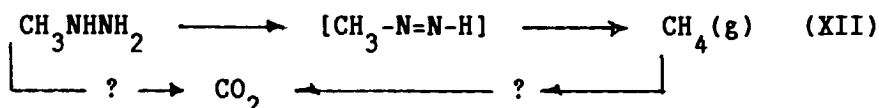
In the case of hydrazines, the first modern study to elucidate the metabolism of hydrazine was made by McKennis and co-workers (1955)(43). The in vivo disposition of hydrazine was studied by administering hydrazine (15 mg/kg, intravenous, i.v.) to two dogs and measuring the amount of hydrazine excreted in the urine. In 48 hours after initial dose 30-40% of the hydrazine was excreted unchanged. Hydrazine metabolites were not detected.

Yard et al., 1957 (44) and El Masiri et al., 1958 (45) examined the in vivo metabolism of substituted hydrazines. They recorded the isolation of hydrazine in the urine of rabbits 24 hours after intraperitoneol, i.p. injection of glutamylhydrazine. Information on the ratio of hydrazine formed relative to the amount of drug given was not available. However, from this data the metabolism of substituted hydrazine indicates a cleavage of the following type:



Some pharmacokinetic studies were also made. Pinkerton et al., (1967) (46) established, using  $^{14}\text{C}$ -monomethylhydrazine as substrate, that 25-40% of initial i.v. dose given to rats was excreted over a 24 hour period in the urine and isolated unchanged. Autopsies showed that the non-excreted radiolabeled carbon was found localized mostly in the liver but also in the kidney, bladder, blood serum and pancreas.

How the material was bound to these areas was not determined. About the same time, Dost et al. (47) studied the fate of  $^{14}\text{C}$ -methylhydrazine in rats and found that 40% of an i.p. dose is respired during the first 24 hours in the form of 20 to 25%  $^{14}\text{CO}_2$  and the remainder as  $^{14}\text{CH}_4$  indicating the presence of the following kind of reaction (XII):

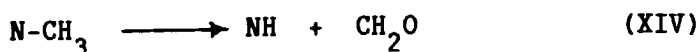


Whether the  $\text{CO}_2$  originates by oxidation of the carbon residue in the original hydrazine or in the product is unclear (though the former is more likely).

Prough and co-workers (1969)(48) extended the study of substituted hydrazine metabolism by investigating the in vitro microsomal directed metabolism of methyl-, ethyl-, n-propyl, and n-butylhydrazine. They demonstrated that these hydrazines were metabolized to the parent hydrocarbons with a possible mechanism such as: (XIII)



Prough's group (Wittkop et al., 1969) (49) also isolated formaldehyde from the in vitro microsomal-directed metabolism of methylhydrazine, 1,1-dimethylhydrazine, 1,2-dimethylhydrazine and procarbazine and suggested that a N-demethylase action was taking place and proposed the following reaction:





The enzyme system used in both these studies was localized in the microsomal fraction taken from rat livers and was specific for N-demethylation and hydrazine metabolism.

The metabolism required both NADPH and molecular oxygen. Induction of methylhydrazine metabolism was possible by pretreatment of microsomal source animals with known cytochrome P-450 inducers (i.e. phenobarbital) prior to sacrifice. Metabolic inhibition was also observed when cytochrome P-450 inhibitors were administered to microsomal suspensions prior to substrate addition. This indicated cytochrome P-450 as the major microsomal enzyme responsible for methylhydrazines metabolism.

The first paper that discussed in vivo metabolism of 1,1-dimethylhydrazine was by Back and co-workers in 1963 (50). They gave sublethal doses of  $^{14}\text{C}$ -1,1-dimethylhydrazine i.v. to rats and monitored the urine for radiolabeled products. During the first five hours 30-50% of the given dose was excreted in the urine. After this the animals were sacrificed and the remainder of the dose was not found in any one specific site but evenly distributed throughout the body.

Dost et al., (1966)(47) also used  $^{14}\text{C}$ -1,1-dimethylhydrazine to study 1,1-dimethylhydrazine in vivo metabolism. Rats were given sub-acute doses of the labeled material i.p.. After ten hours, 30% of the material was respired as  $^{14}\text{CO}_2$ . No  $^{14}\text{CH}_4$  was observed. Dost determined that the detoxification system can apparently be saturated since a similar experiment using the same species of animal and test conditions but using convulsive doses of  $^{14}\text{C}$ -1,1-dimethylhydrazine resulted in significantly lower output of respiratory  $^{14}\text{CO}_2$  in just a few hours after administration.

Prough et al., (1980) (11) using microsomal cytochrome P-450 from phenobarbital pretreated rats demonstrated the formation of a new spectral species. Formation of the spectra required NADPH, molecular oxygen and 1,1-dialkylhydrazine. The spectra showed distinct alpha and beta absorbance transitions between 500 and 600 nm along with the large absorbance bands at 438 and 449 nm characteristic of low-spin hemoprotein complexes. The time required to form the complex and the fact that NADPH and molecular oxygen is necessary suggests that the hydrazine is being metabolized to a form that forms a hemoprotein complex. Complex formation could be induced by using the known cytochrome P-450 inducer phenobarbital during animal pretreatment and inhibited by adding SKF-525A in microsomal suspension prior to substrate addition. These results pointed to cytochrome P-450 being the enzyme part of the spectral-complex.

Using a cytochrome P-450 reductase antibody, the formation of the complex was markedly inhibited when it was added to microsomal suspensions prior to substrate addition. This suggests that the metabolite was generated by the cytochrome dependent monooxygenase system.

Formation of the metabolite-complex inhibited other cytochrome P-450 dependent drug metabolism both in vivo and in vitro experiments. The rate of oxygen consumption during cytochrome P-450 directed metabolism of 1,1-dimethylhydrazine drops drastically following the administration of substrate. This drop in O<sub>2</sub> consumption and the absence of the ferrous-type binding spectra (found normally in anaerobic cytochrome P-450 spectra) indicates the abortive nature of the cytochrome P-450 catalyzed oxidation of 1,1-dimethylhydrazine.

What finally developed from this work was the proposal that 1,1-dialkylhydrazines are metabolized by cytochrome P-450 to a reactive form such as a nitrene intermediate and that it binds to the enzyme such that further oxidation by the enzyme is inhibited. Support for this proposal is based on the fact that the abortive complex exhibits difference binding spectra similar to nucleophilic carbene-heme complexes indicating that the reactive intermediate is carbene like in electronegative character and that both this abortive complex and diazene-generated complexes stabilize cytochrome P-450 in the ferric state.

Because 1,1-dialkylhydrazines are not completely metabolized by the cytochrome system it was necessary to investigate other monooxygenase systems that might be responsible for 1,1-dialkylhydrazine metabolism. Because the Ziegler enzyme plays an important role in secondary and tertiary amine metabolism it was of interest to investigate what part it took in the metabolism of 1,1-dialkylhydrazine.

Prough (11) demonstrated that the enzyme was indeed responsible for at least the metabolism of 1,1-dimethylhydrazine. Prough suggested that the metabolism occurs via oxidative dealkylation to form formaldehyde and monomethylhydrazine. The solublized, purified enzyme he used was taken from the liver of old sows killed in slaughter houses. The stoichiometry of hydrazine oxidation was examined by using a limiting amount of hydrazine substrate and noting the substrate dependent extent of NADPH oxidation and  $O_2$  consumption. When incubated with the Ziegler enzyme, formaldehyde and monomethylhydrazine are formed stoichiometrically from 1,1-dimethylhydrazine. HPLC analysis of ethyl acetate extracts of the reaction mixture showed only these products and not tetramethyltetrazene.

Prough suggested that these results are consistent with the formation of an azomethinimine intermediate with rearrangement to hydrazone. The formation of minor quantities of methane and the complete absence of tetramethyltetrazene supports two possible pathways: formation of a diazene intermediate that tautomerizes to the azomethinimine or the formation of an azomethinimine tautomer directly from the initial oxidation product. However, because the reaction was done at high pH (8.4), the tautomerization pathway is favored. (see Figure 15)

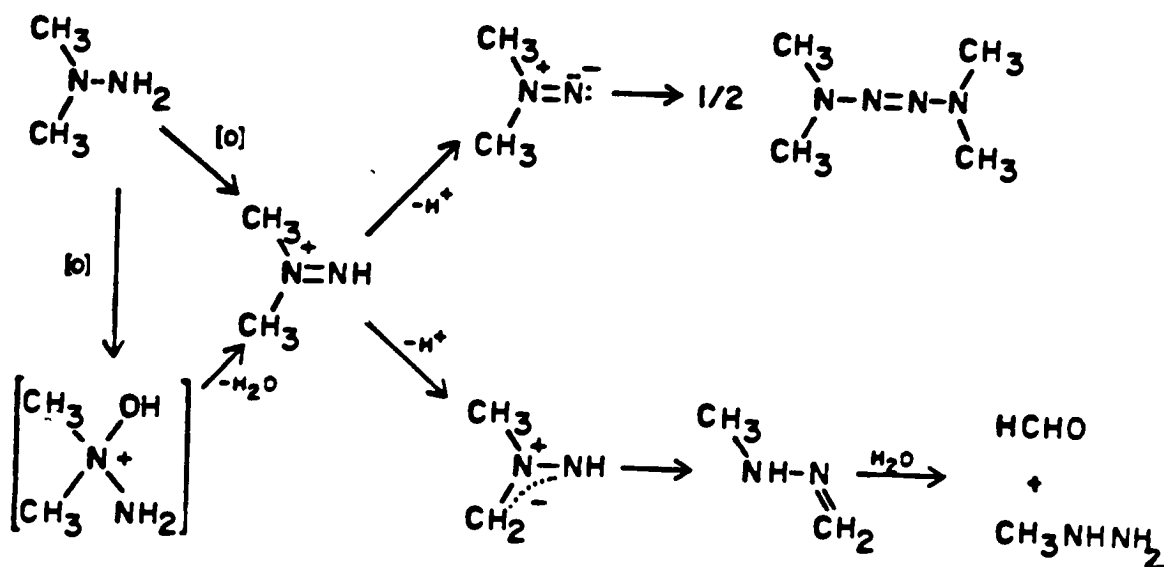


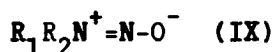
Figure 15: The chemical and proposed mechanism for the the Ziegler enzyme (MAO) directed metabolism of 1,1-dimethylhydrazine (Prough *et al.*, 1981)(11).

## CHEMISTRY OF NITROSAMINES

### GENERAL PROPERTIES:

Aliphatic nitrosamines are generally stable yellow liquids or solids at room temperature (1,1-dimethylnitrosamine b.p.= 154°C, 1,1-diethylnitrosamine, b.p.= 173°C) and soluble in water. Aromatic nitrosamines tend to become less stable when heated at atmospheric pressure and are insoluble in water.

The electronic interaction and the electronic structure of the nitrosamine is uncertain; however, there are some very definite conclusions that one can draw from the physical properties. The two nitrogens and the two alpha carbons in IX are all planar, and only the hydrogens or substituents on the alpha carbons are not in the plane of the nitrosamine function (N-N-O).



The nitrosamine function is angular with respect to the two nitrogen's (N-N-O bond angle of 114°) and therefore rotation is restricted and leads to Z and E isomerism about the N-N bond.

Delocalization of the electrons from the amino nitrogen results in a highly polar molecule with a high electron density on the oxygen (the canonical form of nitrosamine is shown as IX). This delocalization of charge is consistent with aliphatic nitrosamines being soluble in water and polar solvents.

The ultraviolet spectrum of nitrosamines show absorbances below 400 nm with maxima in the range of 340-385 nm. Infrared spectra of nitrosamines have strong bands at 1421-1476 ( $\nu_{N-O}$ ), 1352-1367 and 1266-1290  $\text{cm}^{-1}$ . The N-O stretching frequency of nitrosamines are typically lower than that

of the N=O function in monomeric, tertiary, aliphatic nitroso compounds (1511-1495  $\text{cm}^{-1}$ ) thus, supporting the canonical structure IX and electron delocalization. Table 1. summarizes some typical N-O stretching frequencies.

The actual position of the absorptions is determined by the type of nitrogen substituent bond and the type of substituent (i.e. aliphatic, aromatic, non-carbon substituents, etc. ).

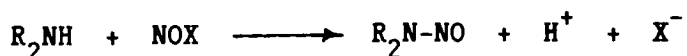
Table 1: Typical N-O stretching frequencies. (Silverstein, et al., 1981)(51)

<u>Compound</u>	<u>N-O function</u>	<u>N-O Stretching Frequency</u>
Nitramine	$\begin{array}{c} \text{N}-\text{N}-\text{O} \\   \\ \text{O} \end{array}$	Symmetrical N-O stretch (1389-1259 $\text{cm}^{-1}$ ) Asymmetrical N-O stretch (1661-1499 $\text{cm}^{-1}$ )
Nitroso	R-N=O	With monomeric, tertiary, aliphatic substituents (1585-1539 $\text{cm}^{-1}$ ) With aromatic, monomeric substituents (1511-1495 $\text{cm}^{-1}$ )
Nitrosamines	N-N=O	with aliphatic substituents (1421-1476 $\text{cm}^{-1}$ )

The  $^1\text{H}$ -nmr spectra of 1,1-dimethylnitrosamine gives two equal absorptions at  $\delta$  3.76 and 2.96, attributed to the methyl groups trans and cis to the oxygen respectively.

#### REACTIONS OF NITROSAMINES:

Preparation of Nitrosamines - This simply involves the nitrosation of aliphatic or aromatic secondary amines by a nitrosating species:



In acidic solutions, an electrophilic pathway is involved with dinitrogen trioxide reacting with the free amine to form the corresponding N-nitrosamines.

Nitrosamines can be formed from secondary amines in nitrous acid and sodium nitrite. Free radical pathways offer methods that use neutral or alkaline aqueous solutions of dinitrogen tetroxide and nitric oxide as the nitrosating agent.

Certain tertiary and quaternary amines may be converted on nitrosation into secondary nitrosamines and carbonyl compounds (Figure 16).

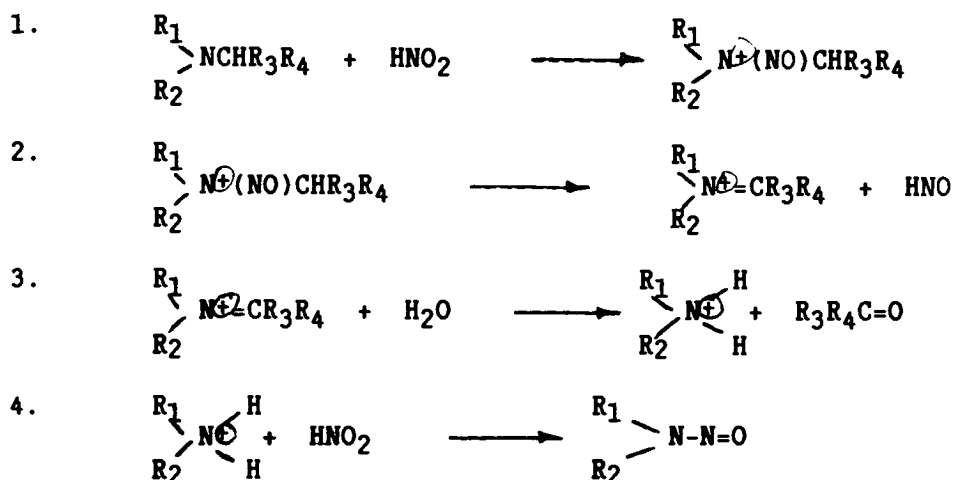
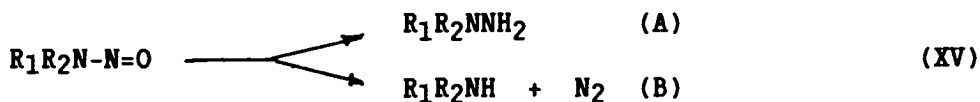


Figure 16: Nitrosation of a tertiary amine.

Reduction of Nitrosamines - There are numerous reduction reactions involving nitrosamines that have as end products either secondary amines or 1,1-dialkylhydrazines.

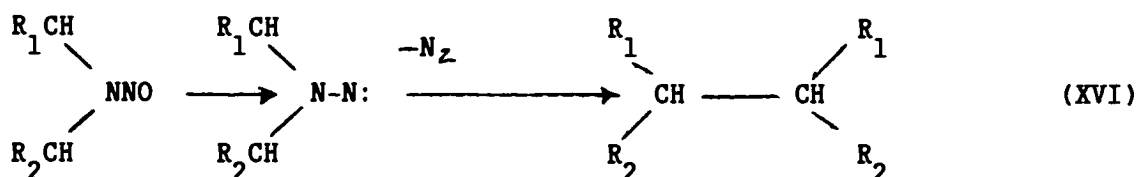


An example is an unsymmetrical dialkyl nitrosamine being reduced by zinc in acetic acid to the corresponding hydrazine (A). If the substituents on the nitrosamine are larger than n-propyl then this same reduction would result in production of the secondary amine (B).

Two other examples of nitrosamine reduction to hydrazine products are: the reduction of 1,1-dimethylnitrosamine in the presence of hydrogen catalyzed by palladium and reduction of 1,1-dimethylnitrosamine in the presence of  $\text{LiAlH}_4$  in anhydrous diethyl ether or THF.

Mixing 1,1-dimethylnitrosamine with hot alcohol in low pH solution will form the dimethylamine, however chilling the reaction and adding  $\text{MgSO}_4$  to the mixture will result in formation of 1,1-dimethylhydrazine.

Reduction of the nitrosamine in lithium in liquid ammonia or with sodium dithionite results in tetrazene or bialkyl formation (XVI).



The mechanism responsible for the reaction involves formation of a diazene that decomposes to the tetrazene or bialkyl (bialkyl formation shown).

Oxidation of Secondary Nitrosamines - Oxidation can occur at either nitrogen atom, oxygen, or substituent.

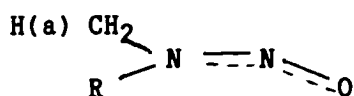


Figure 17: Possible reaction sites of nitrosamines. (R = H, alkyl, allyl groups)

Oxidation at the alpha hydrogens is affected by the nitrosamine's stereochemical form. The relative acidity of the alpha hydrogens is a direct consequence of the compound's stereochemistry. Deuterium exchange at hydrogens alpha to a nitrosamine function occurs most rapidly with that hydrogen which is in-plane with the nitroso group or pro-Z and attached by a bond perpendicular with the atoms of the nitrosamine function.



This indicates that the most acidic hydrogen is that which is pro Z and perpendicular to the nitrosamine group as illustrated with the conformationally biased system, 1-nitro-4-t-butylpiperidine (Lyle *et. al.*, 1979)(52)(Figure 18).

The  $^1\text{H}$ -nmr spectrum of the compound in Figure 18 shows four distinct signals for the four different alpha hydrogens. Using proton nmr to follow the degree of deuterium exchange, Lyle and his group found that it was the pro-Z alpha hydrogen which undergoes exchange most readily.

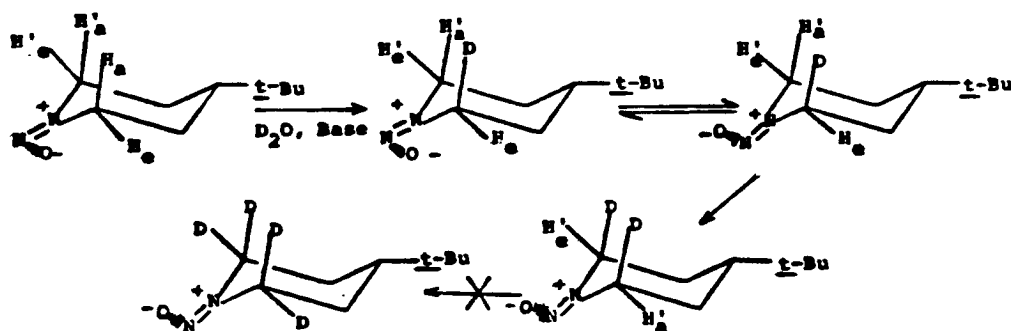
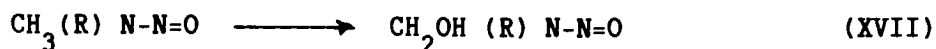


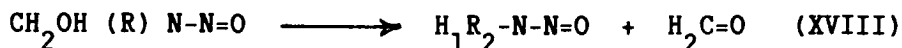
Figure 18: Relative acidity of alpha protons as determined by the conformational effect of deuterium exchange on a conformationally biased system.

As previously described in oxene chemistry, there are a number of methods for breaking hydrogen-carbon bonds.

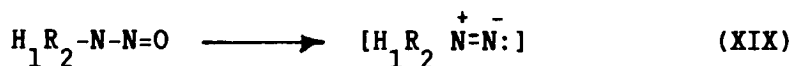
Oxidative dealkylation of methyl alkyl nitrosamines involves hydroxylation on the methyl group to give alpha-hydroxymethylnitrosamines (XVII).



This hydroxy nitrosamine is very unstable and loses formaldehyde to form the primary alkylnitrosamine (XVIII).



The unstable nitrosamine rapidly rearranges to the alkyl diazonium ion (XIX).



The diazonium ion may then proceed to form tetrazenes or be reduced to a mono alkyl hydrazine. The alpha-hydroxylated species has not been isolated, however, ester and ether derivatives of the hydroxylated have been prepared (Michejda, et al., 1979)(53).

Oxidation at the N-N bond results in denitrosation. This is a common reaction mechanism among aromatic nitrosamines and involves the nucleophilic attack on a protonated nitrous group which facilitates the reaction by forming nitrous acid as a leaving group.

## METABOLISM OF NITROSAMINES

### GENERAL:

In 1982 P.N. Magee (54) wrote that to date the material available indicating that nitrosamines are involved in causing cancer in humans is not sufficient to make conclusions on their carcinogenic mechanisms. Although evidence is provided that nitrosamines are powerful carcinogens, the specific details of their carcinogenic action was (and is ) still lacking.

This defect is due, in part, to the problems involved in acertaining specific products from nitrosamine metabolism. With nitrosamines becoming more apparent in our environment and diet (McWeeny 1983)(55) the need to know exactly how these chemicals are metabolized becomes more crucial.

### METABOLIC MECHANISM:

The generally accepted mechanism of nitrosamine metabolism (and hence carcinogenicity) and whose mechanism was described earlier, is via an hydroxylation at the alpha carbon. The resulting product is the unstable alpha-hydroxy-nitrosamine which decomposes to the diazohydroxide compound. This decomposition product can alkylate nucleic acids (Figure 19). The alkylation of nucleic acids is believed to be achieved via a diazonium ion formed from the decomposition of the alpha-hydroxynitrosamine. This speculation is given substance by experiments performed with deuterated nitrosamines. There appears to be a direct correlation between the kinetic isotope effect and the rate of reaction occurring at the alpha carbon with the rate of production of tumors in animals fed protonated and deuterated forms of 1,1-dimethylnitrosamines (Keefer et al., 1973)(56).

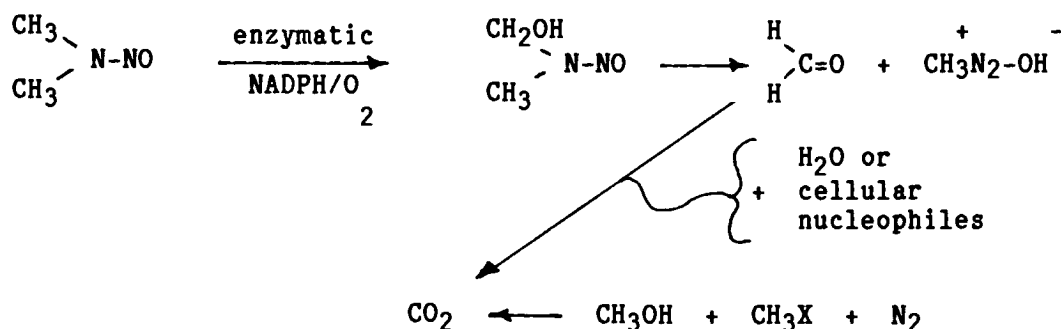


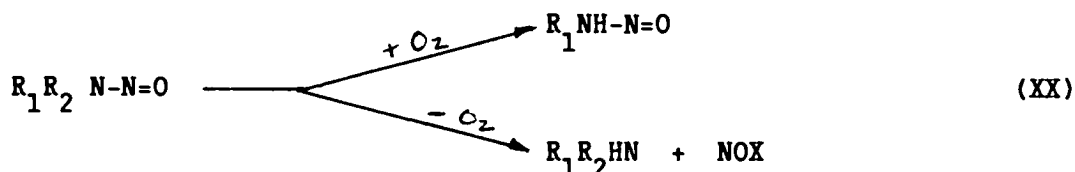
Figure 19: A generally accepted scheme of 1,1-dimethylnitrosamine microsomal directed metabolism.

Magee and Barnes (1967)(57) characterized cytochrome P-450 as the enzyme responsible for the alpha hydroxylation of 1,1-dimethylnitrosamine, leading to subsequent demethylation. They further stated that this reaction is also the rate limiting step and is dependent on the presence of NADPH and molecular oxygen. Further work done on cytochrome P-450 directed metabolism of nitrosamines revealed that the demethylation metabolism of nitrosamine is affected by the amount of substrate present and the amount of the demethylase enzyme present.

The rates of nitrosamine metabolism were determined by measuring the amount of metabolite formed when using microsomes from rats, pretreated with phenobarbital or 3-methylcholanthrene, and low concentration doses of nitrosamine in the presence of NADPH and  $\text{O}_2$ . Repeating this experiment with fresh mixtures of the above materials and with the addition of a cytochrome P-450-inhibiting substance resulted in increased rates of metabolite formation. However at above lethal dose nitrosamine concentrations, the cytochrome P-450 inhibitors had the opposite effect on the rate, decreasing the rate of metabolite formation (Arcos *et al.*, 1977)(58).

These findings led to speculation that there existed, under aerobic conditions, at least two forms of demethylase in microsomes (Appel et al., 1979)(59). (Kroeger-Koepke and Michejda, 1979)(60).

Under anerobic conditions nitrosamines are metabolized via a cytochrome P-450 directed denitrosation mechanism instead of a demethylase mechanism. (Potter and Reed, 1982)(61). (Appel et al., 1979)(59).



Potter and Reed (1982)(61) used purified cytochrome P-450 and mixtures of cytochrome P-450 and cytochrome P-450 reductase and measured the rates of enzymatic denitrosation of nitrosamines. By changing the amounts of reductase present, they observed a synergism between the reductase and cytochrome P-450 supporting cytochrome P-450 as the enzyme responsible for the metabolism of nitrosamines under anerobic and aerobic conditions.

The rate of anerobic nitrosamine metabolism by cytochrome P-450 in the presence of NADPH can be observed by using optical difference absorbance spectra and monitoring the increase in absorbance at 444 nm. The absorbance strength is proportional to the amount of cytochrome P-450-substrate (or metabolite) complex formed (Potter and Reed, 1979)(61).

Cytochrome P-450 when complexed to NO exhibits a characteristic binding spectra with a Soret absorbance at 445 nm and type I spectral changes. This type of spectral change is indicative of the formation of a parmagnetic heme center with subsequent ligand type of binding. During the denitrosation of nitrosamines by cytochrome P-450 this same type of binding spectrum is exhibited.

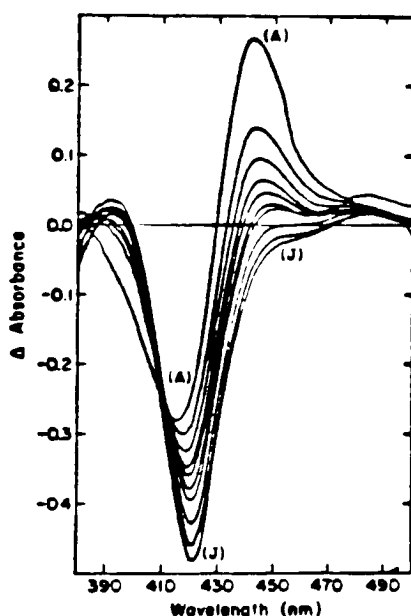
Indeed, Ebel et al., (1975)(62) and O'Keefe et al., (1978)(63) both characterized the distinct optical difference spectra when NO was a ligand of both ferric and ferrous cytochrome P-450. They also observed both Soret and visible maxima of ferrous-NO from substrate binding complexes of both the purified and microsomal cytochrome P-450.

The NO-binding spectra however is not very stable. Potter and Reed found that the both the ferric and ferrous NO complexes were unstable. The addition of substrate (NO) to anaerobic phenobarbital pretreated liver microsomes resulted in the formation of a complex that exhibited ferric type binding spectra. Upon the addition of NADPH the resulting substrate binding spectra changed from a ferric heme type to a ferrous type (Figure 20)(61).

The resulting substrate binding spectra observed for 1,1-dimethylnitrosamine denitrosation directed by cytochrome P-450 is characteristically the same as that obtained when using NO as substrate. However, the substrate binding complex did not have as long a life as that formed when NO was bubbled through a microsomal suspension. In fact the substrate binding complex's spectrum exhibits an ever deepening absorbance minimum at about 421 nm indicating that the complex quickly degenerates. This trough may be the result of the cytochrome P-450-substrate binding complex being transformed to a cytochrome P-420-substrate binding complex. This idea was substantiated by comparing the EPR signals and optical difference spectra produced by a half-hour old cytochrome P-450-substrate binding complex to freshly produced cytochrome P-420-substrate binding complex and finding that both complexes exhibit exactly the same binding spectra EPR signals (Appel et al., 1979)(59).

Denitrosation by cytochrome P-450 under anaerobic conditions and in the presence of NADPH have been observed in nitroso compounds other than nitrosamines. Radiolabelled nitrosoureas were added to phenobarbital-pretreated rat liver microsomes along with NADPH but no  $O_2$ . The microsomes were incubated at  $30^{\circ}C$  for 30 sec. and the resulting substrate binding spectra was that of an NO-heme type of binding spectrum. Organic extraction of the microsomal suspension revealed the presence of the parent urea compound in stoichiometric amounts with NADPH utilized (Potter and Reed, 1979)(61)

---



---

Figure 20: Repetitive scanning of cytochrome P-450 ferrous-NO optical difference spectra generated by the addition of NO gas bubbled into microsomal suspensions containing cytochrome P-450 and cytochrome P-450 reductase. Scans were recorded every 1.5 s from A to J. (Potter and Reed 1979)(61).

## KINETIC ISOTOPE EFFECTS

### DEUTERIUM LABELLED COMPOUNDS:

Urey and co-workers in 1932(64) were the first to discover deuterium and recognize it as the rare and stable heavy isotope of hydrogen. They, along with others, recognized the large mass ratio,  $^2\text{H}/^1\text{H}$ , between deuterium and hydrogen would be useful in the study of biological equilibrium and kinetic experiments.

The effects of isotopic substitution on a reaction mechanism (and on the reactions kinetics) was first formulated in terms of the transition state theory of reactions by Bigeleisen and Mayer (1947)(65). The so-called isotope effect exhibited in appropriate studies is a consequence of molecular vibrational frequencies of the initial and transition states of the hydrogen and deuterium containing compounds. Observing perturbations in this behavior would provide information concerning changes in the vibrational frequencies of the compound in its transition state and its initial ground state.

Kinetic isotope effects on reaction rates can be expressed as primary effects and secondary effects. Simplistically, primary isotope effects are observed in reaction kinetics when the C-D (or C-H) bond is at the reaction center, that is, the C-D (C-H) bond is broken during the rate limiting step. Secondary isotope effects are observed when nonexchangeable deuterium is present near but not at the reaction center (Katz and Crespi, 1971)(66).

Primary isotope effects are fairly straight forward in their explanation if one were to use bond stretching frequencies that can be observed in IR spectroscopy.



A common stretching frequency of a C-H bond will occur at or around the 2900-3100  $\text{cm}^{-1}$  region and that of C-D bond around 2055-2200  $\text{cm}^{-1}$  region.

Harris and Wamser (1976)(67) explain that this difference in the stretching frequencies between C-H and C-D is a result of the increase in mass in deuterium. The lower stretching frequency observed for the C-D bond also indicates a lower energy. Kinetic isotope effects then, are a result of zero-point vibrational energy differences between C-D bonds and C-H bonds. Figure 21 illustrates the zero-point vibrational energy difference of approx. 1.2 kcal in favor of the C-H bond. This means that the energy required to weaken or break a C-H bond is less than that required to do the same to a C-D bond.

In chemical reactions, the magnitude of the kinetic isotope effect is related to the type of bond breaking in the reaction and the transition state structure. A primary isotope effect's observed magnitude depends on the extent of hydrogen bond (or deuterium bond) fracturing in the transition state (67). The base catalyzed elimination reaction of 1-bromo-2-phenylethane exhibits a large isotope effect (67) of  $k_H/k_D=7.1$ . Exhibitions such as this are indicative of the nearly complete H-C bond breakage in the transition state. Secondary kinetic effects usually exhibit a lesser rate change because the hydrogen bond that breaks is not participating in the transition state but does effect the overall reaction rate.

Secondary isotope effects are a result of the deuterium being in close proximity to the reaction center but not in it. Thus these effects can be a result of inductive, steric and of hyperconjugative influences. They can also arise from changes in molecular bond hybridization such as that which occurs in a reaction whose reactants pass from the ground state to a transition state complex.

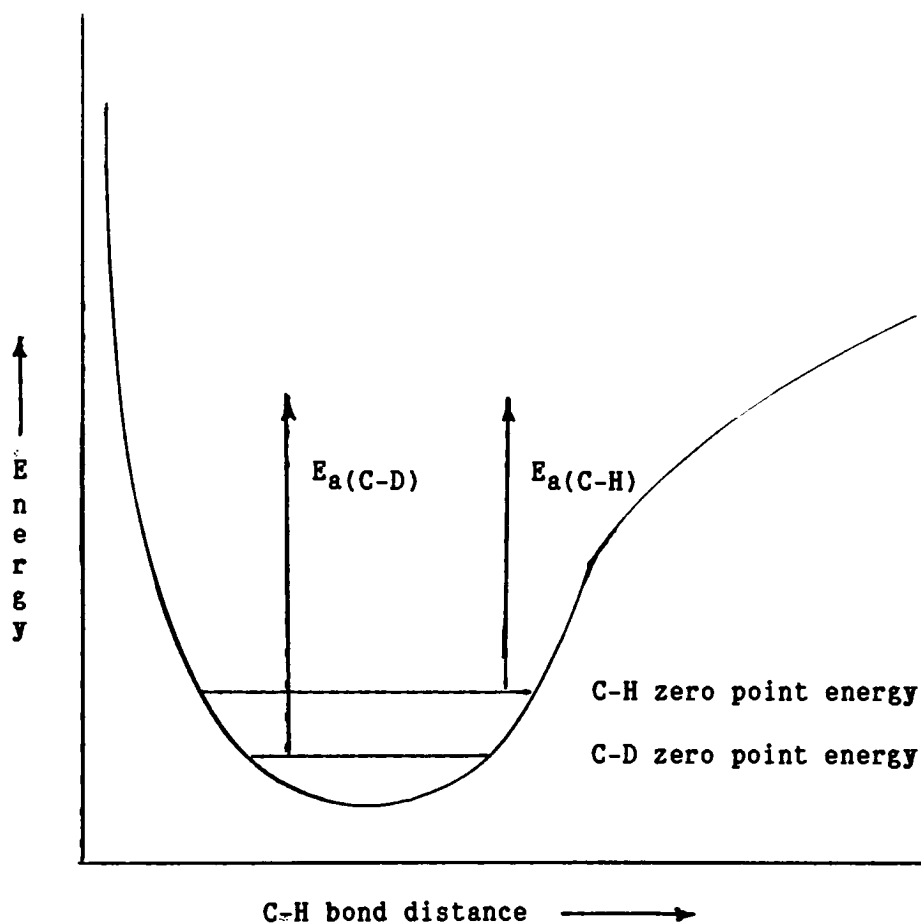
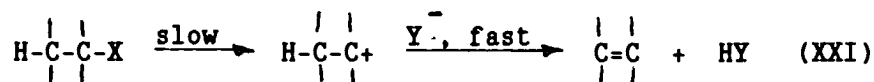


Figure 21: Zero-point vibrational energy as the source of kinetic deuterium isotope effects. (Wamser and Harris, 1976)(67).

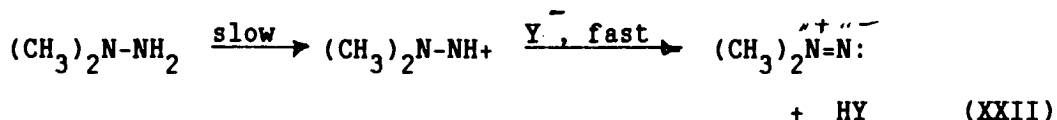
## KINETIC ISOTOPE EFFECTS IN ELIMINATION REACTIONS:

Michjeda et. al. (60) has proposed an elimination of mechanism in the enzymatic dealkylation of 1,1-dimethylnitrosamine. Also, Prough (11) has provided evidence that 1,1-dimethylhydrazine is metabolized to monomethylhydrazine and formaldehyde via an elimination mechanism.

Elimination reactions driven by carbocation formation (E1) proceed according to reaction (XXI):



Similarly:



Both reactions would exhibit primary isotope effects if the hydrogen at the beta position in reaction (XXI) or at N2 were deuterated and broken during the rate limiting step (Fry, 1964)(68)

The extent of secondary isotope effects felt from deuterium-labelled methyl groups in reaction (XXII) would be directly related to the role they play in the formation of the transition state.

The magnitude of isotope effects also has relevance to the reaction mechanism (Collins and Bowman, 1970)(69). The chemical formation of a diazonium ion from 1,1-dimethylhydrazine with subsequent formation of the tetrazene, has been shown to follow a mechanism whereby the hydrazine losses its N2 hydrogens without the loss or exchange of hydrogens from the two methyl groups (11,40,42). The mechanism is elimination followed by dimerization (see Figure 15).

Alternately, Hines (27) has proposed that enzymatic oxidation of 1,1-dimethylhydrazine involves the formation of a quaternary ammonium ion or the immediate oxidation to the acid stable diazenium ion which in aqueous base is tautomerized to the azomethanimine that can undergo a 1,2 rearrangement to formaldehyde and methylhydrazone. Under these conditions, primary isotope effects will be observed when the methyl hydrogens are labelled and the tautomerization/rearrangement step is rate limiting (see Figure 15).

## ENZYMATIC REACTIONS AND KINETIC ISOTOPE EFFECTS:

Collins and Bowman (1970)(69) and Richards (1970)(70) offer chapters in their books dedicated to primary and secondary kinetic isotope effects in enzyme catalyzed reactions. There are also whole symposiums dedicated to kinetic isotope reactions in metabolic reactions such as The Annual International Conference on Stable Isotopes.

Multistep processes, such as those that occur in enzymatic reactions obscure basic kinetic isotope effects by complicating rate factors. Biological mechanisms may become altered or completely re-routed as a result of deuterium labelling (Horning et al., 1979)(71) (Mira et al., 1980)(72). Alterations of substrate binding and transport to the enzyme's catalytic or binding sites may also effect the overall observed kinetic effect (Lu et al., 1980)(73)

The following are some examples of enzymatically controlled reactions involving changes in products, kinetic rates or entire pathways.

Primary kinetic isotope effects have been observed in the cytochrome P-450-dependant dealkylation of caffeine (71). Horning et. al., in 1979 used deuterium labelled and protonated forms of caffeine to show that a shift in metabolic pathways was possible by simply exchanging protons with deuterium at key positions on caffeine.

Normally, caffeine is dealkylated in the liver by microsomal cytochrome P-450 resulting in theobromine as the ultimate metabolite. Theoretically, by measuring the amount of theobromine produced the rate of caffeine metabolism can be measured. However, when deuterium was exchanged for all of caffeine's hydrogens the rate of caffeine metabolism to theobromine was doubled.

Also of interest was a change in metabolic products when only selected sites were deuterated. When only those hydrogens at the nine position methyl group where exchanged with deuterium the metabolic products were theophylline and not the expected theobromine. The amount of theophylline produced was stoichiometric with the amount of 1 position labelled caffeine utilized.

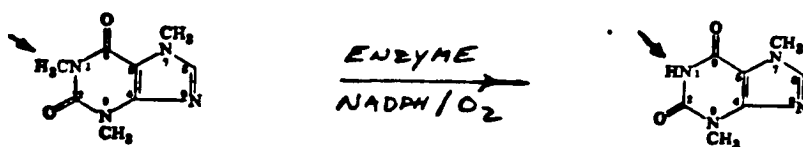


Figure 22 a: Hepatic metabolism of caffeine to theobromine.

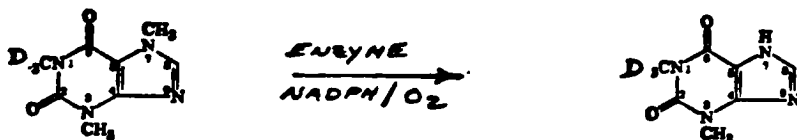


Figure 22 b: The Hepatic metabolism of 1-(d<sub>3</sub>-methyl)-caffeine to theophylline.

A similar set of experiments that illustrate the metabolic pathway shifts were done by Miwa and co-workers (1980)(74). They observed a small primary kinetic effect on  $V_{max}/K_m$  for 7-ethoxycoumarin-d<sub>2</sub> and 1,1-dimethylhydrazine-d<sub>6</sub> during oxidative dealkylation by purified cytochrome P-450 enzyme system. 7-Ethoxycoumarin-d<sub>2</sub> exhibited an isotope effect ( $k_H/k_D$ ) for  $V_{max}/K_m = 3.1$  whereas N,N-dimethylaniline exhibited an effect ( $k_H/k_D$ ) for  $V_{max}/K_m = 0.95$ .

However, when only one of the two methyl groups on 1,1-dimethylaniline was deuterium labelled the observed isotope effect ( $k_H/k_D$ ) increased,  $V_{max}/K_m = 1.6$ . They cited intramolecular methyl exchange at the enzyme site to be the cause for the effect with the loss of a methyl hydrogen as the rate limiting step.

## EXPERIMENTAL



## CHEMISTRY

### DEUTERATION OF 1,1-DIMETHYLNITROSAMINE:

Materials - The following materials were purchased from outside sources. With the exception of methylene chloride and reference 1,1-dimethylnitrosamine all materials were used without further purification:

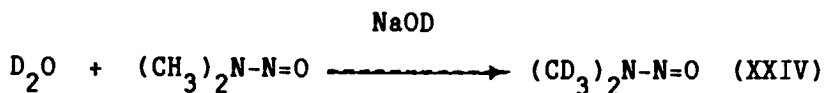
Aldrich Chemical Co.: sodium hydroxide (deuterated, NaOD; 40% in D<sub>2</sub>O)) and (gold-label) 1,1-dimethylnitrosamine.

J.T. Baker Chemical (New Jersey): deuterium oxide (99.96% D<sub>2</sub>O), methylene chloride, conc. sulfuric acid, sodium hydroxide pellets, anhydrous calcium chloride and anhydrous magnesium sulfate.

Methylene chloride was kept anhydrous by storing it in a 3 liter round bottom flask with 250 grams of CaCl<sub>2</sub>. A distillation head was attached to the holding flask to facilitate distilling fresh, dry methylene chloride when needed. 1,1-Dimethylnitrosamine was distilled through a 10 inch fractionating column packed with glass helices and collected over a boiling range of 156-157°C.

Deuterium exchange on sodium hydroxide - As an alternative to Aldrich supplied NaOD solutions, NaOD solution was made by dissolving 5 grams of NaOH in 25g of D<sub>2</sub>O. This was kept at 25°C for about an hour after which the solvent was evaporated. The deuterium treatment followed by evaporation was done four times to insure complete exchange. Deuterated NaOH was made only when needed and kept in a dessicator until used. (Keefer et. al., 1970)(75).

Deuteration of 1,1-Dimethylnitrosamine procedure - The deuteration procedure is from that used by Keefer, et al., in 1970 (75) (XXIV).



In a 300 ml round bottom flask 25 mls of 1,1-dimethylnitrosamine was added to 100 mls of (99.9%  $\text{D}_2\text{O}$ )  $\text{D}_2\text{O}$  and 15 mls of 40% NaOD in  $\text{D}_2\text{O}$ . The mixture was allowed to reflux for one hour and then cooled. The solution was slowly acidified by adding 10 mls of conc.  $\text{H}_2\text{SO}_4$  through the top of the refluxing condenser. An ice bath was used to keep the solution from boiling.

When the solution was cooled to room temperature it was decanted into a 1000 ml separatory funnel and extracted six times with 100 mls of ( $\text{CaCl}_2$  dried and freshly distilled) methylene chloride. The combined methylene chloride extracts were dried over anhydrous magnesium sulfate, then decanted into a 1000 ml single neck round bottom flask. The methylene chloride was distilled off using a 10 inch fractionating column packed with glass helices. The remaining 24 ml of yellow residue was added to a clean and dried 300 ml round bottom flask and treated to another addition of caustic deuterated water. This procedure was repeated three times.

The yellow residue at the finish of the fourth extraction clean up step was distilled in a distillation apparatus (Kontes) consisting of a single piece 50 ml pear shaped flask connected to a 5 inch fractionating column. The entire apparatus was wrapped in foil during the distillation. The collected distillate had a boiling range of 156-157°C.

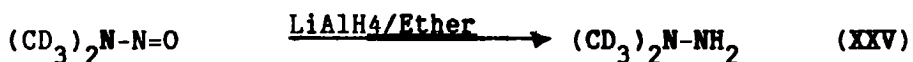
The final distillate was analyzed for purity by injecting a one microliter sample into a Perkin-Elmer Sigma 3B gas chromatograph equipped with flame ionization detector (FID) and a 6' X 1/8" ID glass column packed with 10% carbowax 20M/2% KOH on 80/100 chromsorb W AW (Supelco). Helium was used as the carrier gas and was set at a flow rate of 30 ml/min. The instrument's oven temperature was ramp programmed with a starting temperature at 70°C and a final one of 200°C. Temperature increased at a rate of 2°C per minute from 70 to 170 and 5°C per minute up to 200. Detector and injector temperatures were kept isothermal at 220°C for the entire separation. The recorder chart speed was kept at two cm per min.

Inspection for complete deuteration of the methyl hydrogens was done by mass spectroscopy at the University of Rochester, Chemistry Department (Rochester, NY). These results are discussed in the results section of this paper.

## REDUCTION OF 1,1-DIMETHYLNITROSAMINE TO 1,1-DIMETHYLHYDRAZINE:

Materials - The following materials were obtained from J.T. Baker Chemical Co. (New Jersey) and used without further purification: diethyl ether, reagent grade acetone, sodium hydroxide pellets, oxalic acid, and anhydrous ethanol. The lithium aluminum hydride and picric acid used were obtained from Aldrich Chemical Co. (Wisconsin). 1,1-Dimethylhydrazine was purchased from Eastman Kodak Chemical Co. (Rochester, New York) and was purified by fractional distillation through a 10 inch column packed with glass helices and collected at a boiling range of 62-63°C.

Reduction procedure - The procedure used in this experiment was adapted from Scheuler and Hanna's (1951)(76) method for reducing protonated nitrosamines in the presence of lithium aluminum hydride and anhydrous ether.



All glassware used during the reduction was dried in a 110°C oven for one hour. The glassware was either cooled in a desiccator or kept under NaOH dried nitrogen atmosphere for a period of fifteen minutes prior to use. A 1000 ml round bottom flask with three straight necks was used as the reduction reaction vessel. Because of diethyl ether's volatile nature it was better to add the ether to the reducing agent rather than the reverse, for this reduced the amount of foaming and loss of ether. [Safety precautions had to be taken in the form of bringing the hood's safety glass down.]

Whitish-grey  $\text{LiAlH}_4$  (25.0 g) was carefully weighed into a dry plastic weighing boat. The boat and contents were placed in a desiccator during any delays prior to the start of the reduction reaction.

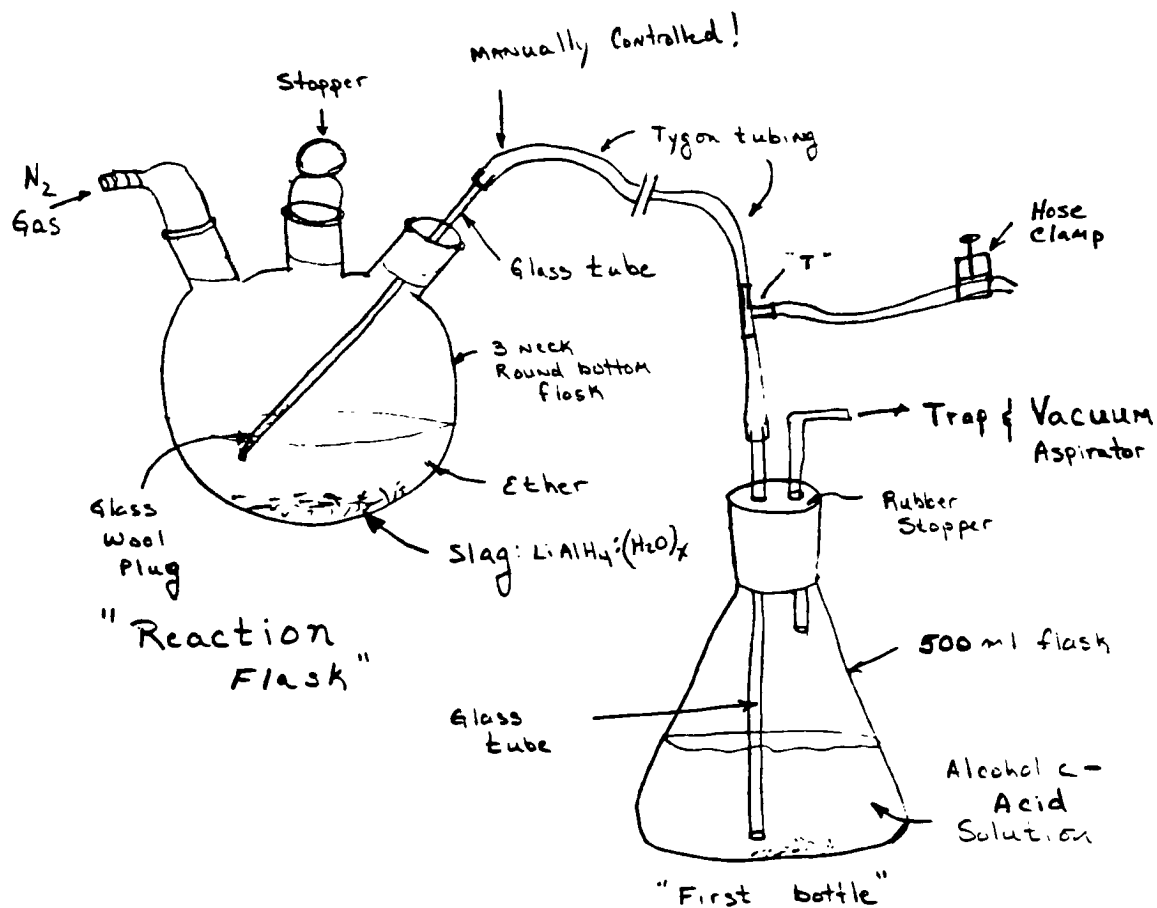


Diagram of the reaction vessel and suction-filtration bottle

To the first neck of the flask was connected a 500 ml dry ice-acetone type condenser which itself was stoppered with a  $\text{CaCl}_2$  drying tube. The center neck housed a mechanical stirrer with a teflon stirring arm. The third neck held the nitrogen inlet tube.

Prior to the start, first dry nitrogen was used to deoxygenate the flask. The nitrogen flush was used until the ether had been added after which the volatile ether prevented air from entering the flask. After fifteen minutes of  $\text{N}_2$  flush a dry ice-acetone slurry was made in a 500 ml beaker and added to the condenser. The preweighed  $\text{LiAlH}_4$  was then added to the flask followed by 250 ml of anhydrous diethyl ether (ether). Another 50 ml dose of ether was used to wash the remaining hydride residue from the weighing boat into the reaction flask. The third neck was stoppered and a heating mantle placed under the flask but not turned on!

The ether and hydride mix was gently stirred by the overhead stirrer for fifteen minutes. When the refluxing of the ether calmed the mixture was heated and boiled for 30 minutes. This refluxing step is useful for activating the hydride. Even though the ether-hydride mixture was at room temperature, the ether in the reaction flask continued to reflux, a result of the presence of active hydride. After cooling the refluxed mixture, the stopper was removed from the third neck and replaced by an oven dried 500 ml graduated equal-pressurizing addition funnel. With the addition funnel's stopcock closed, 25.00 ml of unsymmetrical dimethylnitrosamine (limiting reagent for yield calculation) and 250 ml of anhydrous ether were added to it.

Once the ether in the flask reached a constant reflux rate, the solution had to be cooled prior to the nitrosamine addition. This was done by replacing the heating mantle with an ice bath.

During this cooling stage, more dry ice/acetone slurry was made up and stored in a liter Dewar flask.

Once the refluxing had subsided to a constant rate the condenser was filled half-way with the dry ice/acetone coolant mixture and 25 ml of the diluted nitrosamine was slowly added to the flask at a rate of 1 ml per minute. The reaction had to be monitored during this addition stage and a constant level of coolant in the condenser had to be maintained throughout the experiment. Once 25 mls had been added, the stopcock was closed and the mixture gently stirred. The addition of the nitrosamine resulted in an increased evolution of gas and heat. This indicated that reaction was taking place. Ten minutes after this happened addition of the nitrosamine was resumed.

It took about an hour and a half to deliver all the ether-nitrosamine solution. Following this reaction period, the dropping funnel was rinsed with several small portions of ether and stoppered. The ice bath was removed and the reaction mixture was stirred for an additional two hours. The ice bath was replaced after the two hours and the reaction stopped by slowly adding 25 ml of ice cold distilled water. This was followed by slowly adding 25 ml of ice cold 15% aqueous NaOH. When this had been added, 75 ml of ice cold distilled water was used to further quench the reaction. The order of addition is very important for proper formation of hydrated lithium aluminum hydride crystals. If this order was not followed, the resulting hydrated lithium aluminum hydride mush would soon prove unworkable. Following this last addition of water, the mechanical stirrer was stopped and the white slag was allowed to settle to the bottom of the flask.

Because the newly-formed hydrazine would be dissolved in both the aqueous and organic layer, an extraction method had to be devised to keep the hydrazine from being air oxidized. To do this, the ether layer had to be removed and a stable hydrazine salt needed to be formed before hydrazine was air oxidized.

The addition funnel was replaced with a glass stopper while a system of three gas washing bottles was set up. All but one of the bottles were equipped with an open tube that could be submerged in an alcoholic oxalic acid solution. The third bottle was a cold finger condenser that acted as vapor trap. The tubes were connected by tygon tubing rinsed with ether prior to use and connected to a tap water aspirator. The system was connected such that the ether was bubbled through the oxalate solutions.

The ether was carefully drawn into the first wash bottle containing approximately 100 mls of 5 M oxalic acid in 95% ethanol. This first bottle was protected from the solid slag particles by a plug of glass wool in the opening of its aspirator tube. The aspirator tube was used like a drinking straw and adequately pulled the ether away from the oxidized slag mass. It was important not to aspirate any of the water into oxalate solution because oxalic acid would react with the oxidized slag. As the reaction product came over into the oxalic acid, a white precipitate immediately formed. The bottle holding the oxalic acid mix needed to be changed several times because of the large volume of ether involved in this process. The residual slag was washed five times with fresh ether and extracted using the above method. Once the acid salt of the 1,1-dimethylhydrazine was formed there was little danger of the hydrazine being oxidized to its respective tetrazine.



After the five extraction procedures, any residual hydrazine left in the hydride slag was discarded. Any unreacted nitrosamine left in the reaction mix would be carried through to the oxalic acid solution or remain behind in the hydride slag. The nice part about the oxalate salt is that it is specific for hydrazines and will not react with any residual nitrosamine.

The above reaction was attempted using the protonated form of nitrosamine. It was repeated several times using both the protonated and the deuterated forms with derivative salts being either the oxalate (mp.  $142^{\circ}\text{C}$ ) or picrate (mp =  $147^{\circ}\text{C}$ ).

Reaction Products Identification - The hydrazine-acid salts were characterized using mixed melting points. Using commercial 1,1-dimethylhydrazine, salts of 1,1-dimethylhydrazine were formed by treatment with each of the respective acids:

Hydrochloric acid salt (hygroscopic in air no melting point)(76),

Picric acid salt (lit. value mp =  $146^{\circ}\text{C}$ )(76) (actual mp = 146-147)

Oxalic acid salt (lit. value mp =  $143^{\circ}\text{C}$ )(76) (actual mp = 142-143)

Tartaric acid salt (lit. value mp =  $147^{\circ}\text{C}$ )(76) (act. mp = 145-146)

All salt derivatives were dried at room temperature and under vacuum in an apparatus equipped with paraffin wax as an organic vapor trap for protecting the vacuum pump. Mixed melting point tests were done by mixing commercial 1,1-dimethylhydrazine-oxalate salt with the reduced deuterium product-oxalate salt. No melting point depression was observed.

The oxalate salt was also checked for purity by high performance liquid chromatography (HPLC), and for degree of hydrogen exchange by infrared and mass spectroscopy.

The HPLC separation of the hydrazine from nitrosamine or tetramethyltetrazene was done on a Varian 5000 Liquid chromatograph using an isocratic solvent system consisting of 10 mM ammonium acetate in 60% methanol in water (pH 7.6) at a 1.0 ml per min flow rate. The chromatogram was obtained by measuring the absorbance of the effluent at 277 nm with time on a Varian variable wavelength UV/Vis spectrophotometric detector. The instrument was equipped with a uBondapak C<sub>18</sub>, uncapped, 30 cm X 4 mm column.

The 1,1-dimethylhydrazine-d<sub>6</sub>-oxalate salt was analyzed by mass spectroscopy at the University of Texas at Dallas , Dallas, TX by Dr. R.A. Prough. The protonated form, 1,1-dimethylhydrazine-oxalate salt was analyzed by mass spectroscopy at the University of Rochester, Rochester, NY.

Infrared analysis of nujol mol and KBr pellet of 1,1-dimethylhydrazine-d<sub>6</sub> (and H<sub>6</sub> )-oxalate salt derivatives were done on a Perkin-Elmer 257 infrared spectrophotometer equipped with diffraction grating.

Product yields were calculated by the amount of oxalate and picrate salt formed. Using commercial protonated 1,1-dimethylhydrazine, complete conversion of free hydrazine to salt was observed. Reduction product-oxalate salt accounted for an average of 48% of the added nitrosamine.

Isolation and purification of the free hydrazine product was attempted by atmospheric and vacuum distillation of the ether layer. A 3 foot fractionating column packed with glass helices was used for all distillations.

## METABOLIC STUDIES

### RAT HEPATIC MICROSOMAL CYTOCHROME P-450 STUDIES:

Materials - NADPH, NADH, DL-sodium isocitrate, isocitrate dehydrogenase (type IV), glucose oxidase (type II), catalase (from bovine liver, 10,000-25,000 u/ml), Tris(hydroxymethyl)aminomethane (Tris), glycine, 5' cAMP and ninhydrin spray were purchased from Sigma Chemical Company (St. Louis, Mo.). Carbon monoxide and nitrogen were obtained from the Linde Division, Union Carbide Corporation (New York, New York). Sodium dithionite, magnesium chloride, potassium chloride, potassium ferricyanide, potassium bromate, EDTA, formaldehyde, monomethylhydrazine, n-octylamine, 1,1,4,4-tetramethyltetrazine and N,N-dimethylaniline were obtained from Aldrich Chemical Company (Wisconsin). Ethyl acetate was purchased from J.T. Baker Chemical Company (New Jersey).

Assay of Hydrazine Concentration - Potassium ferricyanide in glycine buffer at a pH of 8.4 was reduced by either 1,1-dimethylhydrazine or its deuterated form. The stoichiometry of reduction for  $K_3Fe(CN)_6$  is twice the amount of hydrazine present. This reduction reaction was measured on a Cary 14 at 420 nm ( $\epsilon = 1.04 \text{ mM}^{-1} \text{ cm}^{-1}$ ) (Prough et al., 1981)(11) in a 3.0 ml cuvette that was thermostated at 25 °C for 30 minutes. Absorbance changes were monitored on a strip chart recorder, speed 1 in/min, with 0-0.1 A units full scale.

The reaction mixture consisted of 0.200 ml of 30 mM  $K_3Fe(CN)_6$  and 2.8 mls of 0.2 M glycine buffer solution. The remaining volume was made up with either 0.01 or 0.005 ml of approximately 25 mM hydrazine solution.

Microsome Preparation and Animal Pretreatment - Male Sprague Dawley CD rats (Charles River Laboratories, Wilmington, MA.) (200-250 gms) were maintained ad libitum on standard laboratory chow and injected i.p. with phenobarbital in 0.9% saline (80 mg/kg) daily for four days then starved 16-18 h prior to sacrifice.

This procedure was adopted from a method by Remmer et al., (1967)(25). The microsomes used in all of these experiments were prepared the livers of four phenobarbital pre-treated Sprague-Dawley rats. Their little heads were chopped off and their bodies were gently squeezed of excess blood and gutted. The livers were carefully removed with a sharp pair of surgical scissors and placed in a beaker containing ice cold sucrose buffer (0.25 M sucrose and 0.001 M EDTA solution).

After all the rats were sacrificed, the livers were removed from the buffer, quickly weighed and then placed in a volume of buffer which was four times their weight. The livers were minced by scissors, added to homogenizing tubes and homogenized with a teflon tipped homogenizer. Skill was required in passing the teflon tip through the livers without damaging them.

After four passes of the homogenizer through the tissue, the homogenates were cleared of nuclei and cellular material by pouring the homogenate into four polycarbonate tubes and centrifuging at 6000 rpm for ten minutes at 4 °C. The resultant supernatant was carefully decanted into four more polycarbonate tubes and spun at 12000 rpm at 4 °C for another ten minutes. The supernatant is decanted into two 30 ml polycarbonate, sealable, tubes with caution not to pour any of the white mitochondrial material into the bottles during this step.

The tubes were capped and spun at 108,000 rpm at 4 °C for one hour. The supernatant from this step was poured off and discarded leaving a brownish-pink pellet lining the bottom of the centrifuge tubes. This pellet was resuspended by homogenizing in a 0.1 M Tris-0.1 M KCl-0.01 M MgCl<sub>2</sub> solution, buffered at a pH of 7.6. Enough buffer solution was used to fill the tubes. The tubes were capped and spun at 40,000 rpm at 4 °C for one hour. The pellets were removed from the tubes and resuspended in fresh Tris-MgCl<sub>2</sub>-KCl buffer and refrigerated until they were used.

Determination of microsomal protein, cytochrome b<sub>5</sub> and cytochrome P-450 - Protein concentrations were estimated by the method of Lowry et al., (1951)(19). The specific amount of microsomal cytochrome b<sub>5</sub> and P-450 were calculated by a method by Omura and Sato (1964)(2). An aliquot of the stock microsomal suspension was diluted to approximately 1 mg/ml protein in 6.5 ml of Tris-MgCl<sub>2</sub>-KCl buffer solution (pH 7.6). Samples of the diluted aliquots were placed in both the reference and sample 1 cm cuvette and placed in an Aminco, model DW-2, double-beam scanning spectrophotometer (American Inst. Co. Silver Springs, Md.).

The amount of cytochrome b<sub>5</sub> was determined by difference spectroscopy by first generating a baseline indicative of equal light absorbance in both cuvettes. The cytochrome b<sub>5</sub> was reduced in the sample cuvette by adding 20 mM of NADH following the addition of an equal volume of buffer to reference cell. The difference spectrum of the reduced form minus the oxidized form of the cytochrome b<sub>5</sub> exhibited a Soret absorbance maximum at 425 nm, a minimum at 411 nm, and can be quantitated by measuring the Soret peak height relative to baseline and using a 425 minus 411 nm differential molar absorptivity of 185 mM cm<sup>-1</sup>.

The cytochrome P-450 is quantitated also by difference spectroscopy immediately following the cytochrome  $b_5$  determination by gently bubbling the sample cuvette with pure CO gas. Both cuvettes were then treated to a small scoop of sodium dithionite (5-10 grains = 0.0100 gm) and thoroughly mixed with a plastic stick. The cuvettes were again bubbled with CO gas and difference spectra recorded. The resulting difference spectrum of the CO gas-treated microsomes yields a Soret maximum at 450 nm and a minimum at 490 nm and was quantitated by using the 450 minus 490 differential molar absorptivity of  $91 \text{ mM}^{-1} \text{ cm}^{-1}$ \*.

Optical Absorbance Difference Spectroscopy - The spectral complex formed by the substrate used and cytochrome P-450 was monitored on the Aminco spectrophotometer. The reaction mixture consisted of a final volume of 6.5 ml composed of Tris- $\text{MgCl}_2$ -KCl buffer (pH 7.6), rat liver microsomal material with a final concentration of 1.0 mg protein/ml, an NADPH regeneration system (1.5 IU/ml\* isocitrate dehydrogenase, 15 mM DL-sodium isocitrate, and 1.0 mg/ml of 5'cAMP). Both the sample and reference cuvette held 2.85 ml of the above solution when the baseline was recorded in the region of 390 nm to 690 nm at a chart speed of 5.0 nm per sec. and at a sensitivity of 0.5 or 1.0. To the sample cuvette, 100  $\mu\text{l}$  of substrate was added followed by the addition of an equal volume of buffer solution to the reference cell; the resulting spectra was recorded. The reaction was initiated by the rapid addition of 10  $\mu\text{l}$  of 20 mM NADPH to both cuvettes.

Kinetic Studies - The kinetic studies were also done on the Aminco instrument and the same reaction mixture combinations, but for kinetic studies the instrument was used in the dual beam wavelength/time base mode. Reaction rates were obtained by measuring the absorbance difference between 438 nm and 510 nm using substrate volumes of 50 to 200  $\mu$ l of 25 mM hydrazine-oxalate solutions and initiated by NADPH addition. The amount of complex formed was quantitated by determining the molar absorptivity of  $115 \text{ mM}^{-1} \text{ cm}^{-1}$

Anaerobic experiments were performed by adding an oxygen scavenger system to the reaction mixture. The system consisted of 7 IU/ml glucose oxidase\* and 2 IU/ml catalase\*. This material was mixed with 1.5 IU/ml isocitric acid\* and 1.0 mg/ml 5-AMP to make a final volume of 5.5 mls diluted in Tris-MgCl<sub>2</sub>-KCl buffer. This solution was made nearly anaerobic in about 2 min. by bubbling a gentle stream of nitrogen gas through it. The gas was removed from but kept over the solution while 1.0 ml of a solution consisting of 75 mM glucose, 0.5 IU/ml (1.3 ml/100 ml buffer) isocitrate dehydrogenase, and 1.0 mg protein/ml of rat liver suspension was added and thoroughly mixed. The resultant mixture was kept under nitrogen prior to use. During the reaction, the headspace of the cuvettes were first purged with nitrogen, kept under nitrogen while the solutions were added and tightly sealed with cuvette tops and parafilm. For about two minutes before the addition of substrate or NADPH the cell compartment of the spectrophotometer was flushed with a brisk stream of nitrogen gas. Five minutes were allowed for the oxygen scavengers to do their work, from the time an addition was made to the time the binding spectra were taken.

## HYDRAZINE N-OXIDATION BY MICROSOMAL FLAVIN CONTAINING MONOOXYGENASE:

Materials - The purified flavin-containing monooxygenase (EC 1.14.13.8, dimethylaniline monooxygenase (N-oxide forming)) was provided by Drs. R.M. Hines and R.D. Prough. (The University of Texas at Dallas, Dallas, Texas.). n-Octylamine was from Aldrich Chemical Co. (Wisconsin). Buffers and other reagents were obtained from sources listed in previous section on cytochrome P-450.

Assay of Hydrazine Concentration - (See previous section on cytochrome P-450.)

Experimental Design - Assay of the stock enzyme solution's activity and all initial rate data were performed by monitoring, spectrophotometrically, the rate of NADPH oxidation at 340 nm using a Cary 14 double beam spectrophotometer (Varian Inst., Palo Alto, CA.). The spectrophotometer was equipped with a chart recorder set at a speed of 1 in/min. with a pen deflection of 0.01 absorbance units (Au) per inch (full scale = 0.1Au). All absorbance data were recorded, as the change in absorbance as a function of time (Slope = in/min). Data were later converted from inches/min to absorbance units/min. and recorded.

The instrument's cell holder was thermostated at 25 °C during all assay's. Two quartz 1.0 ml cuvettes were matched for identical optical density at 340 nm, marked as sample and reference cells and used accordingly throughout the study.



Buffer used in all assays was 1 mM Tris-EDTA buffer solution (described earlier in cytochrome P-450 section of rat microsome preparation). A 1.19 mM n-octylamine solution was made up using buffer as diluent. Final concentration of n-octylamine in the cell was 1 mM. Exact proportions for n-octylamine and buffer are listed in Table 2. Each buffer was made up as a 1 liter stock solution and refrigerated until needed. Thirty minutes prior to running any assay, a 50 ml aliquot of the buffer was incubated at 25 °C. All assays were run using the incubated buffer.

Stock solutions of 20 mM NADPH and 0.06 mg active protein/ml enzyme were made separately and refrigerated or kept on ice until used. Enzyme was made up to an enzyme content of 0.06 mg active protein/ml based on activity using 1,1-dimethylaniline as substrate and Vmax value of 950 nMoles NADPH/min/mg-protein. (See enzyme's activity assay below.) Hydrazine and 1,1-dimethylaniline solutions were made up fresh on the day of use. The hydrazine solutions were standardized daily using the above listed assay for hydrazine.

Both reference and sample cell had a total volume of 1 ml. Each held 0.840 mls of the appropriate buffer, 0.050 ml enzyme solution, and 0.010 ml 20 mM NADPH solution. An additional 0.100 ml of non-n-octylamine containing buffer was added to the reference cell in place of substrate. When necessary, additional, non-n-octylamine containing buffer was added with the substrate to bring the substrate's volume contribution of the sample cell to 0.100 ml. All reagents were mixed in the reference cell and placed in the instrument prior to sample cell work-up. A fresh reference cell was made up for each sample assay.

The order of addition of material to the sample cell was buffer and enzyme, NADPH, then substrate. Changes in absorbance due to addition of enzyme, NADPH and substrate were monitored for 3,5 and 10 minutes, respectively. The pen position was returned to the enzyme's established baseline following each addition of NADPH and substrate to the sample cell.

The substrate's actual or net absorbance change was calculated by subtracting the endogenous NADPH absorbance change from the substrate's observed absorbance change. See Table 8 a & b for specific data.

Assays of Enzyme Activity - The activity of the stock solution of enzyme was determined daily by using the above experimental design and an enzyme saturating concentration of 2.5 mM of 1,1-dimethylaniline as substrate and the appropriate buffer. (See Table 2 for cell conditions). Dimethylaniline's actual absorbance change (the net absorbance change) was used to calculate the enzyme's "active" protein content.

"Active" protein content was calculated using an absorptivity for NADPH of  $3.22 \times 10^{-3} \text{ nMoles}^{-1}\text{-cm}^{-1}$  at 340 nm and using a  $V_{\text{max}}$  value of 950 nMoles NADPH/min/mg protein for the maximal rate of oxidation due of 1,1-dimethylaniline (Prough 1981) (11). (Conditions under which  $V_{\text{max}}$  were obtained are described in Table 7 in the results section. See the results section for a sample calculation.)

Table 2: Sample and reference cell conditions for monitoring active protein content and rates of NADPH oxidation by the flavin-containing monooxygenase enzyme and suitable substrate. Cell Size: 1 ml

<u>Cell Contents:</u>	<u>Sample Cell</u>	<u>Reference Cell</u>
Buffer Solution <sup>1</sup> :	0.840 ml	0.840 ml
Enzyme:	0.050 ml	0.050 ml
NADPH:	0.010 ml	0.010 ml
Substrate Concentrations:		
A. 1,1-dimethylhydrazine-d <sub>6</sub>	0.020-0.100 ml	none
B. 1,1-dimethylhydrazine	0.020-0.100 ml	none
C. 1,1-dimethylamine	0.050 ml	none
Additional Buffer:	80-0 ul	0.100 ml
(No n-octylamine added.		
In the sample cell, this is		
dependent on substrate amount)		
:		
Total Solution volume:	1.000 ml	1.000 ml

<sup>1</sup> Buffer Solution: 1 mM Tris, 1 mM EDTA, buffered to pH 8.4 at 25 °C  
or 1.19 mM n-octylamine<sup>2</sup>, 1 mM Tris, 1 mM EDTA, buffered to pH 8.4 at  
25 °C.

<sup>2</sup> N-octylamine concentration was 1 mM in a final cell volume of 1 ml.

Initial Rates of Hydrazine N-Oxidation - Rates were measured spectrophotometrically by monitoring the oxidation of NADPH at 340 nm using the same conditions described in the experimental design section.

Manipulating the substrate concentration with buffer solution brought the final substrate's volume contribution to 0.1 ml. Substrate concentrations were for the deuterated: 0.47 to 2.35 mM and 0.38 to 1.90 mM in the presence n-octylamine. For the protonated hydrazine the concentrations were: 0.62 to 3.10 mM and 0.42 to 1.68 mM in the presence of n-octylamine. (See Table 8 a & b in the results section for actual substrate concentrations.)

Reciprocal plots of the substrate concentration verses the reciprocal of the rate of oxidation were evaluated using the Lineweaver-Burke equation. During these reactions, the amount of NADPH, and enzyme were held constant, while the substrate concentration was varied.

Quality of data was estimated with a linear regression analysis using Stat-Pro statistical software (Wadsworth Electronic Publishing, Boston, Mass.) on an Apple IIe computer, 64K, with extended 80 column text card. (Apple Computers, Inc. , 20525 Mariani Avenue, Cupertino, California, 95014.

Chemical Oxidation Procedures - 1,1,4,4-Tetramethyltetrazene was prepared by the McBride and Kruse (1957)(40) method. Potassium bromate is reduced by 1,1-dimethylhydrazine or its deuterated form, by adding 0.1 M concentration of the hydrazine and titrating it with a known amount of  $\text{KBrO}_3$  to a yellow end-point.

Hydrazine (0.77 mls of 0.1 M) was added to 10 ml of ice cold concentrated HCl in a 250 Erlenmeyer flask. The two were mixed completely with plenty of ice.

The ice-slurry was maintained at  $-10^{\circ}\text{C}$  while approx. 40 mls of 0.5 N  $\text{KBrO}_3$  was titrated to a permanent yellow end-point. Following the titration, 30 mls of 5.0 N  $\text{NaOH}$ , that was previously chilled to  $0^{\circ}\text{C}$ , was added to the titration solution to bring its pH to about 11. The resulting solution was extracted three times, each using 15 mls ethyl acetate.

The combined acetate layers were dried over anhydrous sodium sulfate, filtered, then concentrated to 1/4 the original volume via a  $\text{N}_2$  gas concentrator. The solution was analyzed by HPLC for all possible oxidation products and UV spectra for presence of tetrazene.

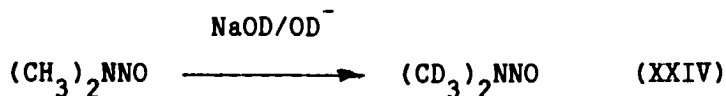
HPLC separations were done on a Waters HPLC, equipped with a Zorbax  $\text{C}_{18}$  (10  $\mu\text{m}$ , 25 cm X 4.5 mm) column and the same isocratic solvent system and other conditions described in the section detailing the purity of the 1,1-dimethylhydrazine-oxalate salt.

Enzyme Oxidation Products - Both  $\text{d}_6$  and protonated 1,1-dimethylhydrazine were used as substrates in analyzing enzyme oxidation products. Into each of two 50 ml extraction tubes was placed 0.480 ml of either  $\text{d}_6$  or protonated 1,1-dimethylhydrazine along with 2.4 ml of Tris-EDTA buffer solution, 0.150 ml of purified enzyme solution and 0.020 mls of 20 mM of NADPH solution. The resulting solution was incubated at  $25^{\circ}\text{C}$  in a shaker type water bath for one hour. Following the incubation period the solutions were extracted with three, 3 ml portions of ethyl acetate.

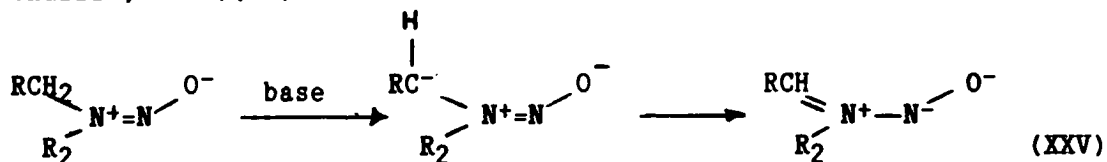
The combined acetate layers were dried over anhydrous sodium sulfate, filtered and concentrated to 1/4 the original volume via a  $\text{N}_2$  gas concentrator. The resulting concentrate was then analyzed by HPLC for all possible products using the same HPLC conditions as in the previous section.

DEUTERATION OF 1,1-DIMETHYLNITROSAMINE:

Mechanism and reaction - According to Keefer (75), exchange of hydrogens on each of the two methyl groups of 1,1-dimethylnitrosamine occurs by virtue of their relative acidities. In the reaction (XXIV) and



under alkaline conditions, N-nitroso derivatives bearing at least a primary alkyl substituent (in this case, a methyl group) will undergo hydrogen exchange at the alpha carbon atom. This exchange is subject to stereoelectronic control resulting in the formation of a corresponding carbanion (XXV). The lability of the alpha protons to exchange is attributed to the stability of this carbanion (dianion) (Challis and Challis, 1982)(76).



Slightly caustic conditions and repeating the boiling process four times will ensure complete exchange (75). A strongly alkaline solution was avoided to prevent possible hydroxylation side reactions that could result in methyl nitrosamine formation such as those in reactions XVII and XVIII.

Purity and Proof of Structure - Analysis of the exchanged material required its indentification as 1,1-dimethylnitrosamine-d<sub>6</sub> and assurance that the material produced was as pure as necessary.

Prior to any analysis, samples of purchased and exchanged 1,1-dimethylnitrosamines were each fractionally distilled and collected over a boiling range of 155-156°C.

Analysis by gas chromatography\*, gave evidence of some impurities in the exchanged form. These were identified by retention time and a standard addition method to be residual methylene chloride and impurities that were in the initial starting stock nitrosamine. Methylene chloride's (82) use as a solvent\* with lithium aluminum hydride and the extensive clean-up procedures during the hydrazine isolation process alleviated most risks in these impurities imparting any effects to the overall reduction reaction's performance.

Following the purity inspection, the process of identifying the material as fully exchanged 1,1-dimethylnitrosamine-d<sub>6</sub> was done by mass, <sup>1</sup>H-nmr and infrared spectroscopy.

The objective for using a mass spectrometer was to determine the extent of deuterium exchange. Complete deuterium exchange of the six methyl hydrogens in 1,1-dimethylnitrosamine-d<sub>6</sub> would produce a mass spectrum containing a molecular ion peak at mass 80. Similarly, the non-deuterated analog would have a mass spectrum containing a molecular ion peak at mass 74. Incomplete exchange would be apparent in the exchanged sample's spectrum by the presence of peaks in the mass range of 79 to 74.

Figure 23 a is the mass spectrum of the protonated form. The molecular ion peak at mass 74 is also the base peak, that is, it is the largest peak in the spectrum. The Table adjacent to the spectrum normalizes each peak with respect to the base peak. Figure 23b is the mass spectrum of 1,1-dimethylnitrosamine taken from the literature (78). Figure 24 is the normalized mass spectrum of the exchanged material however its base peak is at mass 28 and has a prominent peak (approx. 21%) at mass 80 with no other peaks in the mass range of 79 to 74.

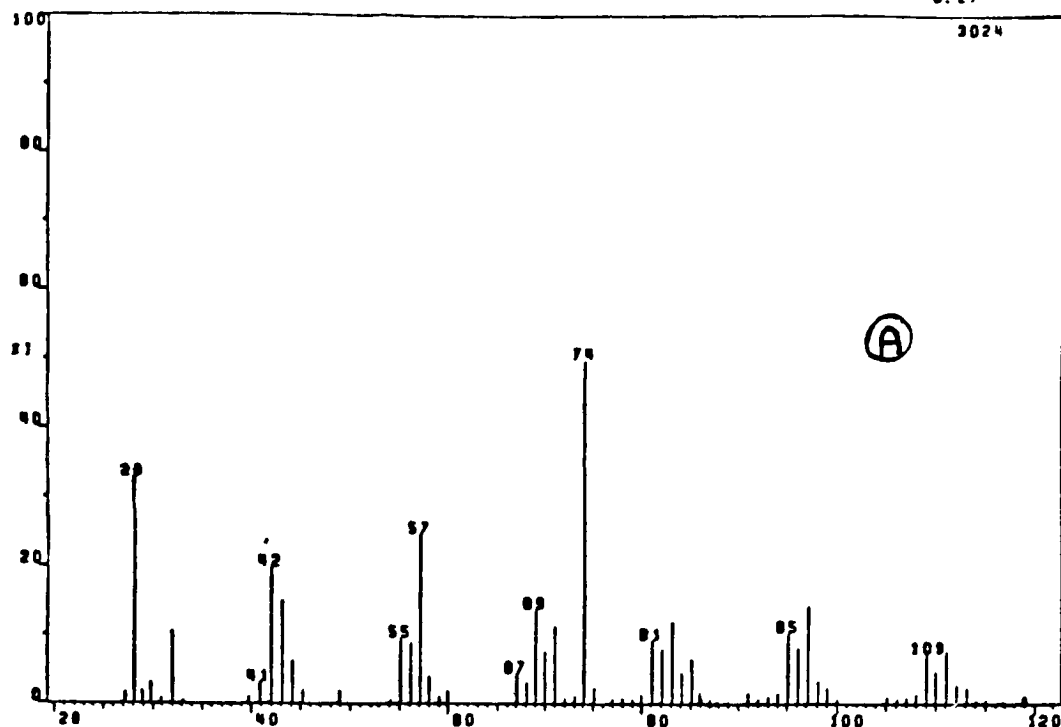
Although the peak at mass 80 was not the base peak it did indicate that a substantial portion of the material had incorporated six deuterium atoms. The sensitivity was intentionally increased to view the mass range of 79 to 74 for incomplete exchange products and none were found.

Peaks resulting from potential side reaction products, such as N-methylnitrosamine- $d_3$  (mass 63) and 1,1-dimethylamine- $d_6$  (mass 47), were also absent from the exchanged product's spectrum.

Spectra from both the exchanged and protonated nitrosamines contained prominent peaks at masses of 28, 42, 57, and 69. These peaks probably resulted from fragmentation of the molecular ion or the parent ion group,  $N-N-O^+$ . Especially prominent in both spectra is the peak at mass 28. It was probably caused by the  $N_2^+$  ion fragment. Other peaks appearing above the expected molecular mass are the result of the molecular ion fragments dimerizing in the ion beam of the instrument.

This dimerization is common in nitrosamine mass spectroscopy. Determining the composition of each of the fragments is difficult and can only be accurately decided by highly accurate mass measurements. These dimers are responsible for peaks in the spectrum ranging from two to three times the molecular weight of the nitrosamine used.





052.0 BY 0: 0127 TIC:  
CCD BASE INT.: 20004 S/S SCAN:  
SAMPLE 05

PEAK NO.	MASS	INT. BASE	PEAK NO.	MASS	INT. BASE
1	27.2	3.97	94	96.1	16.10
2	29.1	65.90	95	97.1	29.41
3	29.0	3.97	96	98.1	6.55
4	29.0	6.10	97	99.0	4.06
5	29.0	1.93	98	100.0	1.42
6	30.9	1.62	99	100.1	1.79
7	31.9	21.10	100	100.1	1.22
8	33.1	0.00	101	107.1	1.05
9	39.0	2.00	102	108.0	2.95
10	40.9	0.99	103	109.0	14.65
11	41.7	0.40	104	109.2	0.40
12	41.9	0.95	105	110.0	0.26
13	42.0	39.60	106	111.0	15.10
14	43.1	25.00	107	111.0	0.40
15	44.1	12.67	108	112.1	9.32
16	45.1	3.74	109	113.1	4.60
17	46.9	3.44	110	114.1	0.99
18	54.1	0.96	111	115.0	1.12
19	55.1	19.10	112	116.0	0.73
20	56.1	17.72	113	116.9	1.09
21	57.1	49.34	114	118.0	2.41
22	58.1	7.07	115	120.0	1.99
23	59.0	1.02			
24	59.9	3.60			
25	67.1	0.73			
26	68.0	6.79			
27	69.0	27.91			
28	70.0	19.10			
29	71.0	22.49			
30	72.1	1.99			
31	73.1	2.19			
32	74.1	100.00			
33	75.1	4.40			
34	77.1	1.09			
35	78.0	1.99			
36	79.0	1.19			
37	80.0	2.90			
38	81.0	10.39			
39	81.9	0.40			
40	82.1	19.04			
41	83.1	23.01			
42	84.1	0.96			
43	85.1	12.96			
44	85.9	3.17			
45	86.1	1.79			
46	87.0	1.32			
47	87.9	0.73			
48	89.0	0.64			
49	91.0	2.70			
50	92.0	1.32			
51	93.1	1.92			
52	94.1	2.00			
53	95.1	20.50			

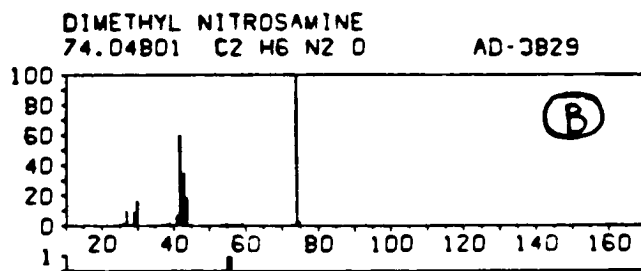
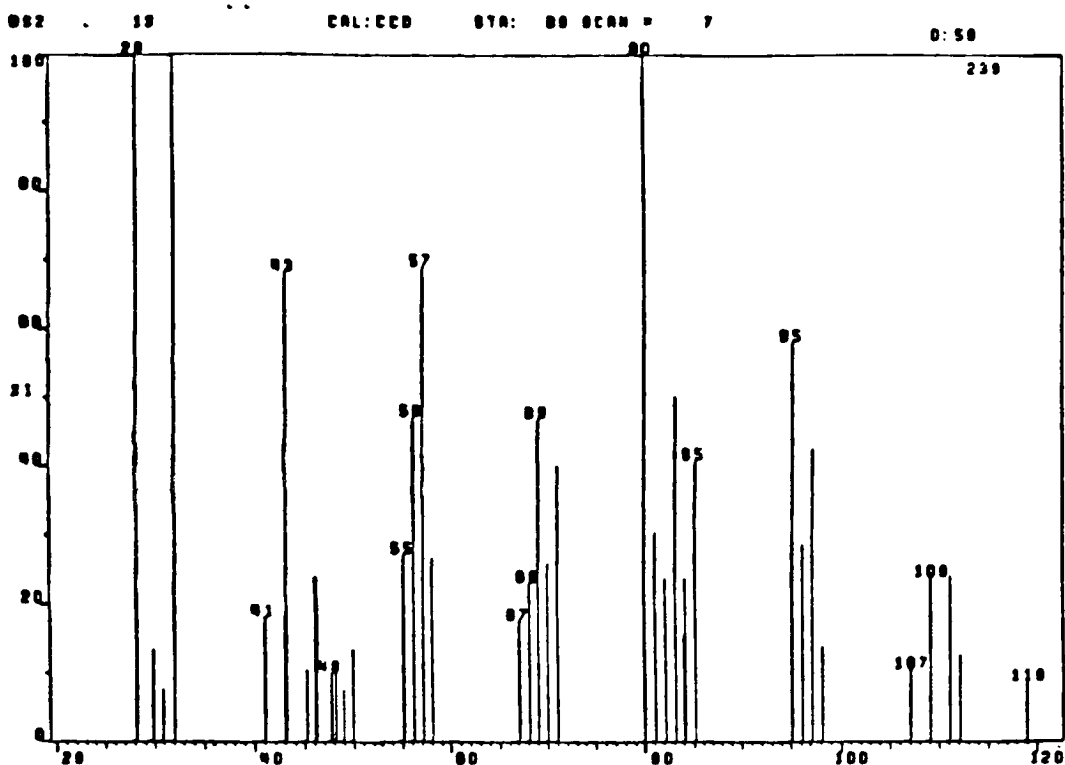


Figure 23: a. Mass spectrum of 1,1-dimethylnitrosamine.

b. Mass spectrum of 1,1-dimethylnitrosamine from the literature. (78)

CAUTION: The Table includes peak number, mass and percentage of the base peak.



052.10 DT 0: 0:  
CC3 DMAC INT

PEAK NO.	MASS	INT. PCT
1	28.1	100.00
2	29.0	2.70
3	30.9	1.06
4	31.0	20.63
5	40.9	9.73
6	43.1	9.91
7	43.1	34.19
8	43.1	9.17
9	43.1	0.00
10	47.7	0.00
11	49.1	2.43
12	49.9	1.06
13	49.9	9.70
14	55.1	9.64
15	56.1	9.91
16	57.1	14.32
17	58.1	9.06
18	67.1	9.03
19	68.0	4.77
20	69.9	9.72
21	69.9	9.80
22	71.0	9.33
23	80.0	20.73
24	81.0	0.34
25	82.1	4.95
26	83.1	10.42
27	84.0	9.21
28	84.1	4.95
29	85.1	9.91
30	95.1	12.07
31	96.1	9.09
32	97.1	0.03
33	98.1	2.06
34	107.0	2.17
35	109.0	4.95
36	111.0	9.09
37	112.1	2.60
38	119.0	1.02

Figure 24: Mass spectrum of 1,1-dimethylnitrosamine-d<sub>6</sub>.  
CAUTION: The Table includes peak number, mass and percentage of the base peak.

Typical peaks resulting from dimers are seen in both sample spectra at mass 57 and 60 (78). Unfortunately, as typical as they are, they have not been identified with great accuracy (78).

Finally, the presence of residual methylene chloride in the exchanged material may have provided peaks to the spectra which could further complicate proper identification of fragment peaks.

Proton nuclear magnetic resonance spectroscopy, ( $^1\text{H}$ -nmr) was not available prior to reduction of the nitrosamine. However a sample was kept in a freezer and examined by  $^1\text{H}$ -nmr sometime after the metabolic studies in Dallas were completed.

As noted earlier, 1,1-dimethylnitrosamine has a structure such that in a magnetic field, protons on the two methyl groups will exist as two separate sets of magnetically equivalent hydrogens. The resulting  $^1\text{H}$ -nmr spectrum of 1,1-dimethylnitrosamine will contain two equal sized peaks ( $\delta = 2.96$  and  $3.76$ ). The peak further upfield ( $\delta = 2.96$ ) or closer to a reference peak is the result of shielding (Figure 25) effects from the nitrosamine's pi bonds.

Deuterium will not display signals in  $^1\text{H}$ -nmr spectra. Therefore, the disappearance of the peaks in the  $^1\text{H}$ -nmr spectrum would establish the extent of deuterium exchange.

Figure 26 is the  $^1\text{H}$ -nmr spectrum of 1,1-dimethylnitrosamine and Figure 27 is the spectrum of the deuterated material. The protonated form has as expected two equal sized peaks at approximately  $\delta = 2.91$  and  $3.65$  ppm. Both the exchanged material and purchased nitrosamine were diluted in  $\text{DMSO-d}_6$  with TMS used as reference.

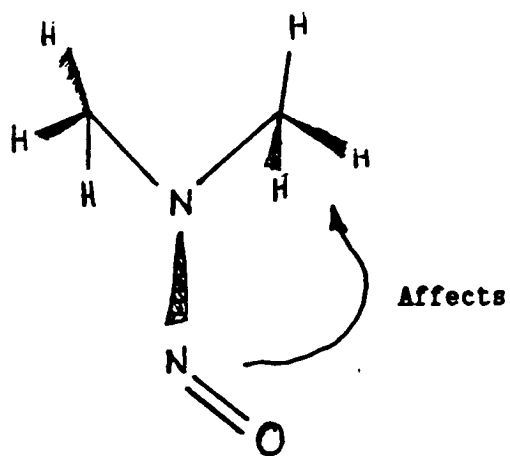


Figure 25: Proton deshielding for 1,1-dimethylnitrosamine.

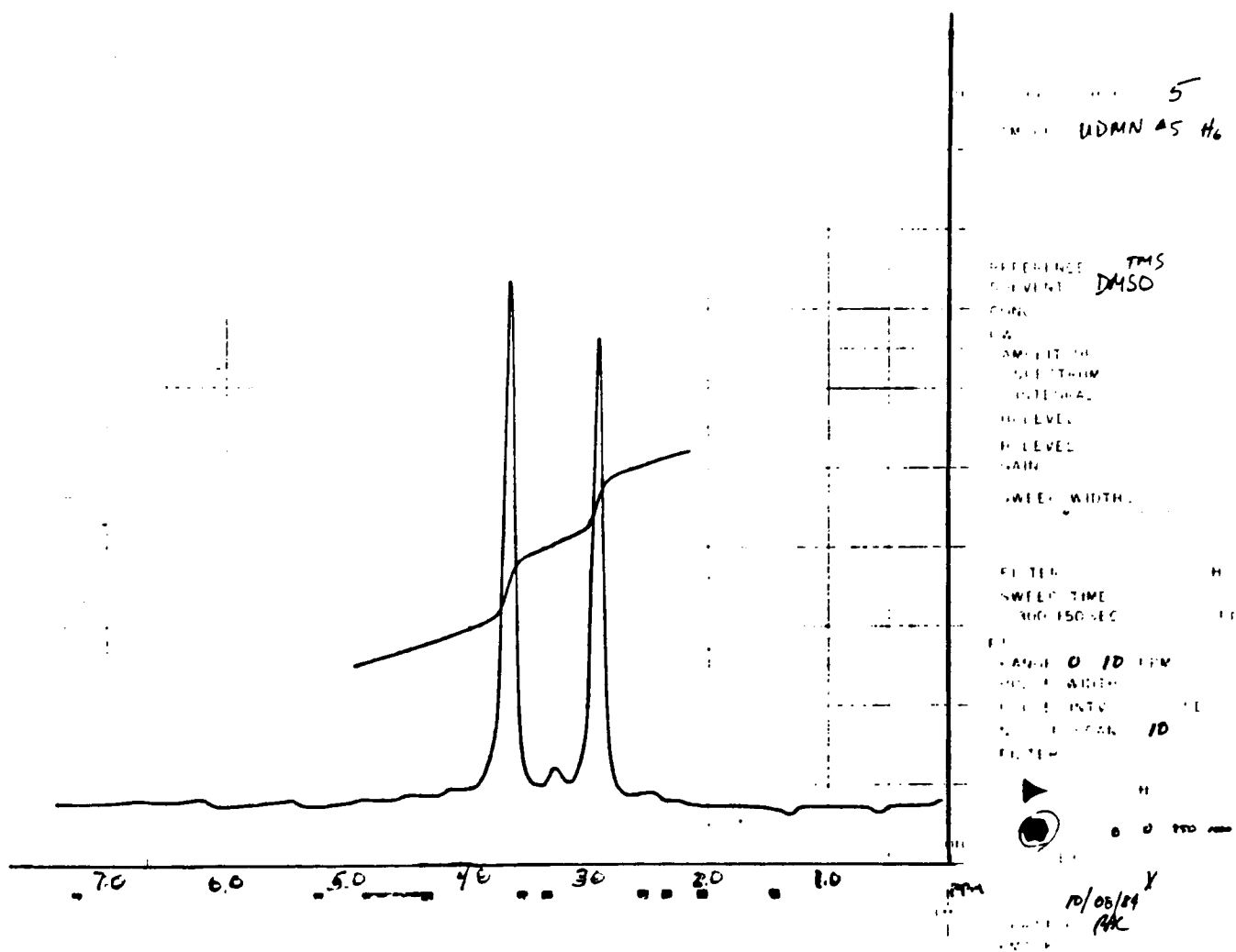


Figure 26  $^1\text{H}$ -nmr spectrum of 1,1-dimethylnitrosamine.

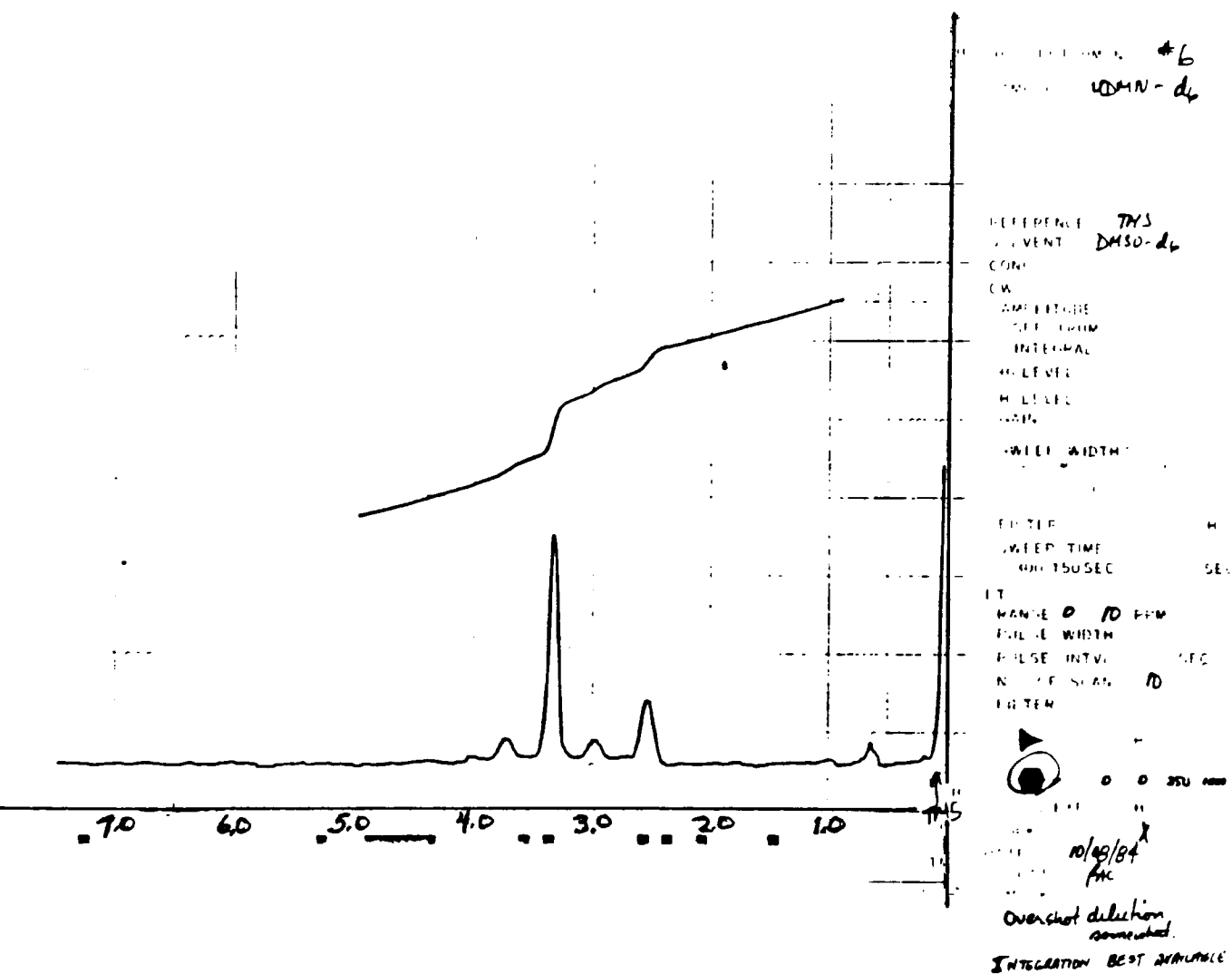


Figure 27  $^1H$ -nmr spectrum of exchanged nitrosamine (1,1-dimethylnitrosamine- $d_6$ ).

The peak positions deviated slightly from the literature values given above. Deviations were probably due to instrument to instrument variations.

Figure 27 is the spectrum of the exchanged material that contains two small peaks at  $\delta = 2.51$  and  $\delta = 3.31$  ppm. Obviously, there is still some unexchanged nitrosamine remaining.

The following attempts were made to clarify unsettling points in the  $^1\text{H}$ -nmr spectra:

1. Because methylene protons absorb far downfield from that of the nitrosamine's methyl proton's absorption region, peaks resulting from residual methylene chloride are not considered a possible cause for the protons in the exchanged product's  $^1\text{H}$ -nmr spectrum.
2. Impurities in the sample may have added to the number of protons in the sample but without proper identification and their quantification an accurate description of the role they play in providing protons cannot be done.

The presence of hydrogen on the nitrosamine, at the time the  $^1\text{H}$ -nmr spectrum was taken, would indicate that the exchange process was not complete, thus, in conflict with the results and the conclusion made from mass spectrometry. Ultimately, the material that needed to be completely exchanged and pure was the hydrazine-salt therefore the weight of this  $^1\text{H}$ -nmr data will be evaluated at the end of the hydrazine discussion.

Infrared spectra of 1,1-dimethylnitrosamine typically exhibit absorbances that are summarized in Table 3.

Table 3: Infrared spectra typical of 1,1-dimethylnitrosamine (51)

<u>ABSORBANCE MODE</u>	<u>POSITION (cm<sup>-1</sup>)</u>	<u>INTENSITY</u>
C-H stretch	2950-2900	Moderate
N-O stretch	1421-1476	Strong
N-O stretch vibration	840-875	Moderate

Infrared spectra of both deuterated and protonated 1,1-dimethylnitrosamines were produced on Perkin-Elmer 257 Grating Spectrophotometer. Referring to the spectrum in Figure 28, the medium absorbance at 2940 cm<sup>-1</sup> (A) was due to the C-H stretching. In the exchanged materials spectrum, Figure 29 The C-D stretch is apparent with a cluster of absorbances at 2250 (med.) to 2125 and 2075 (both medium) cm<sup>-1</sup> indicative of deuterium exchange.

Other absorbances typical of nitrosamines, such as the N-O stretch at 1450 cm<sup>-1</sup> and C-N stretch at 870-800 cm<sup>-1</sup> were apparent in both spectra.

According to Hooke's law, the mass difference that exists between deuterium and hydrogen would cause the deuterium's C-D stretching and bending frequencies to be reduced by a factor of 2<sup>1/2</sup>, relative to hydrogen (51). The C-H stretch is relatively weak in the IR spectrum of both 1,1-dimethylnitrosamine and respective hydrazine. An intensity reduction of 2<sup>1/2</sup> in the absorbances centered at 2200 cm<sup>-1</sup> probably results from the C-D absorbance. These weak absorbances appear as a small cluster of absorbance at 2200 cm<sup>-1</sup>.



Any infrared-sensitive functional group changes that may have occurred during the exchange process would also have been detected during this analysis.

In comparison to spectra taken from the literature, (Figure 30) (79) both the deuterated and the protonated form exhibit strong absorbances at or around  $1421\text{-}1476\text{cm}^{-1}$  due to N-O stretching. This absorbance in both spectra was good indication that the material had not undergone a reaction at the N-N-O site.



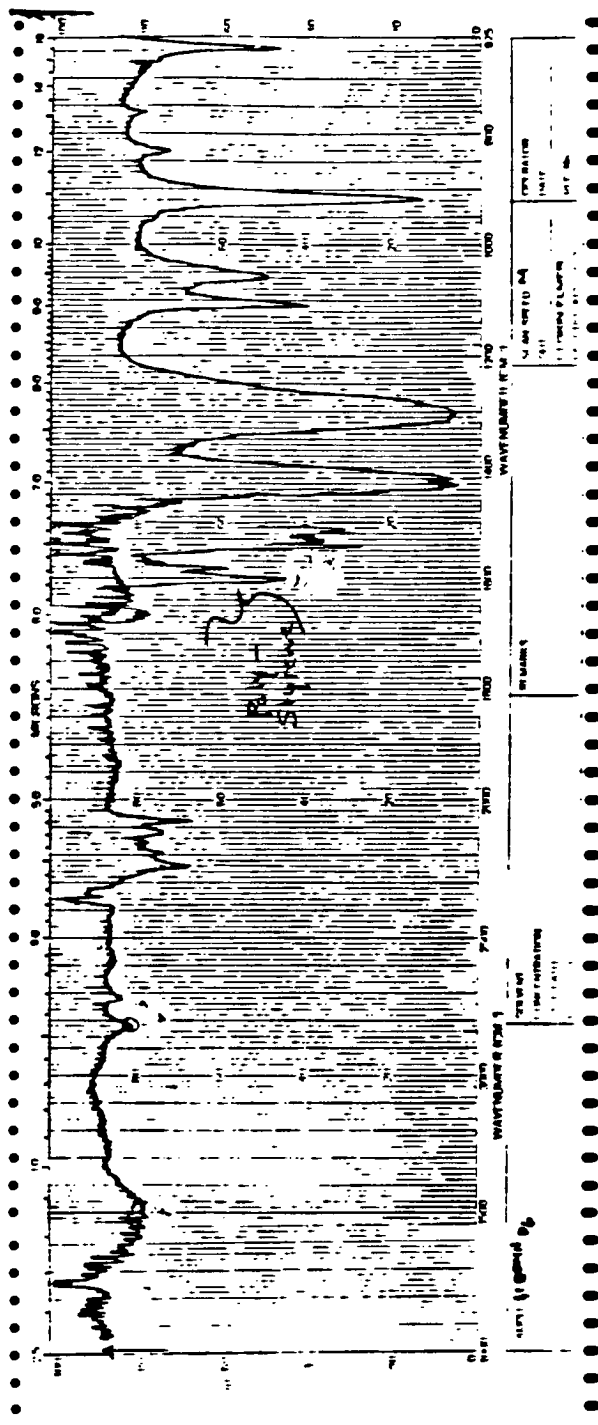


Figure 29: The IR spectrum of exchanged material. (1,1-dimethylnitrosamine- $d_6$ ), neat. (Source: experimental result)

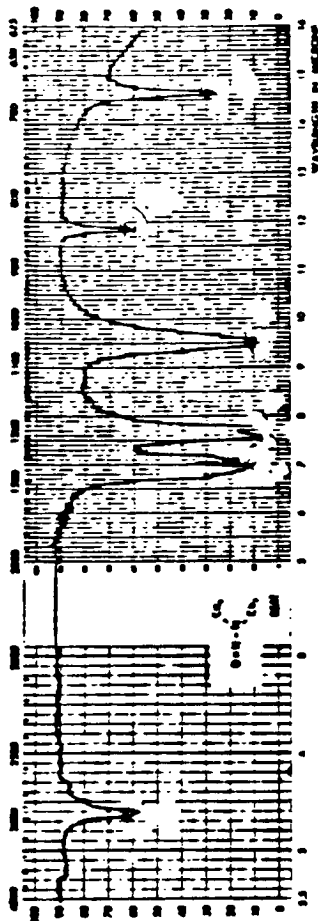
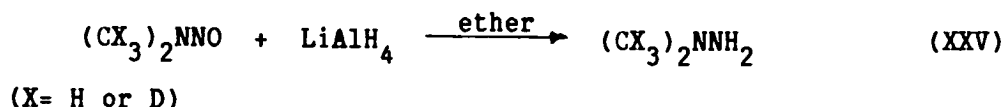


Figure 30: The IR spectrum of 1,1-dimethylnitrosamine, (Source: literature (79))

# REDUCTION OF 1,1-DIMETHYLNITROSAMINE OF 1,1-DIMETHYLHYDRAZINE:

1,1-Dimethylnitrosamine was reduced to its respective hydrazine by treating the nitrosamine with a strong reducing agent, lithium aluminum hydride in anhydrous diethyl ether (XXV).



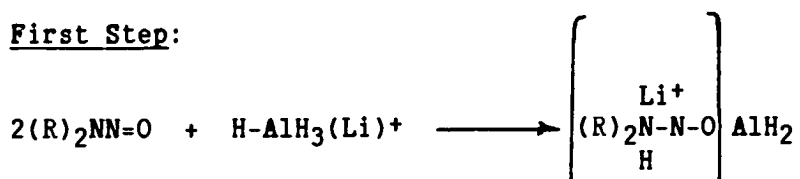
The reduction mechanism is believed to be similar to amide reductions (76,77) with ether aggregates of lithium and alumino hydride ions reacting with the nitrosamine.

Below is an outline of the reaction and some of the observations that were made during the reaction.

The first step in the reaction was the transfer of a hydride ion which resulted in forming a complex. This complex formation was readily apparent by the reaction mixture changing from a yellowish green to red in color just before a violent evolution of heat and gas occurred.

---

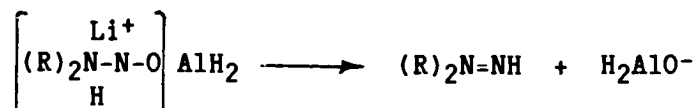
## First Step:



The second step was the decomposition of the tetrahedral complex with the elimination of  $H_2AlO^-$ .

---

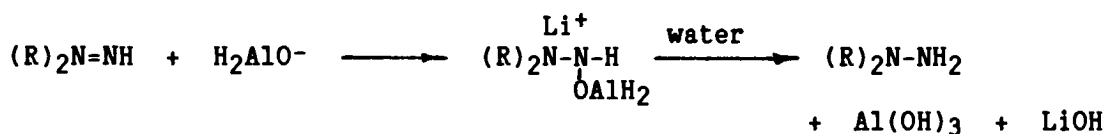
Second Step:



Addition across the N=N bond was done by another hydride ( $\text{H}_2\text{AlO}^-$ ) supplied by a second mole of  $\text{LiAlH}_4$  with the N-O bond hydrolyzed by the addition of water.

---

Third Step:



Once the reaction was quenched, material caught in the traps had to be identified.

Because of the sensitivity of the hydrazine to heat and air, it was necessary to use the hydrazine in its acid salt form. A key point in the analysis of the reduction product-salt was to identify the product as the proper hydrazine salt. The salt's purity was evaluated by mixed melting points, Thin Layer and High Performance Liquid Chromatography, TLC and HPLC, respectively.

First, purity was investigated by mixed melting point. An authentic sample of 1,1-dimethylhydrazine-oxalate salt was mixed with the prepared (reduction product) hydrazine-oxalate salt. A sharp melting point at  $142-143^\circ\text{C}$  (lit value  $143^\circ\text{C}$ )(40) was observed.

When the picrate was made its mixed melting point also showed no depression from the literature value (lit. value, 146-147°C, experimental value 146°C)(40).

These results indicate that the salts of the authentic hydrazine and those of the reduction product were of the same material. The fact that there was no melting point depression in either the picrate or the oxalate justified the use of more sensitive means of ascertaining purity.

The thin layer chromatography (TLC) procedure involved spotting a 12" X 12" TLC plate coated with silica gel (Eastman Laboratory Chemical, Rochester, NY) with monomethylhydrazine, 1,1-dimethylhydrazine, 1,1-dimethylhydrazine-oxalate salt, 1,1-dimethylnitrosamine and the reduction product salt. The solvent system, 50:50 methanol:10% oxalic acid, eluted only one spot for the reduction product and that spot had an  $R_f$  value equal to 1,1-dimethylhydrazine. Development of the chromatogram was done using ninhydrin, sulfuric acid, and an iodine chamber.

The absence of a nitrosamine, respective tetrazines or other impurities in the reaction product's TLC was good indication that oxalic acid was selective in forming a salt with only the hydrazine and that the glass wool plugs in the aspirator tubes kept the lithium aluminum hydride out of the traps.

The oxalate salt was also checked for purity by HPLC. HPLC offers the sensitivity, selectivity and reproducibility characteristic of gas chromatography with the added feature that heat sensitive materials may be easily chromatographed.

The HPLC chromatograms of both the commercial hydrazine and reduction product's salts exhibited only two peaks. These peaks corresponded to oxalic acid and hydrazine. Standard addition of impurities was used to check both the commercial hydrazine and the reduction product for unreacted or undesirable side reaction products. No undesirables were found.

In all chromatograms there was no evident peak belonging to either the nitrosamine, impurity or tetrazene even though their detection was within the limits of the instrument. Equivalent retention times of both the reaction product salt and the authentic hydrazine salt indicate both materials were identical.

Once the reduction product's purity had been evaluated, complete deuterium incorporation and retention had to be established. This analysis required the use of mass,  $^1\text{H}$ -n.m.r. and infrared spectroscopy.

Mass spectrometry was the first spectral analysis available for characterizing the reduction product's oxalate salt. Figures 31-33 are the spectra of protonated (31) and deuterated (32) hydrazine oxalate salts and the spectrum of 1,1-dimethylhydrazine (33) (Aldrich).

An important feature in all spectra is the molecular ion peak at the respective free base molecular weight. For the protonated hydrazine, this peak is at mass 60 and at mass 66 for the  $\text{d}_6$ -form. Other common prominent peaks to all spectra are summarized in Table 4.

The M-1 peak, seen in Figure 31 and 33 at mass 59, was probably caused by the loss of an alpha proton which is common for protonated alpha carbon containing amines. Analogous to the M-1 peak is the M-2 peak appearing in the deuterated material's spectrum at mass 64.



The presence of the oxalic acid in the sample makes interpreting the spectrum of the salts difficult. The oxalic acid easily fragments and obscures the fragments originating from the hydrazine(s). The free base liquid hydrazine has relatively few peaks to contend with and those peaks present are reviewed in Table 4.

Table 4: Common fragments and possible structures from Figures 31-33.

---

<u>FRAGMENT</u>	<u>MASS</u>	<u>% OF BASE PEAK</u>		
		<u>PROTONATED</u>	<u>DEUTERATED</u>	<u>PROTONATED (liq)</u>
N=N+	28	61.5	36.7	24.1
CH <sub>3</sub> -CH <sub>3</sub> +	30	100	5.5	26.5
CO <sub>2</sub> +	44	4.94	100	12.5
(CH <sub>3</sub> ) <sub>2</sub> NH+ or CO <sub>2</sub> H+	45	9.7	73.1	63.3
<sup>+</sup> CD <sub>2</sub> =N-CD <sub>3</sub> +	46	NA	78.1	NA

---

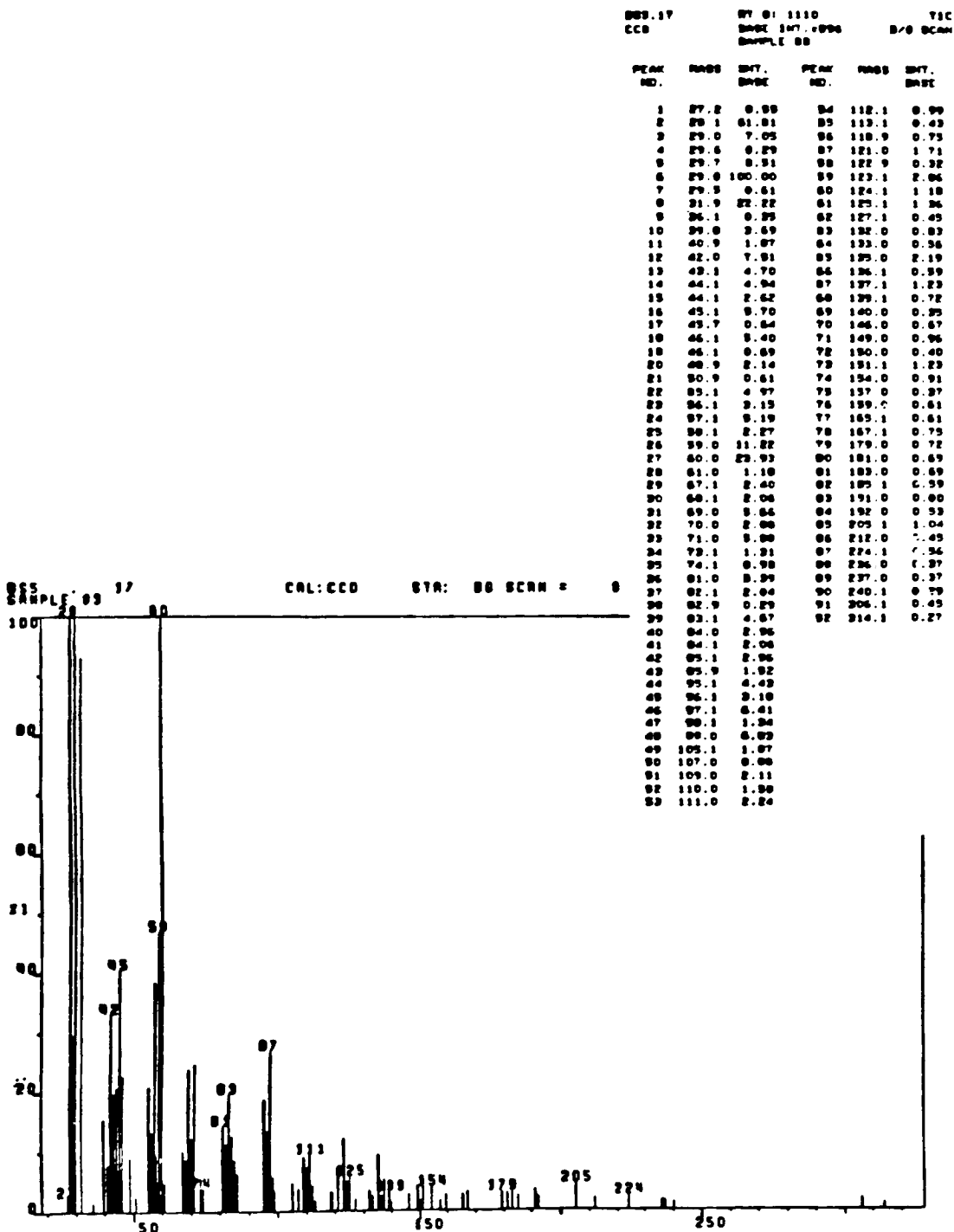


Figure 31: Mass spectrum of 1,1-dimethylhydrazine-oxalate salt

PEAK NO.	RTSS	INT. BASE	PEAK NO.	RTSS	INT. BASE	PEAK NO.	RTSS	INT. BASE
1	29.1	26.73	94	82.1	1.36	107	139.9	1.44
2	29.0	0.60	95	83.1	3.74	108	141.0	0.81
3	29.0	0.39	96	84.1	1.61	109	143.0	1.00
4	29.0	0.47	97	85.1	2.23	110	145.0	1.15
5	30.9	1.07	98	86.1	0.44	111	146.0	1.39
6	32.0	0.23	99	87.0	0.81	112	147.0	0.65
7	32.0	3.32	60	89.9	1.23	113	148.0	0.78
8	33.1	2.59	61	90.0	0.42	114	149.0	1.78
9	34.2	0.49	62	91.0	1.91	115	150.0	0.73
10	36.1	1.78	63	92.0	0.61	116	151.0	1.10
11	39.0	0.08	64	94.1	0.05	117	152.0	0.42
12	40.9	0.91	65	95.1	2.64	118	153.0	0.93
13	42.0	2.54	66	96.0	0.71	119	154.0	2.69
14	43.1	1.93	67	98.1	2.12	120	155.1	0.73
15	44.1	100.00	68	97.1	2.61	121	156.0	0.93
16	45.1	73.06	69	90.1	0.08	122	157.0	0.51
17	45.2	0.47	70	98.9	0.37	123	159.0	0.98
18	46.0	0.39	71	99.0	1.29	124	160.0	0.78
19	46.1	78.14	72	101.0	0.34	125	161.0	3.37
20	46.2	0.38	73	103.0	0.48	126	162.0	0.78
21	47.1	2.25	74	105.0	0.93	127	163.0	1.42
22	48.1	21.73	75	106.1	0.83	128	164.0	0.91
23	49.0	1.76	76	107.0	0.81	129	165.1	0.56
24	51.0	0.63	77	108.0	1.07	130	167.0	0.95
25	53.1	2.78	78	109.0	2.30	131	168.0	0.46
26	54.1	0.22	79	110.0	1.06	132	169.0	0.78
27	54.2	2.00	80	111.0	2.64	133	171.0	1.22
28	57.1	0.45	81	112.1	0.08	134	173.0	0.80
29	58.1	1.03	82	113.1	0.94	135	174.1	0.94
30	59.0	1.29	83	115.1	0.64	136	176.0	4.79
31	59.9	1.29	84	116.0	1.95	137	177.0	14.95
32	60.0	3.08	85	118.9	1.27	138	178.0	2.08
33	62.1	0.39	86	120.0	0.49	139	179.0	0.49
34	63.1	0.90	87	121.0	1.61	140	180.0	1.07
35	64.1	14.09	88	122.0	0.99	141	182.0	0.90
36	65.1	7.91	89	123.1	1.44	142	183.0	0.83
37	66.1	62.49	90	124.1	0.83	143	185.0	0.76
38	67.0	1.03	91	125.1	1.61	144	187.1	0.90
39	67.1	2.29	92	126.0	0.99	145	189.0	1.07
40	68.0	0.05	93	126.1	0.99	146	190.0	0.99
41	68.9	0.03	94	126.8	0.74	147	191.0	3.92
42	69.9	2.44	95	129.0	0.94	148	192.0	1.71
43	71.0	0.97	96	129.9	0.49	149	193.1	0.78
44	73.0	1.95	97	131.0	0.44	150	194.1	0.96
45	74.0	2.27	98	132.0	1.91	151	195.0	0.91
46	77.0	0.94	99	133.0	1.44	152	196.0	0.32
47	78.0	0.78	100	134.0	1.06	153	197.0	0.46
48	78.0	0.37	101	135.0	5.23	154	198.0	0.96
49	79.0	0.66	102	136.0	0.91	155	199.0	0.66
50	79.8	1.49	103	137.0	1.93	156	201.0	0.51
51	80.0	0.68	104	138.0	0.93	157	204.0	0.44
52	81.0	1.75	105	138.9	0.46	158	204.1	0.39
53	81.1	1.11	106	139.0	0.46	159	204.1	0.39

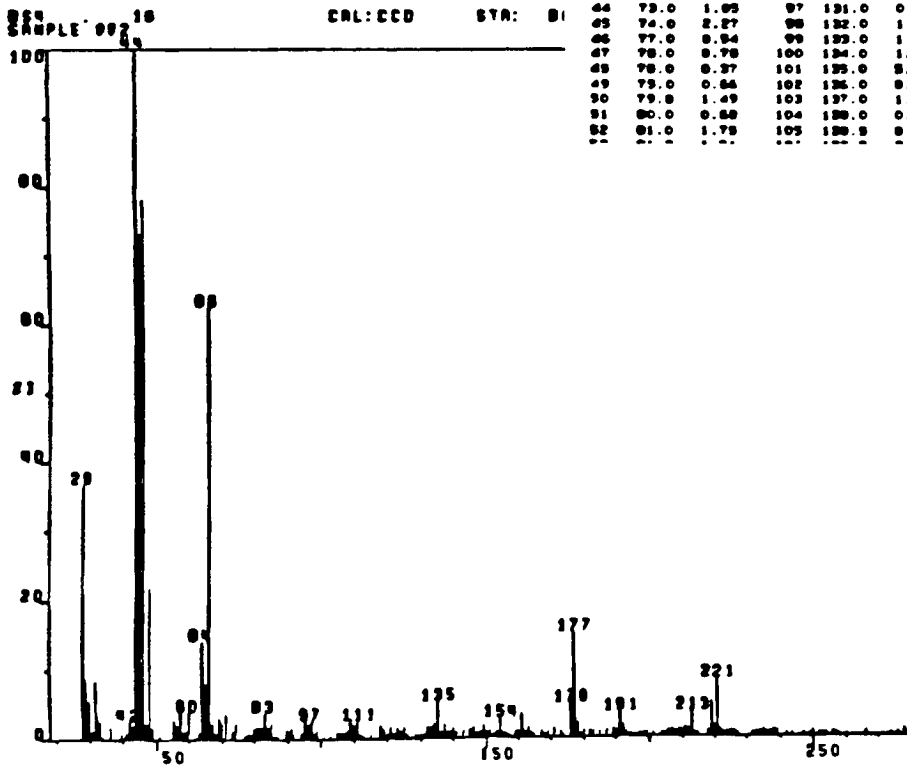


Figure 32 Mass spectrum of the reduction product (1,1-dimethylhydrazine-d<sub>6</sub>-oxalate salt).

UDMH -  $H_6$  liquid.

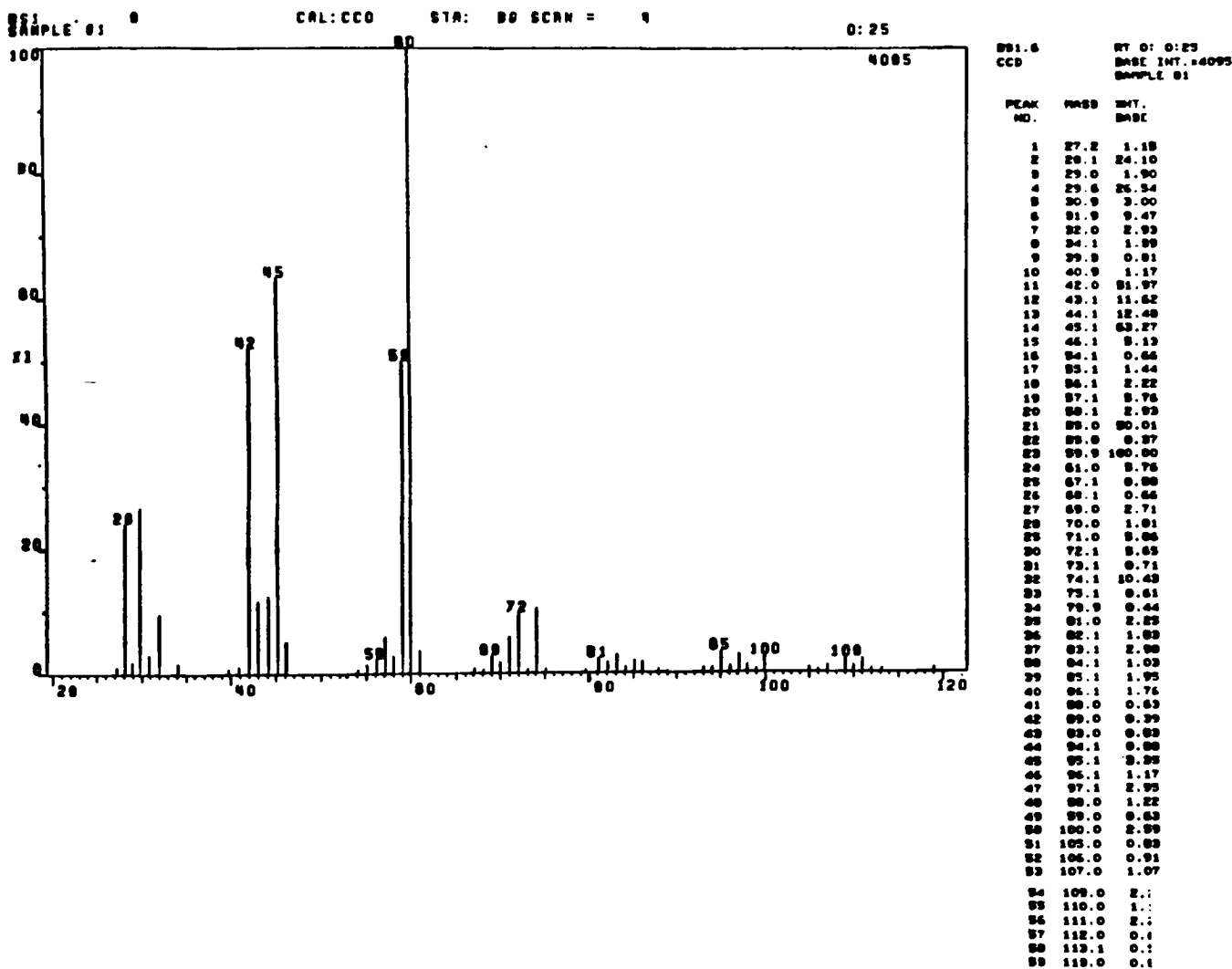


Figure 33: Mass spectrum of 1,1-dimethylhydrazine, neat, liquid.

The infrared spectra in Figures 34-36 are those of 1,1-dimethylhydrazine (neat), 1,1-dimethylhydrazine-oxalate salt and the oxalate salt of the reduction product, respectively.

Of interest in all of these spectra, particularly the reaction product's is the absence of the N=O stretch ( $1421\text{--}1476\text{ cm}^{-1}$ ).

The strong absorbance in Figure 34 at  $3100\text{--}3410\text{ cm}^{-1}$  is due to N-H stretch on the non-alkylated amine portion of the hydrazine. It appears that the N-H stretch is weakened by the presence of the oxalate in both of the oxalate salts spectra.

The strong set of bands in Figure 34 at  $2750\text{--}3000\text{ cm}^{-1}$  are due to two sets of methyl protons stretching (C-H stretching). Exchange of these protons with deuterium caused this stretching frequency to decrease. The strong band at  $1600\text{ cm}^{-1}$  is due to N-H bending or scissoring and the band at  $1450\text{ cm}^{-1}$  is the result of the dimethyl C-H bending. The band at  $800\text{ cm}^{-1}$  is possibly due to N-H wag, however, neat amine samples have the tendency to exhibit broad N-H wag absorbances.

Figures 35 and 36 are more difficult to interpret because of the oxalate's presence. In contrast to the nitrosamine analog's infrared spectra, neither of the hydrazine-oxalate salts should have the N=O str. band at  $1421\text{--}1476\text{ cm}^{-1}$ . The presence of the oxalate, however, obscures this area of the spectrum, possibly because of the carboxalate anion that accompanies salt formation.

The carboxalate characteristcally has two strong absorbances; the first absorbance band occurs at  $1650-1550\text{ cm}^{-1}$  resulting from asymetrical stretching and the a weaker second absorbance band at  $1400\text{ cm}^{-1}$ . Both of these absorption bands play a role in the band broadening in the spectra. Typically, dissolving the carboxylate in carbon tetrachloride is done to exhibit the IR spectrum but the two hydrazine salts failed to appreciably dissolve in the solvent.

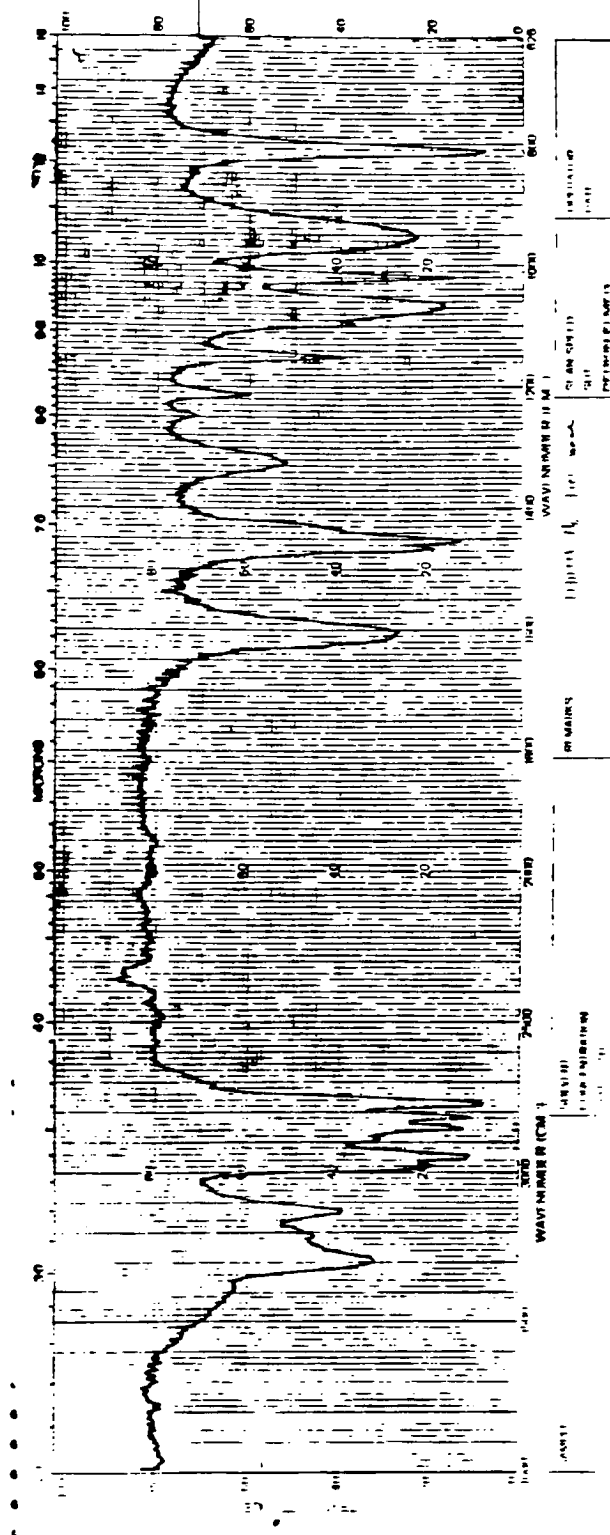


Figure 34: Infrared spectrum of 1,1-dimethylhydrazine, neat, liquid.





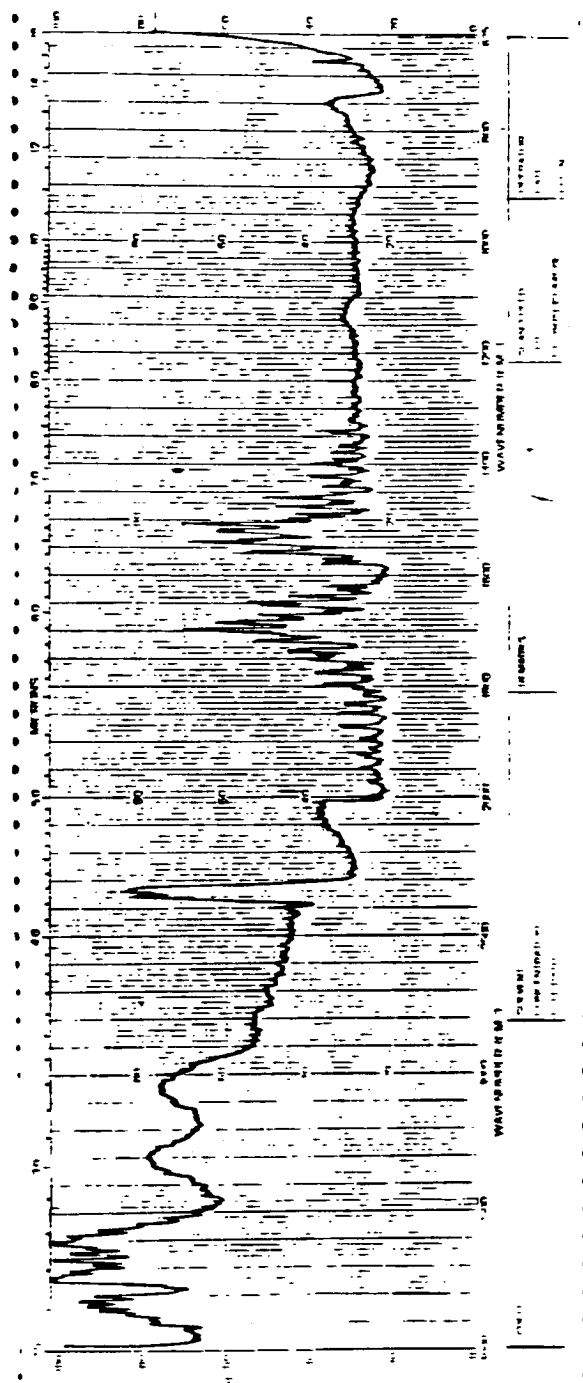


Figure 36: Infrared spectrum of reduction product (1,1-dimethylhydrazine- $d_6$ -oxalate salt) (KBr pellet).

Proton nmr spectra of oxalic acid, the free base, liquid 1,1-dimethylhydrazine, 1,1-dimethylhydrazine-oxalate salt and exchanged reduction product (1,1-dimethylhydrazine-d<sub>6</sub>-oxalate salt) are in Figures 37-40.

The salts were not soluble in any solvent except D<sub>2</sub>O which made it difficult to use TMS as an internal reference. Oxalic acid produces an <sup>1</sup>H-nmr spectrum containing one large singlet peak at  $\delta$  5.75 ppm (Figure 37) and so it was used as an internal reference when TMS was not practical.

Protonated hydrazine (diluted liquid form, Figure 38 a and b) has a large singlet peak at  $\delta$  2.28 ppm (TMS reference) due to the six magnetically equivalent dimethyl protons. The dissolved salt of the protonated hydrazine derivative, (Figure 39) also exhibits a singlet peak but it is slightly displaced downfield due to the deshielding effects by the oxalic acid.

The diluted free base 1,1-dimethylhydrazine however has a small broad peak in its spectrum at  $\delta$  3.30 ppm. This small peak is due to the two amine proton's facile exchange properties and the strong effect by the adjacent nitrogen's electrical quadripole moment. These amine protons typically exhibit a broad peak under poor resolution. However, with better resolution the broad peak is actually a series of smaller peaks. (Figure 38b, 1,1-dimethylhydrazine, <sup>1</sup>H-nmr spectrum taken from the literature), (80). Theoretically, because the oxalate hinders the amine proton's exchange, the formation of the oxalate salt should have severely broaden the two amine protons absorbance peak and pushed the peak far downfield. This may explain the absence of this peak from either Figures 39 or 40.

Both oxalate salts exhibit the large oxalic acid singlet peak and only the spectrum of 1,1-dimethylhydrazine exhibits an additional singlet peak due to the dimethyl protons. Figure 40, the deuterated form's spectrum, contains only the oxalate peak. Obviously, the chemical shift of the pure oxalate protons will be different than the chemical shift observed for an oxalate salt. The oxalate shift should however be almost the same when comparing the protonated hydrazine salt to the deuterated salt. Because of distance, physical and chemical interactions, the difference in alkyl substituents on the hydrazine will have a minor effect on oxalate's chemical shift.

These  $^1\text{H}$ -nmr spectra would indicate that the oxalate salt of the reduction product contains no protons equivalent to those of the dimethyl protons on 1,1-dimethylhydrazine.

The protons encountered in the nitrosamine  $^1\text{H}$ -nmr spectra were most likely caused by incomplete exchange. Why those incompletely exchanged nitrosamines were not reduced or recovered as incompletely exchanged hydrazine is unknown.

One possible reason for the presence of only the fully exchanged 1,1-dimethylhydrazine may be that the deuterated form is more resistant to air oxidation. Under conditions similar to the highly basic reaction quenching solution (15% NaOH), small alkyl chain length and non-branched hydrazine derivatives are easily oxidized to their respective tetrazenes. Large alkyl chains branched at the alpha carbon tend not to be as sensitive to air oxidation.

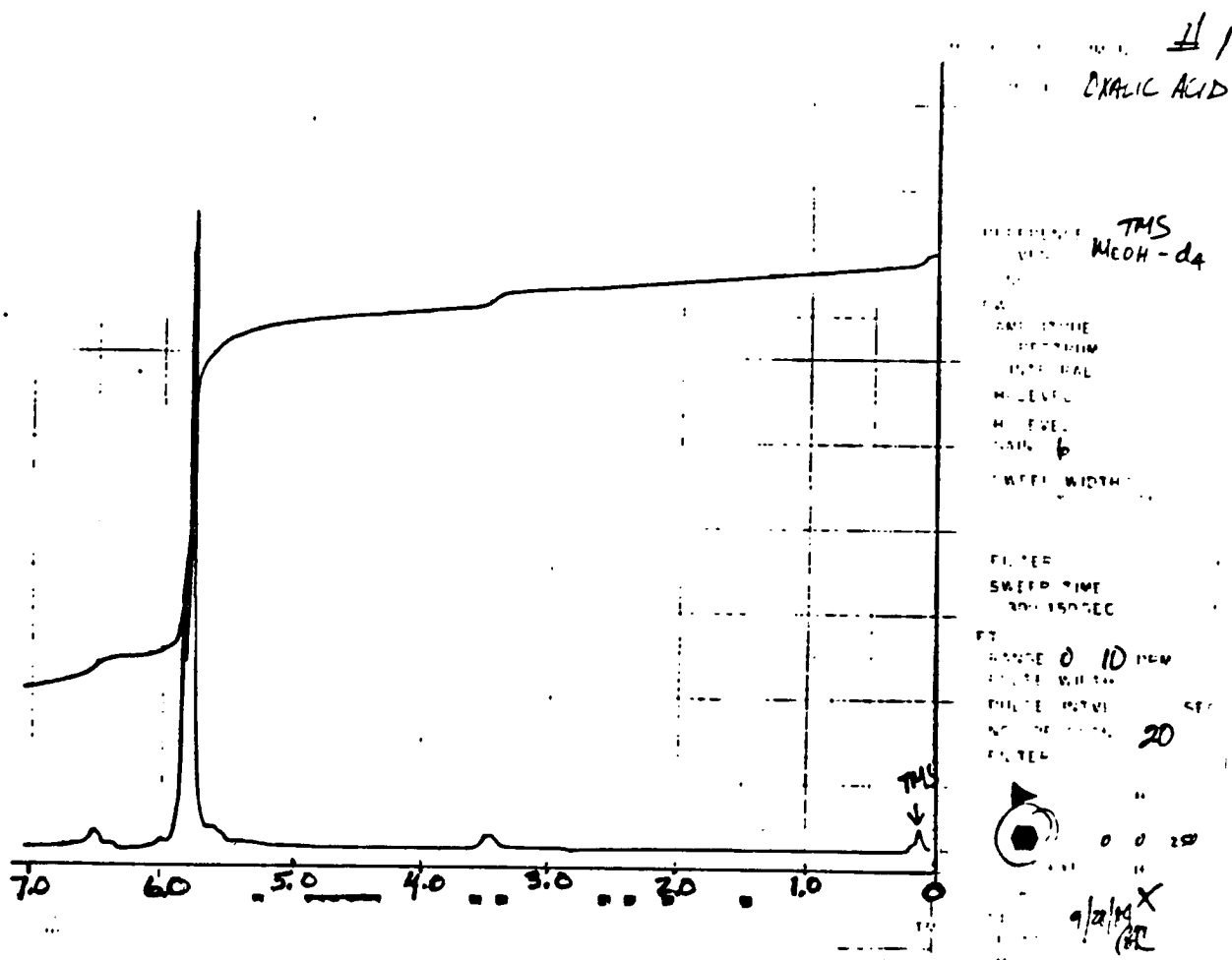
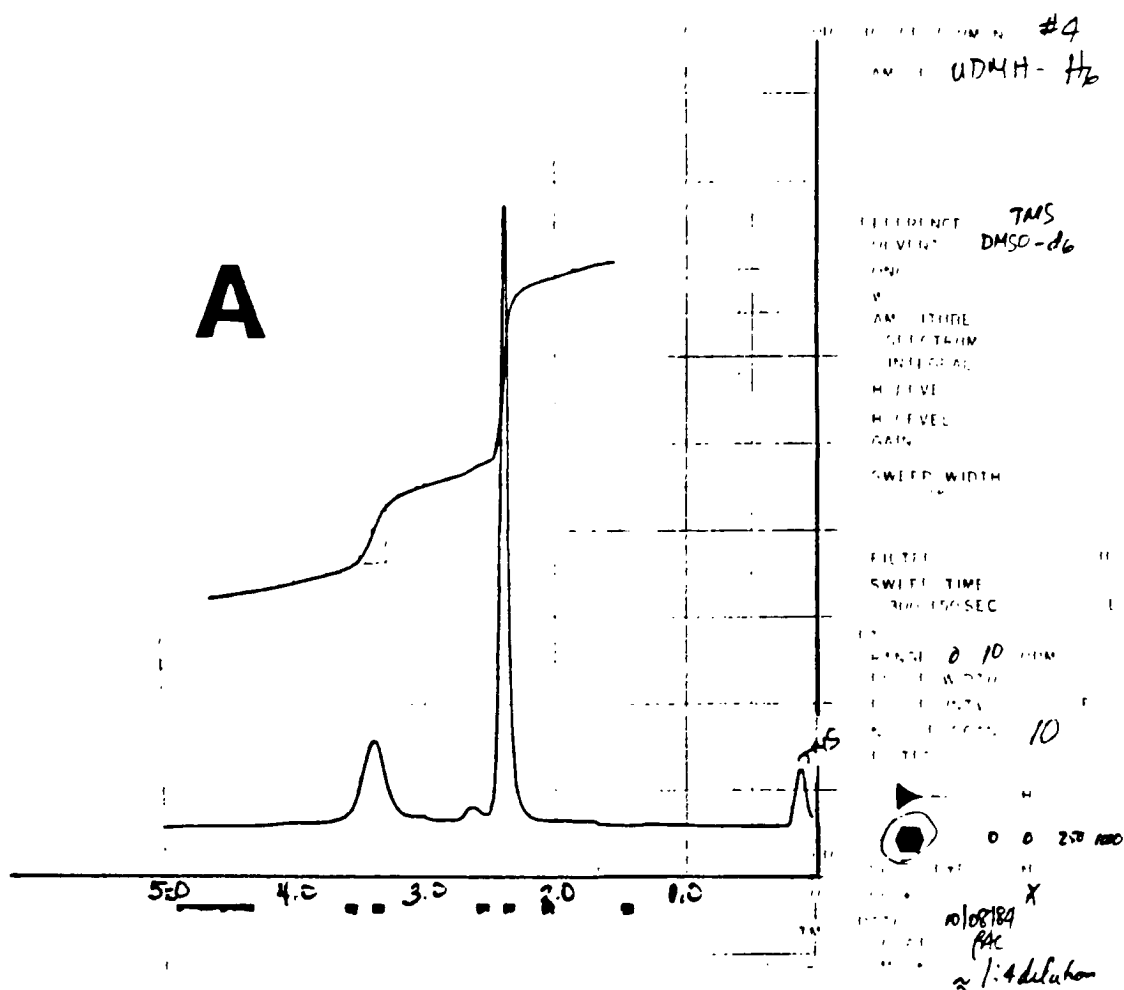


Figure 37:  $^1\text{H}$ -nmr spectrum of oxalic acid, diluted in  $\text{DMSO-d}_6$ , TMS reference.



**B**

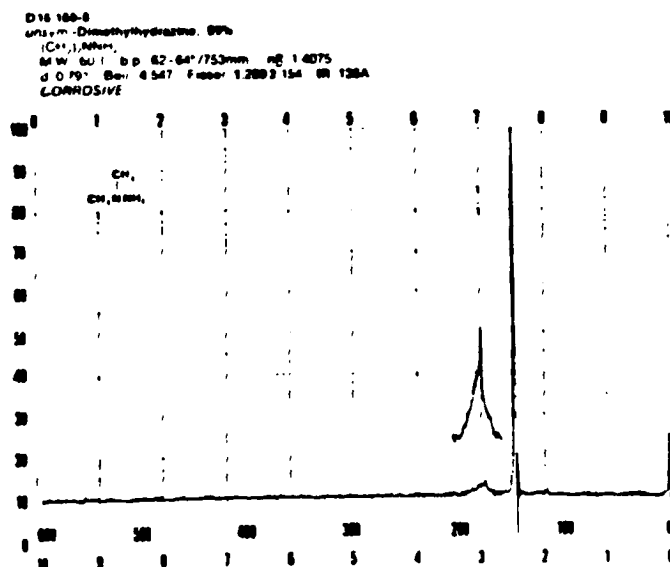


Figure 38: A. <sup>1</sup>H-nmr spectrum of 1,1-dimethylhydrazine, liquid, diluted in DMSO-d<sub>6</sub>, TMS reference.

B. <sup>1</sup>H-nmr spectrum of 1,1-dimethylhydrazine, liquid, from the literature (80).

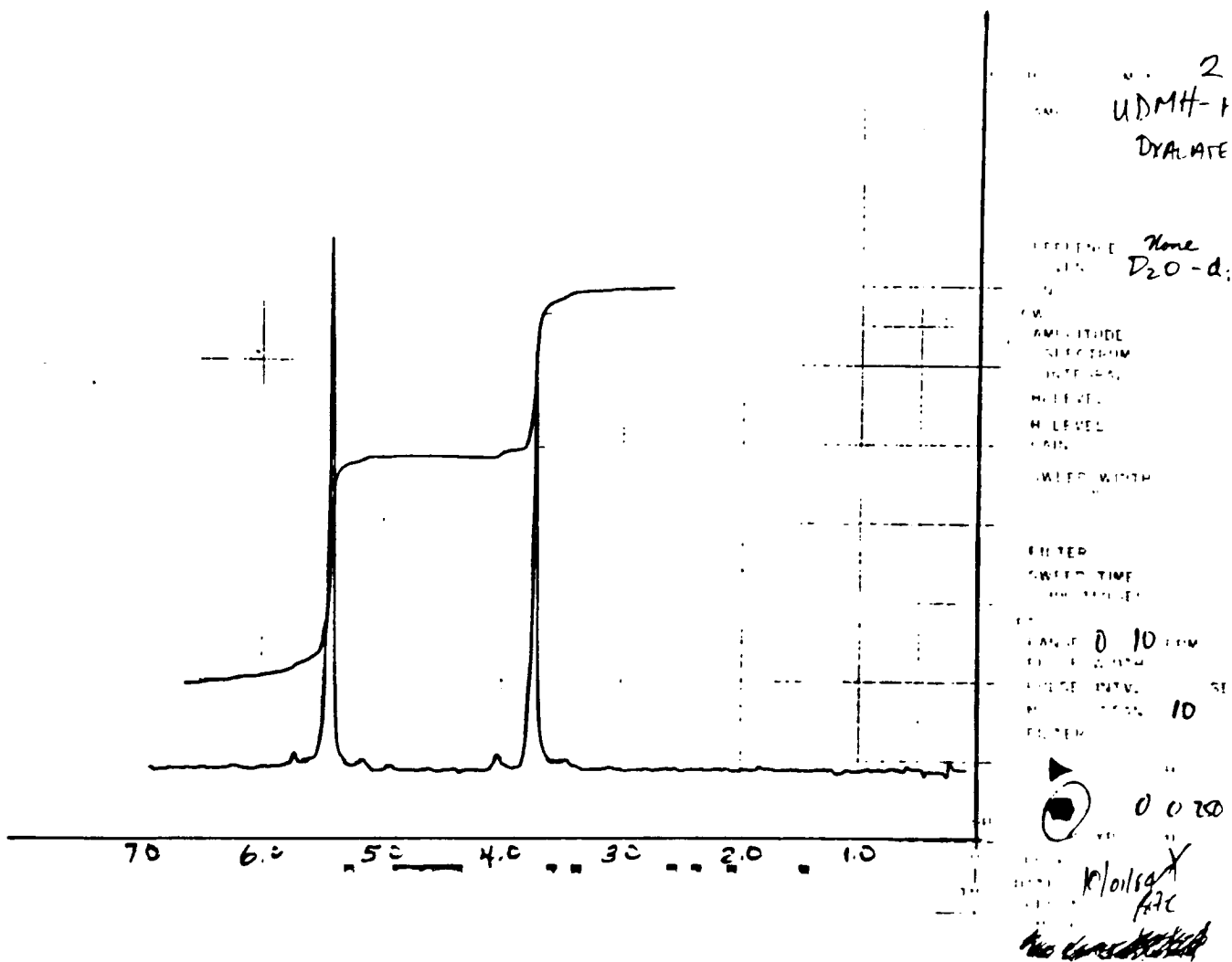


Figure 39: <sup>1</sup>H-nmr spectrum of 1,1-dimethylhydrazine-oxalate salt.  
Diluted in D<sub>2</sub>O, oxalate reference.

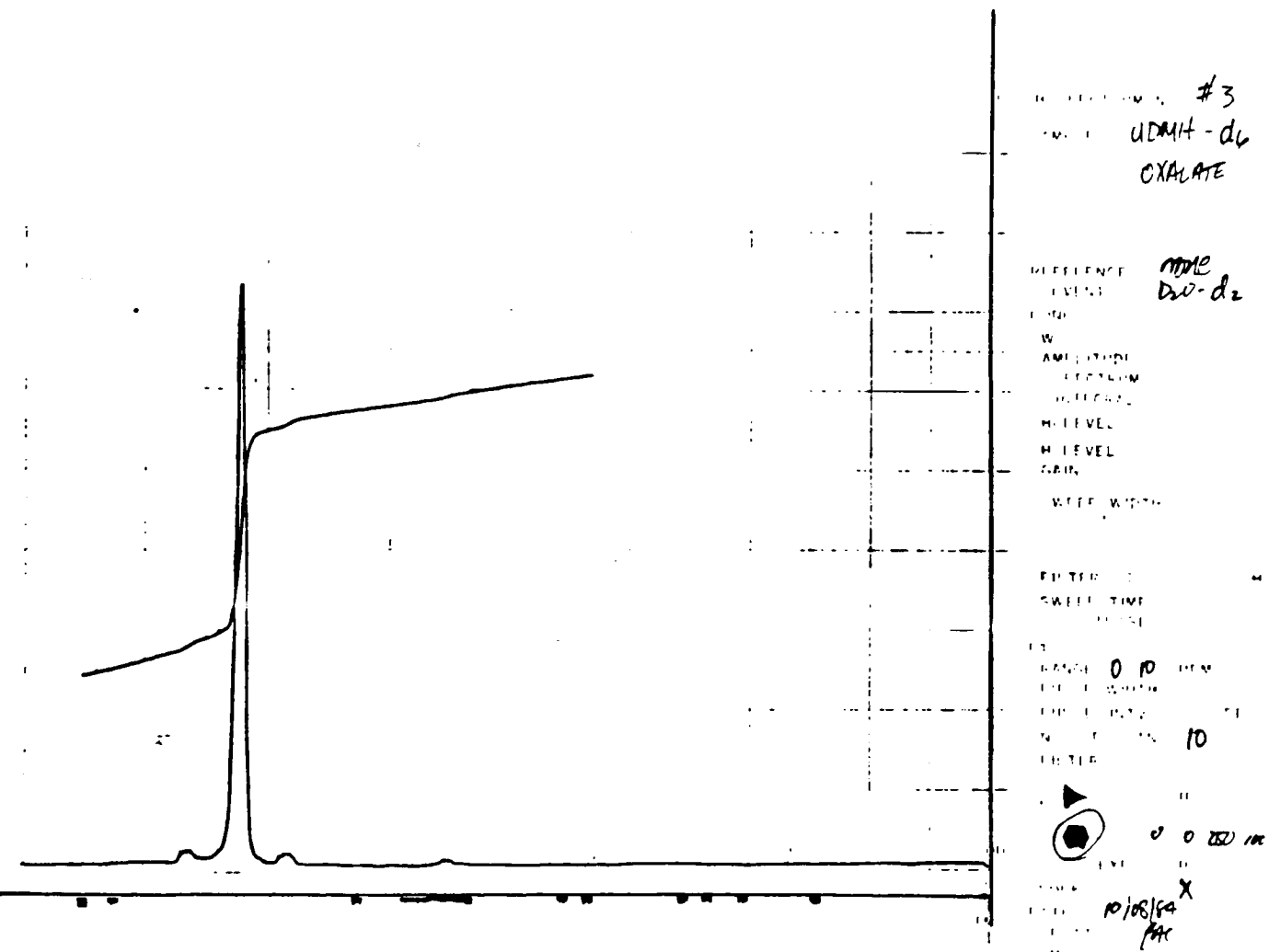


Figure 40:  $^1\text{H}$ -nmr spectrum of reduction product (1,1-dimethylhydrazine- $\text{d}_6$ -oxalate salt) . Diluted in  $\text{D}_2\text{O}$ , oxalic acid reference.

## RESULTS AND DISCUSSION SUMMARY:

From this data the following results may be considered:

1. The formation of the oxalate salt provided a specific and complete method of isolating the hydrazine product from a reaction mixture.
2. The presence of methylene chloride or other impurities in the nitrosamine distillate would not have caused an appreciable deviation in the reduction scheme.
3. From this point, on the reaction product will be considered 1,1-dimethylhydrazine-d<sub>6</sub>.

## MISCELLANEOUS:

Attempts to isolate the the exchanged hydrazine in its pure form were unsuccessful. The hydrazine co-distilled with the ether when steam and fractional distillations were tried.

The order of water-base-water (81) addition at the end of the reduction was essential for proper formation of a managable, crystalline, lithium aluminum hydride residue. If this order is not taken, the resulting material forms an ether-water suspension creating an unmanagable mess.

Centrifuging the suspension was attempted but, because of the toxicity and amount of materials used, this option was not considered practical.



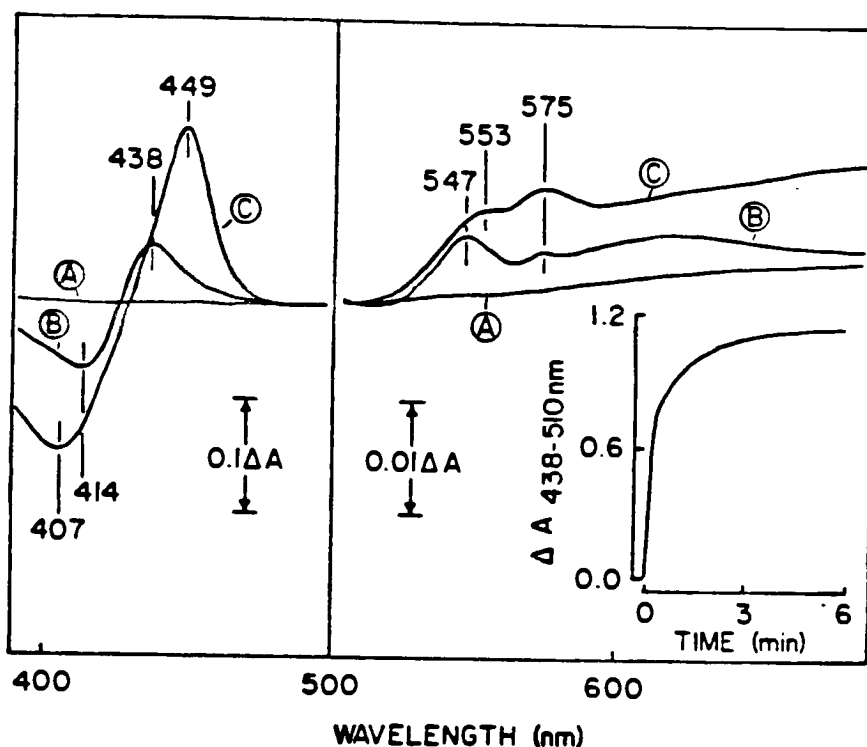
## METABOLISM STUDIES

### OXIDATION OF SUBSTRATE BY RAT LIVER MICROSOMAL CYTOCHROME P-450:

Formation of a spectral complex with the 1,1-dimethylhydrazine derivatives - Prough and co-workers (11) observed that hydrazines were effective as ligands to the heme iron of cytochrome P-450. In the absence of NADPH, disubstituted hydrazines exhibit difference absorbance spectra typical of many nitrogenous ligands to the heme iron of cytochrome P-450 (Schenkman et. al., 1967) (24).

In the presence of NADPH, and under aerobic conditions, the addition of the protonated hydrazine and 1,1-dimethylhydrazine-d<sub>6</sub>, as substrate, to the microsomal suspensions resulted in the formation of a spectral complex. This complex exhibited a concentration-dependent type II difference binding spectra (Prough (11), Figure 41 and 42 A & B). The difference absorbance spectrum, exhibited by each hydrazine derivative substrate, had a Soret absorbance transition with a maximum at 438 nm, a minimum at 414 nm, and alpha and beta absorbance transitions at 575 nm and 547 nm. These spectral properties are indicative of a low spin hemoprotein complex.

Upon standing, the Soret peak's minimum shifted to 407 nm and a bathochromic shift\* placed the maximum at 449 nm occurring with hypochromicity\* (Figure 41). This shift is typical when 1,1-dimethylhydrazine substrate-cytochrome P-450 suspensions (Prough et. al., (11)) approach anaerobiosis but, rapidly returns to the 438 form upon O<sub>2</sub> reintroduction.



Difference Absorption Spectra of the N-Aminopiperidine Metabolite Hemoprotein Complex. Microsomes prepared from phenobarbital pretreated animals were suspended in buffer containing NADPH and a NADPH-regenerating system to a final concentration of 1 mg protein per ml. The suspension was quickly divided into reference and sample cuvettes and a baseline of equal light absorbance recorded (A). Ten minutes after the addition of 1 mM N-aminopiperidine to the sample cuvette, the spectrum of the 438-nm complex was recorded (B). Both reference and sample cuvettes were depleted of oxygen as described in Experimental Procedures and the spectrum of the 449-nm complex recorded (C). In a separate experiment with the spectrophotometer in the dual wavelength/time base mode, the 438 minus 510 nm difference absorbance was measured as a function of time after the addition of 1 mM N-aminopiperidine (inset).

Figure 41: Difference absorption spectra of the N-aminopiperidine metabolite hemoprotein complex: Reprinted from Hine's Thesis. (Hines, 1980) (27)

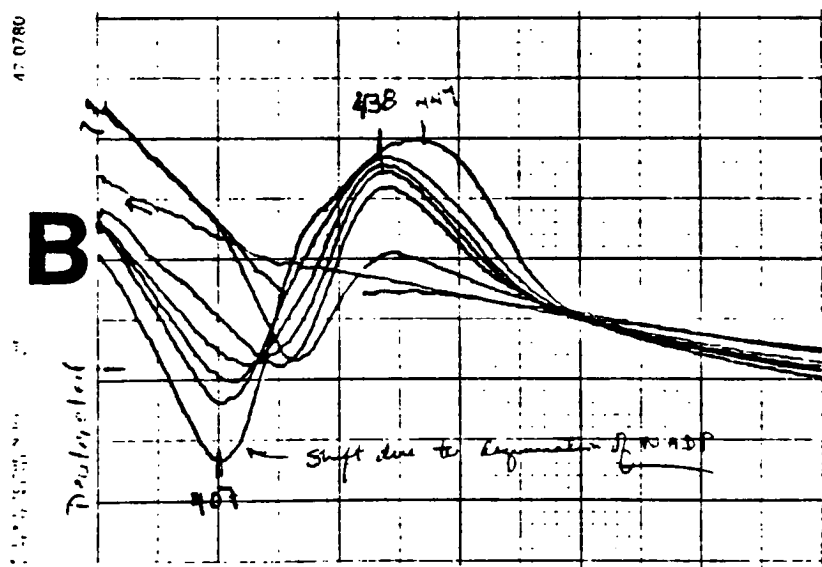
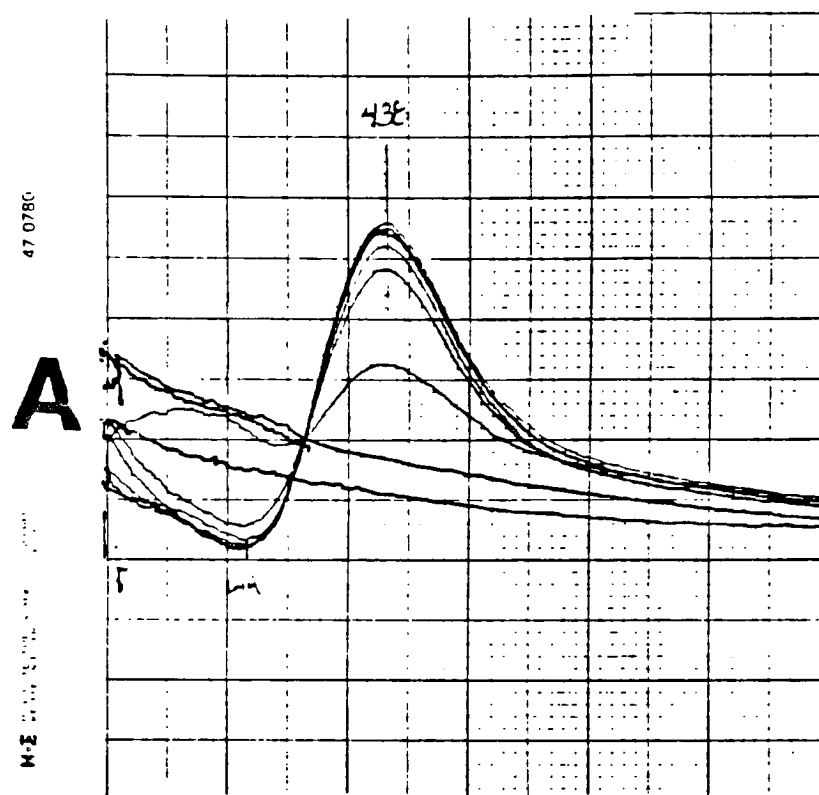


Figure 42: The difference absorbance binding spectra exhibited by cytochrome P-450 in the presence of hydrazine substrate and NADPH. A is with protonated 1,1-dimethylhydrazine as substrate and B is with the deuterated form. See experimental section for conditions.

This oxygen sensitive spectral shift is consistent with a ferric (the 438 nm-complex) to ferrous (the 449 nm-complex) transition of the heme iron to cytochrome P-450. (Prough et. al., (11)) Both exchanged and protonated 1,1-dimethylhydrazine formed the 438 nm complex and both complexes exhibited oxygen sensitivity.

When added as substrates, both the protonated and the deuterated forms of 1,1-dimethylhydrazine formed complexes that resulted in similar spectral forms of microsomal cytochromes. These spectral forms matched those observed by Prough et. al., (11) who characterized the abortive complex formed by 1,1-disubstituted hydrazines and cytochrome P-450.

The formation of the substrate induced spectral complex, using the deuterated and the protonated form, indicates that the presence of deuterium substitution does not alter the rate of formation of the metabolite-cytochrome P-450 complex. It also indicates that both substrates do reach the enzyme and that the enzyme has an affinity for both substrates.

Further work needs to be done in areas such as; characterizing cytochrome P-450's ability to function after the deuterated form is used as substrate, what metabolites are generated and what happens to the enzyme's reaction rate when inhibitors are used during rate studies.

Kinetic studies using the deuterated and protonated 1,1-dimethylhydrazine as substrate to cytochrome P-450 - The experimental conditions were carried out under optimal pH (7.6) and NADPH cuvette concentration of 0.20 mM. Both of these conditions were determined by Prough, et. al., (11). For large substituents on disubstituted hydrazines (such as N-aminopiperidine), the maximal change in absorbance requires about 5 minutes.

Experience with the two forms of 1,1-dimethylhydrazine reveals that the smaller substituents require much less time to achieve a maximum change in absorbance. Both the deuterated and the protonated form of the substrate achieved a maximum change in about one minute.

When actual kinetic studies were attempted, the speed of metabolite complex formation made measuring the initial rate impossible with the equipment available. Figures 41 (insert) and 44 A & B are examples of initial rate measurements made by plotting increases in absorbance difference between 438 and 510 nm vs time for N-aminopiperidine and for both the 1,1-dimethylhydrazine forms.

The 1,1-dimethylhydrazine substrate bound (within seconds) to the cytochrome such that the measured slope would not yield a reliable initial reaction rate. Altering the substrate, NADPH, or microsomal concentration had no effect on the initial reaction rates. Lowering the reaction temperature to 10°C did not slow the reaction enough to get a measurable initial rate.

The fact that both the deuterated and protonated hydrazine react so quickly would indicate that the presence of deuterium does not appreciably affect the enzymes affinity or the mechanism at which the substrate is transported to the enzyme.

Any observable variation in the initial rates of the metabolite-complex would have assisted in elucidating the actual mechanism for metabolite-complex formation.

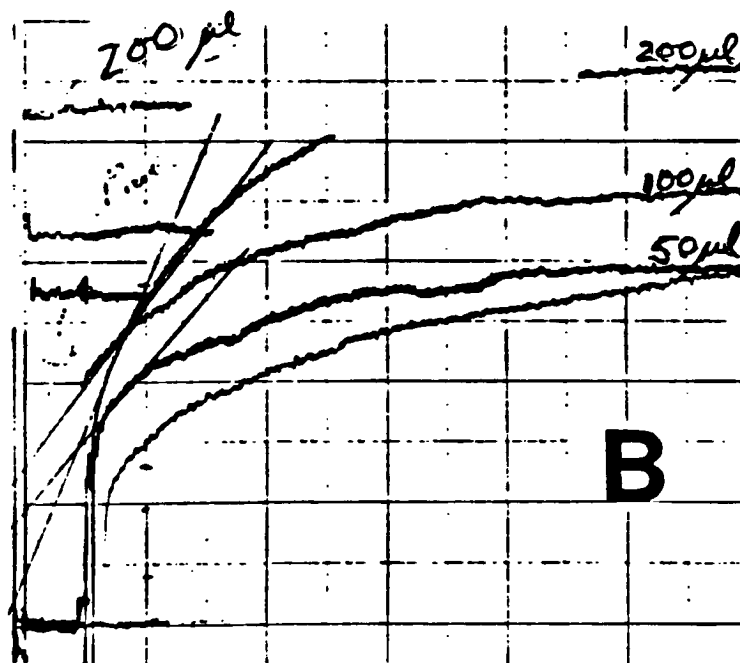
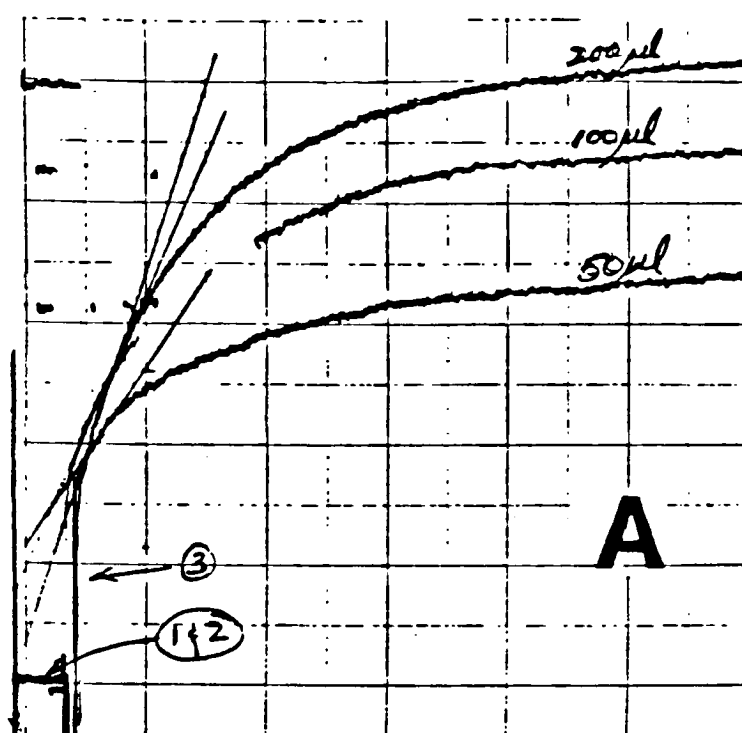


Figure 43: A&B The increase in absorbance difference between 438 and 510 nm for 1,1-dimethylhydrazine substrates. A is the protonated substrate and B is the deuterated form. (Scan rate 50 sec./in., substrate volume 50, 100 and 200  $\mu$ l. 1- Microsomal suspension only. 2- Microsomes and substrate. 3- Reaction initiated by NADPH addition.

Table 5: Hydrazine derivatives and their ability to form the 438 nm-complex  
Reprinted from Hine's thesis. (Hines, 1980)(27)

Hydrazine Derivative	$\Delta A_{438-510 \text{ nm}}^a$
<u>1,1-Disubstituted hydrazines</u>	
<u>N</u> -Aminopiperidine	0.128
<u>N</u> -Aminomorpholine	0.018
<u>N</u> -Aminohomopiperidine	0.114
<u>N</u> -Aminopyrrolidine	0.116
1-Amino-4-methylpiperidine	0.115
1-Amino-4-(8-hydroxyethyl)piperazine	0.023
1-Methyl-1-phenylhydrazine	0.024
1-Amino-2,6-dimethylpiperidine	0.056
1,1-Dimethylhydrazine	0.030

<sup>a</sup> Maximum absorbance difference seen with 1 mM hydrazine substrate. Experiments were performed with microsomes from phenobarbital-pretreated animals at a final concentration of 0.9 mg protein/ml. The abbreviation "nd" denotes the absence of any detectable spectral complex.

Table 5 provides spectral information on hydrazines when placed in aerobic microsomal suspensions containing cytochrome P-450 and NADPH. Using this Table as a guide, further attempts at using deuterated compounds for this type of kinetic work would be best done by using a deuterated form of N-aminopiperidine.

Should kinetic studies be attempted using the 1,1-dimethylhydrazine a stop flow type of spectrophotometer would probably be best suited for determining the rapid rate of complex formation.

### 1,1-Dimethylnitrosamine and cytochrome P-450 binding spectra:

1,1-Dimethylnitrosamine is believed to be an important intermediate in the oxidation of 1,1-dimethylhydrazine, if not, indeed the actual metabolite responsible for the metabolite-complex itself. Prough *et. al.*, (11) failed to show a significant level of nitrosamine content present in the reaction mixtures containing microsomal cytochrome P-450, NADPH, O<sub>2</sub> and 1,1-dimethylhydrazine.

A type I difference binding spectrum is exhibited when 1,1-dimethylnitrosamine is added to a microsomal suspension. However there is no change to the 438 nm spectral form when the reaction is repeated in the presence of NADPH or sodium dithionite under anerobic or aerobic conditions.

It was of interest then to first determine if the deuterium exchanged nitrosamine would have produced the same type I binding spectrum as its protonated analog. Second, to determine, under anaerobic conditions, cytochrome P-450's reducing agent ability. If cytochrome P-450 were to act as a reducing agent, then it is possible that the nitrosamine would be reduced to it's corresponding hydrazine. If this were true, then the in situ formed hydrazine could be metabolized to the metabolite-cytochrome P-450 complex when aerobic conditions were instituted.

In the experiment, when both the deuterated and the protonated nitrosamine were added to microsomal suspensions under anaerobic or aerobic conditions, only the type I difference binding spectrum was exhibited. Upon additon of NADPH or sodium dithionite to either anaerobic or aerobic reaction mixtures no change to the 438 nm complex was evident. There was also no apparent change to the 438 nm complex when the anerobic reaction cuvette was oxygenated.



None of the above studies provided evidence supporting the formation of nitrosamine metabolite spectral complex. It was also interesting that the expected NO binding spectra that Potter and Reed (61) observed, when they introduced 1,1-dimethylnitrosamine to anerobic microsomal suspensions of cytochrome P-450, was not observed here.

## SUBSTRATE OXIDATION BY THE FLAVIN-CONTAINING MONOOXYGENASE:

General - It has been reported that several hydrazines, particularly 1,1-dimethylhydrazine will serve nicely as substrates for the microsomal flavin-containing monooxygenase or Ziegler enzyme (11). A later study by this same group (35) characterized the N-oxidation of hydrazines by the Ziegler enzyme and found that the reaction's stoichiometry was 1:1:1 NADPH,  $O_2$  and substrate (1,1-dimethylhydrazine) with the proposed mechanism presented in Figure 44.

It was of interest then to examine the possible effects of deuterium exchanged 1,1-dimethylhydrazine on the enzyme directed reaction's initial rates. At the same time, any change in the reaction rate may be a result of a change in reaction pathway with subsequent change in products. It was also necessary to investigate any possible change in reaction products.

Prough and co-workers (11) established that the kinetic mechanism operating the monooxygenase directed oxidation of 1,1-dimethylhydrazine, in Figure 44, is a function of NADPH concentration-up to a point. Any further addition of NADPH after that point had no effect on the reaction rates. This report stressed that the rate limiting step was dependent upon both NADPH and hydrazine presence. For this reason, both the NADPH concentration (Figure 45) and the enzyme concentrations were kept constant.

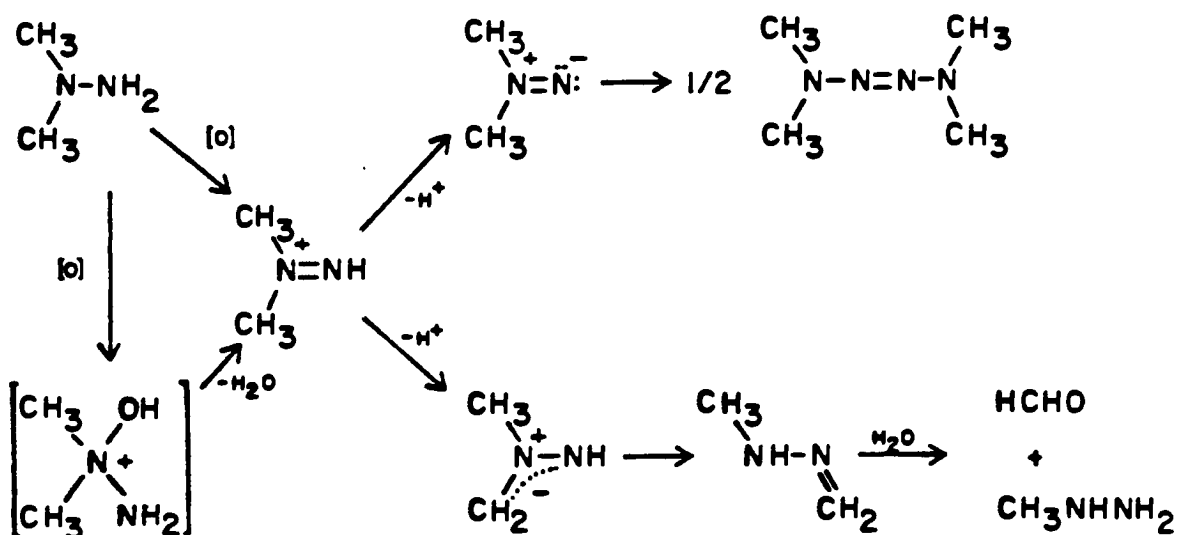


Figure 44: A generally accepted scheme of 1,1-dimethylhydrazine's microsomal directed metabolism. (Prough, 1981) (11)

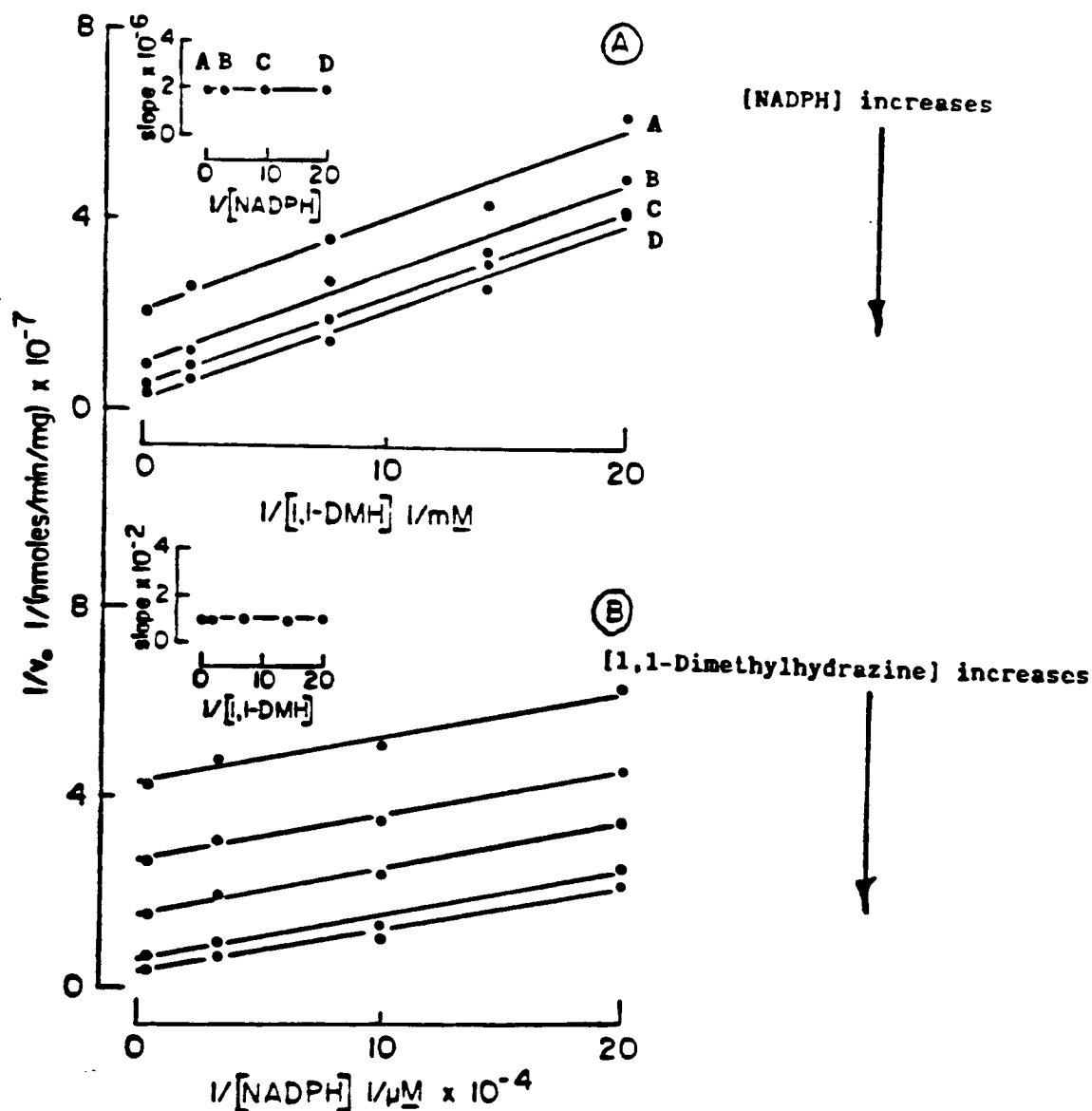
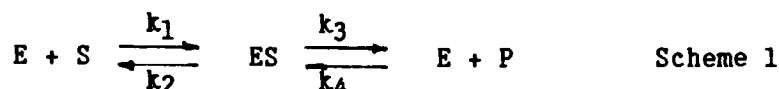


Figure 45: Kinetic analysis of the N-oxidation of 1,1-dimethylhydrazine by the flavin-containing monooxygenase: The reaction conditions were those described by Hines (27). Used 0.1 M potassium phosphate buffer (pH 7.4) at 37°C. A. Double reciprocal plots of initial rate data at 0.2 mM oxygen and variable hydrazine and fixed NADPH conc. The concentrations of NADPH from top to bottom are 5, 10, 30, and 250  $\mu\text{M}$ . B. Double reciprocal plots of initial rate data at 0.2 mM oxygen and variable NADPH and hydrazine. The hydrazine concentrations from top to bottom are 0.07, 0.13, 0.50 and 5.00 mM. Insets show replots of slope versus the concentration of the changing fixed substrate. (Reprinted from Hines Thesis (27)).

Enzyme kinetics - Scheme 1 will be used as the enzyme reaction's simplified rate mechanism. [E] and [S] represent free enzyme and substrate, respectively, which are in equilibrium, ( $k_1$  and  $k_2$ ), with the substrate-enzyme complex, ES. The rate constant,  $k_3$ , is defined as the actual or intrinsic rate constant for the formation of product and free enzyme at substrate concentrations below saturation.



Under the conditions of Scheme 1,  $K_m = [k_2 + k_3]/k_1$ .  $K_m$  is the term known as the Michaelis-Menten constant. Using the Michaelis-Menton equation (I)(83),  $K_m$  is experimentally derived as having the value of the substrate concentration at 1/2 the enzyme's maximal velocity or 1/2  $V_{max}$ . These two terms,  $K_m$  and  $V_{max}$  are important and will be used to characterize the enzyme's reaction mechanism.

$$v_o = \frac{V_{max} [S]}{K_m + [S]} \quad (I)$$

Where:  $v_o$  is the reaction's initial rate.

[S] is the substrate concentration.

$V_{max}$  is the maximum rate of reaction an enzyme may have at saturating substrate concentrations. The rate at which an enzyme reacts with a substrate, under first-order conditions and at substrate concentrations that are below that, needed to saturate the enzyme, is called the initial rate of reaction or  $v_o$ .

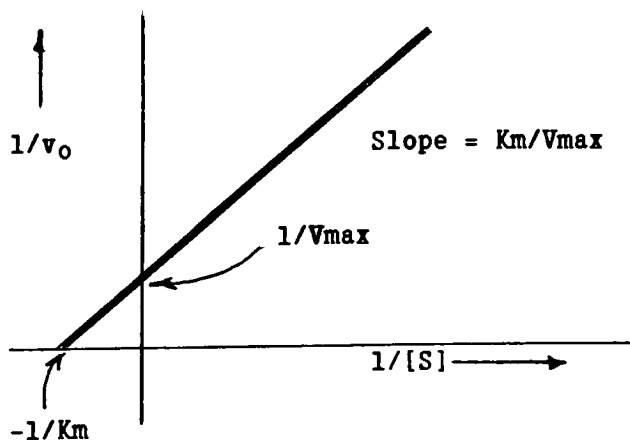
For the reaction to go to completion and substrate to be changed to product, the reverse rate constant,  $k_4$ , must be small, relative to the forward rate constant,  $k_3$ . Under these conditions the breakdown of ES to products is considered irreversible. Thus, the concentration of [ES] depends on  $k_3$ . The velocity of the reaction is then equal to the concentration of the [ES] complex and  $k_3$  or  $v_o = k_3[ES]$ .

Initial rate data or  $v_o$  may be used to calculate both  $K_m$  and  $V_{max}$ . This is easily done with the Lineweaver-Burk equation (II) which is simply an algebraic transformation of the Michaelis-Menton equation.

$$\frac{1}{v_o} = \frac{K_m}{V_{max}} \cdot \frac{1}{[S]} + \frac{1}{V_{max}} \quad (II)$$

By plotting the reciprocal value of the substrate concentration versus the reciprocal value of the respective initial rate, the slope of the resulting straight line is equal to the value of  $K_m/V_{max}$ . The plot's y-intercept is equal to the reciprocal value of  $V_{max}$  ( $1/V_{max}$ ) and the x-intercept is equal to the negative value of the reciprocal of  $K_m$  ( $-1/K_m$ ).

A double reciprocal (Lineweaver-Burk) plot:



Experimental design - In this study, the initial rates were obtained by following the change in absorbance of NADPH at a low substrate concentration and at a fixed enzyme concentration. The following will detail the steps taken to evaluate the enzyme's kinetics.

Enzyme activity and concentration - Activity of the enzyme was checked daily prior to running any hydrazine initial rate studies. Under initial rate conditions, described in the experimental section, (Table 2), 1,1-dimethylaniline (2.5 mM) was used as a substrate to test the enzyme's activity. Using dimethylaniline's net absorbance change, A, and a form of Beer's law (51)(III), the rate of NADPH consumption, c, in units of nMoles NADPH/min-ml, due to 1,1-dimethylaniline oxidation was calculated as 2.92 and 3.05 in the presence of n-octylamine. (See Table 6 A & B.)

$$c = A / e * d \quad \text{(III)}$$

$$[E] = c / V_{\max} \quad \text{(IV)}$$

Where:

c = Rate of consumption of NADPH per unit of time and volume (nMoles/min-ml)

A = Initial rate of change in absorbance (Au-min<sup>-1</sup>)

d = The cell's pathlength (1 ml cell, d = 1 cm)

e = The absorptivity of NADPH at 340 nm (6.22 X 10<sup>-3</sup> ml-nMoles<sup>-1</sup>-cm<sup>-1</sup>)

[E] = The enzyme's active protein content.

To get the enzyme solution's "active" enzyme content of 0.06 mg active protein/ml, the rate, c, was divided by 950 nMoles/min/mg-protein, the V<sub>max</sub> value for dimethylaniline, [(Prough, 1981)(11) (See Table 7 for conditions which dimethylaniline's V<sub>max</sub> was obtained)].

Dimethylaniline is a known substrate for the flavin-containing monooxygenase and is often used to check the activity of the enzyme. In this study, the activity check for the enzyme was also used to estimate the the active protein content of the enzyme solution.

Table 6: Experimental Results: Rates of NADPH oxidation by the flavin-containing monooxygenase using 1,1-dimethylaniline as substrate. Experimental conditions described in Table 2.

SUBSTRATE <sup>1</sup> [dimethylaniline] (mM)	REACTION SLOPE		RATE OF CONSUMPTION <sup>2</sup>	
	NADPH	DIMETHYLANILINE (change in absorbance/min)	NET SLOPE	NADPH (nMoles/min-ml)

A. Without n-octylamine:

2.50	0.0038	0.0220	0.0182:	2.92
------	--------	--------	---------	------

B. With n-octylamine:

2.50	0.004	0.0230	0.019:	3.05
------	-------	--------	--------	------

1 Stock solution of 1,1-dimethylaniline was 50 mM. Used 0.05 ml in 1 ml cell.

2 Consumption is based on the absorptivity of NADPH of  $6.22 \times 10^{-3}$  ml nMol<sup>-1</sup> cm<sup>-1</sup> at 340 nm and equation III on previous page.



Table 7: Michaelis-Menten parameters for selected hydrazine compounds and the flavin-containing monooxygenase enzyme. (Prough (11))

Substrate <sup>a</sup>	$K_m$ mM	$V_{max}$ <sup>b</sup> nmol/min/mg
Dimethylaniline	0.02	950
Methylhydrazine	35.0	1370
Ethylhydrazine	40.0	1350
n-Propylhydrazine	15.0	1520
Isopropylhydrazine	8.3	803
Butylhydrazine	6.9	1480
Phenylhydrazine	3.0	890
Benzylhydrazine	7.0	880
1,2-Dimethylhydrazine	12.0	644
1-Methyl-2-benzylhydrazine	2.0	1260
Procarbazine	5.7	560
$\beta$ -Ethylphenylhydrazine	3.3	1250
1,1-Dimethylhydrazine	0.43	890
1-Methyl-1-phenylhydrazine	0.08	1130
1,2-Dimethylphenylhydrazine	0.38	895
N-Aminopyrrolidine	0.10	960
N-Aminomorpholine	0.61	950
N-Aminopiperidine	0.03	960
N-Aminohomopiperidine	0.17	878

<sup>a</sup> Nonsubstrates: Carbidopa, Hydralazine, Isoniazide, Iproniazide, and Isocarboxazide.

<sup>b</sup> Experiments were performed using purified monooxygenase in 0.05 M Tricine buffer, pH 8.2, at 37 °C.

Because of the differences in this study's conditions and those described in Table 7, a certain element of error may be introduced to the calculated value of the initial rate,  $v_o$ , (in Table 8 a & b) and other values calculated which have mg protein as units (i.e.  $V_{max}$  values). This error; however, will not have any effect on the magnitude of observed differences, if any, when comparing initial rates of deuterated and non-deuterated oxidation.

The absorbance data, for both the enzyme protein content and initial rates, were collected in units of inches/min directly from the chart paper. The absorbance data reported in Table 8 a & b have been converted to absorbance units/min. or Au/min. by using a full scale absorbance value of 0.1 Au at a chart speed of 1 inch per minute. Measurements were done over the specified time(s) outlined in the experimental section. When these times were used, the change in absorbance was linear and easily measured.

Initial rates of substrate metabolic oxidation,  $v_o$  - The experimentally determined initial rates for 1,1-dimethylhydrazine and 1,1-dimethylhydrazine- $d_6$  were determined by first calculating the sample cell's NADPH concentration change as a function of time,  $c$ , (equation I) with respect to a specific substrate concentration. This concentration change was then divided by the sample cell's active enzyme content,  $[E]$ . The active protein content used was 0.003 mg protein/ ml [ (0.06 mg/ml for the stock solution) multiplied by, 0.05 ml used in the sample cell, which was then diluted to 1 ml.]

Table 8a: Experimental Results: Rates of NADPH oxidation by the flavin-containing monooxygenase enzyme using 1,1-dimethylhydrazine-d<sub>6</sub> and 1,1-dimethylhydrazine as substrate without n-octylamine in the buffer solution. Experimental conditions described in Table 2.

SUBSTRATE <sup>1</sup> [hydrazine] (mM)	REACTION SLOPE			RATE OF CONSUMPTION <sup>2</sup> NADPH (nMoles/min/mg)
	NADPH (change in absorbance/min)	HYDRAZINE (change in absorbance/min)	NET SLOPE	
<u>1. 1,1-dimethylhydrazine-d<sub>6</sub> as substrate:</u>				
2.35	0.0035	0.026	0.0225	1206
1.18	0.0035	0.021	0.0175	938
0.94	0.0033	0.020	0.0167	894
0.71	0.0040	0.0195	0.0155	831
0.58	0.0040	0.017	0.0130	697
0.47	0.0030	0.014	0.0110	589
<u>2. 1,1-dimethylhydrazine as substrate:</u>				
3.10	0.0040	0.0213	0.0173	927
2.48	0.0030	0.0160	0.0130	697
1.86	0.0032	0.0160	0.0128	686
1.55	0.0035	0.0150	0.0115	616
1.24	0.0035	0.0126	0.0091	487
0.93	0.0030	0.0113	0.0083	445
0.62	0.0035	0.0100	0.0065	348

<sup>1</sup> Stock solution of hydrazine used:  
deuterated: 19.0 mM  
non-deuterated: 21.0 mM

<sup>2</sup> Consumption is based on the absorptivity of NADPH of  $6.22 \times 10^{-3}$  ml nMol<sup>-1</sup> cm<sup>-1</sup> at 340 nm and using approx. 0.003 mg/ml active protein for the enzyme concentration.

Table 8b: Experimental Results: Rates of NADPH oxidation by the flavin-containing monooxygenase enzyme using 1,1-dimethylhydrazine-d<sub>6</sub> and 1,1-dimethylhydrazine as substrate with n-octylamine in the buffer solution. Experimental conditions described in Table 2.

SUBSTRATE <sup>1</sup> [hydrazine] (mM)	REACTION SLOPE			RATE OF CONSUMPTION <sup>2</sup> NADPH (nMoles/min/mg)
	NADPH (change in absorbance/min)	HYDRAZINE	NET SLOPE	
<u>1. 1,1-dimethylhydrazine-d<sub>6</sub> as substrate:</u>				
1.90	0.004	0.025	0.021	1125
1.50	0.004	0.021	0.017	911
0.95	0.004	0.020	0.016	857
0.65	0.003	0.016	0.013	697
0.38	0.0035	0.013	0.009	482
<u>2. 1,1-dimethylhydrazine as substrate:</u>				
1.68	0.004	0.0175	0.0135	723
1.36	0.004	0.0165	0.0125	670
0.73	0.004	0.0130	0.0090	482
0.42	0.004	0.0100	0.0060	322

<sup>1</sup> Stock solution of hydrazine used:  
deuterated: 23.5 mM  
non-deuterated: 31.0 mM

<sup>2</sup> Consumption is based on the absorptivity of NADPH of  $6.22 \times 10^{-3}$  ml nMol<sup>-1</sup> cm<sup>-1</sup> at 340 nm and using approx. 0.003 mg/ml active protein for the enzyme concentration.

Lineweaver-Burk plots were constructed from the reciprocal values of the reaction's initial rates,  $1/v_0$ , vs the reciprocal value of the substrate concentration in the sample cell,  $1/[S]$ . These reciprocals are listed in Table 9. Lineweaver-Burk plots of the data are exhibited in Figure 46 a & b.

The slope and y-intercept were determined from the data in Table 9 using a statistical linear regression package from Stat-Pro. (The functional slopes and intercepts were used from Stat-Pro's linear regression).

The slope and y-intercept were then applied to the Lineweaver-Burk equation, yielding the values of:

1.  $-1/K_m$  from the x-intercept.
2.  $1/V_{max}$  from the y-intercept.
3.  $K_m/V_{max}$  from the slope

Table 10 summarizes these Michaelis-Menten parameters ( $K_m$ ,  $V_{max}$  and  $V_{max}/K_m$ ).

Standard deviations, ( $SD_I$ 's), for the intercept values were calculated in the regression analysis. The intercept's standard deviation,  $SD_I$ , comes from the reciprocal value's average standard deviation. The Michaelis-Menten parameter's standard deviations,  $SD_M$ , were calculated from the intercept's standard deviation ( $SD_I$ ), using equations V and VI.

$$P = SD_I / \text{Intercept} \quad (V)$$

$$SD_M = P * M \quad (VI)$$

Where:

- $SD_I$  - The standard deviation for the intercept value.
- $M$  - The respective intercept's Michaelis-Menten parameter
- $SD_M$  - The standard deviation for the respective intercept's Michaelis-Menten Parameter

Table 9: Experimental Results: Rates of NADPH oxidation by the flavin-containing monooxygenase using 1,1-dimethylhydrazine-d<sub>6</sub> and 1,1-dimethylhydrazine as substrate

SUBSTRATE [hydrazine] (mM)	RATE OF NADPH CONSUMPTION* (nMoles/min/mg)	1/SUBSTRATE [hydrazine] (mM) <sup>-1</sup>	1/RATE OF NADPH CONSUMPTION* (nMoles/min/mg) <sup>-1</sup> X 10 <sup>-4</sup>
<u>A. Without n-octylamine in the buffer solution:</u>			
<u>1. 1,1-dimethylhydrazine-d<sub>6</sub> as substrate:</u>			
2.35	1206	0.42	8.3
1.18	938	0.85	10.7
0.94	894	1.06	11.2
0.71	831	1.42	12.0
0.58	697	1.70	14.4
0.47	589	<u>2.13</u>	<u>16.9</u>
Standard deviation, SD <sub>I</sub> , (+/-)		0.13	0.6
<u>2. 1,1-dimethylhydrazine as substrate:</u>			
3.10	927	0.32	10.8
2.48	697	0.40	14.4
1.86	686	0.54	14.6
1.55	616	0.64	16.2
1.24	487	0.81	20.5
0.93	445	1.07	22.5
0.62	348	<u>1.62</u>	<u>28.7</u>
Standard deviation, SD <sub>I</sub> , (+/-)		0.09	1.2
<u>B. With n-octylamine in the buffer solution.</u>			
<u>1. 1,1-dimethylhydrazine-d<sub>6</sub> as substrate:</u>			
1.90	1125	0.52	8.9
1.50	911	0.66	11.0
0.95	857	1.05	11.7
0.65	697	1.53	14.4
0.38	482	<u>2.63</u>	<u>20.7</u>
Standard deviation, SD <sub>I</sub> , (+/-)		0.13	0.7
<u>2. 1,1-dimethylhydrazine as substrate:</u>			
1.68	723	0.59	13.8
1.36	670	0.73	14.9
0.73	482	1.36	20.7
0.42	322	<u>2.38</u>	<u>31.0</u>
Standard deviation, SD <sub>I</sub> , (+/-)		0.26	0.3

Table 10: Experimental results: Michaelis-Menten parameters and observed isotope effects for 1,1-dimethylhydrazine-d<sub>6</sub> and 1,1-dimethylhydrazine and the flavin-containing monooxygenase system. Standard deviations, SD<sub>M</sub>, in parentheses.

PARAMETERS <sup>1</sup>	SUBSTRATE	
	1,1-dimethylhydrazine-d <sub>6</sub>	1,1-dimethylhydrazine
<u>A. Without n-octylamine:</u>		
K <sub>m</sub> (mM)	0.82 (.08)	1.70 (.26)
V <sub>max</sub> ( <u>nmoles NADPH</u> ) (min/mg protein)	1664 (166)	1267 (100)
V <sub>max</sub> /K <sub>m</sub> ( <u>nmoles NADPH</u> ) (mM-min/mg protein)	2039	745
D <sub>V</sub>	0.76	
D <sub>V</sub> /K	0.36	
<u>B. With n-octylamine:</u>		
K <sub>m</sub> (mM)	0.83 (.08)	1.22 (.04)
V <sub>max</sub> ( <u>nmoles NADPH</u> ) (min/mg protein)	1549 (135)	1263 (41)
V <sub>max</sub> /K <sub>m</sub> ( <u>nmoles NADPH</u> ) (mM-min/mg protein)	1851	1032
D <sub>V</sub>	0.82	
D <sub>V</sub> /K	0.55	

<sup>1</sup>Where:

K<sub>m</sub> - The -1/x-intercept from Figures 46 a and b.

V<sub>max</sub> - The 1/y-intercept from Figures 46 a and B.

V<sub>max</sub>/K<sub>m</sub> - The 1/slope from Figures 46 a and B

D<sub>V</sub> -The observed isotope effect on the enzyme's maximal velocity;  
V<sub>max</sub>H/V<sub>max</sub>D.

D<sub>V</sub>/K - The observed isotope effect on the enzyme's maximal  
velocity/Michaelis-Menten constant, ratio;  
(V<sub>max</sub>/K<sub>m</sub>)<sub>H</sub>/(V<sub>max</sub>/K<sub>m</sub>)<sub>D</sub> .

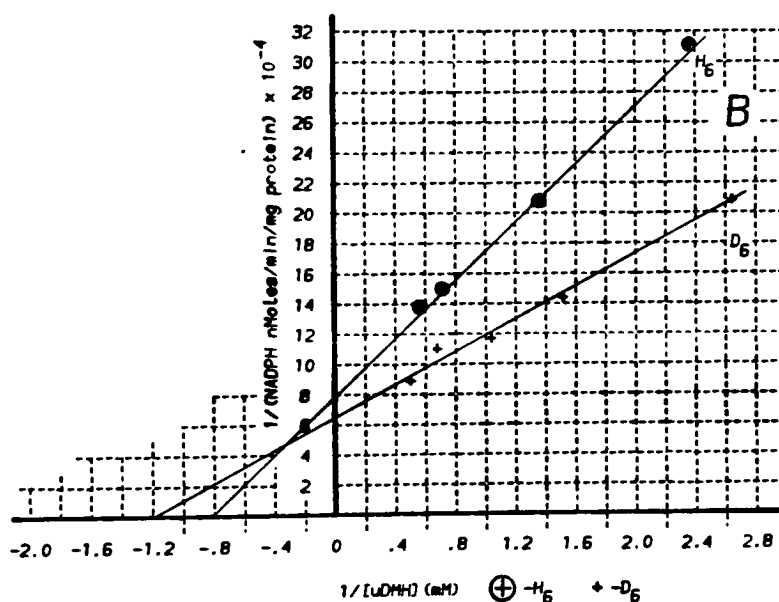
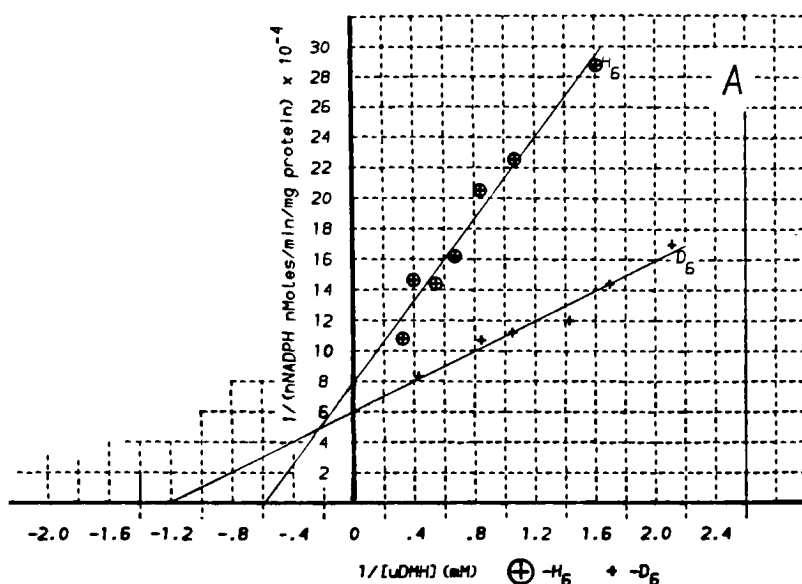


Figure 46: Kinetic analysis of the N-oxidation of 1,1-dimethylhydrazine and its deuterated analog by the flavin-containing monooxygenase: The reaction conditions were those described in the experimental section using 1 mM Tris, 1 mM EDTA buffer (pH 8.4) at 25°C. A. Double reciprocal plot of initial rate data under aerobic conditions and variable (1) 1,1-dimethylhydrazine- $d_6$  and (2) 1,1-dimethylhydrazine with NADPH fixed at 0.20 mM. The hydrazine concentrations from top to bottom are listed in Table 9A. B. Double reciprocal plots of initial rate data of the above reactants with the addition of n-octylamine to the buffer solution are also presented. The concentration data are listed in Table 9B.



Support for Prough's proposed mechanism of 1,1-dimethylhydrazine oxidation may be obtained by examining the kinetic isotope effect's on  $V_{max}$ ,  $V_{max}/K_m$  and  $K_m$ . Under the conditions of Scheme 1, the isotopically sensitive bond breaking step (C-D) should effect the value of the rate constant for the formation of product from the substrate-enzyme complex,  $k_3$ .

Theoretical kinetic isotope effects on  $V_{max}$ ,  $^{D_V}$  - This rate equation relates the observed isotope effect on the maximal velocity,  $^{D_V}$ , to the actual or intrinsic isotope effect,  $k_{3H}/k_{3D}$ . For  $^{D_V}$ , this intrinsic isotope effect is controlled by two factors, the reverse commitment to catalysis, Cr, and the ratio of catalysis, R. Steps preceeding the formation of an enzyme-substrate complex are excluded in this term. Analysis of Scheme 1 permits the derivation of equation VII (Miwa et. al., 1980)(74).

$V_{max}$ Observed Isotope Effect	Intrinsic Isotope Effect	Reverse Commitment To Catalysis [Cr]	Ratio of Catalysis [R]
$^{D_V}$	$k_{3H}/k_{3D}$	$k_{2H}/k_3$	$k_{3H}/k_4$
=	$\frac{k_{3H}/k_{3D}}{1}$	$+$ $\frac{k_{2H}/k_3}{k_{2H}/k_3}$	$+$ $\frac{k_{3H}/k_4}{k_{3H}/k_4}$

(VII)

A large reverse commitment, Cr, means the carbon-hydrogen cleavage is reversible and may approach equilibrium. A large ratio of catalysis, R, term indicates the rate of carbon-hydrogen bond cleavage step is not slow compared to other forward steps. Under irreversible conditions, a large reverse commitment may be ruled out.

Experimental or observed kinetic isotope effects on  $V_{max}$ ,  $D_V$  - The  $D_V$  values observed in the experimental results do not show an observable kinetic isotope effect. ( $D_V = 0.76$  and  $0.82$  in the presence of n-octylamine. See Table 10 for units.) This may indicate that there actually is no intrinsic isotope effect on  $V_{max}$ . It may also mean that any intrinsic isotope effect present is much smaller than the ratio of catalysis term, R.

Theoretical kinetic isotope effects on  $V_{max}/K_m$ ,  $D_{V/K}$  - Kinetic isotope effects in  $D_{V/K}$  provide information on the binding dynamics of the substrate to the mixed-function monooxygenase (Miwa et. al., 1980)(74).

Analysis of Scheme 1 permits the derivation of equation VIII (Miwa et. al., 1980)(74).

Observed Isotope Effect		Intrinsic Isotope Effect		Commitment to Catalysis
$D_{V/K}$	=	$\frac{k_{3H}/k_{3D}}{1}$	+	$\frac{k_{3H}/k_2}{k_{3H}/k_2}$

(VIII)

This rate equation relates the observed isotope effect in the pseudo-first order rate constant,  $V_{max}/K_m$  to the actual or intrinsic isotope effect,  $k_{3H}/k_{3D}$  and to the ratio,  $k_{3H}/k_2$ . The ratio,  $k_{3H}/k_2$ , describes the efficacy of the ES complex to productively go forward through catalysis via  $k_{3H}$  relative to dissociating nonproductively to free E and S via  $k_2$ . So, it ( $k_{3H}/k_2$ ) is a measure of the commitment to catalysis of the ES complex (Miwa, 1980)(74).

An isotope effect,  $D_{V/K}$ , according to the above rate equation can only be observed if the commitment of catalysis term is small by comparison to the intrinsic isotope effect. As this term approaches zero the observed isotope effect will equal the intrinsic isotope effect.

Experimental or observed kinetic isotope effects on  $V_{max}/K_m$ ,  $^D V/K$  -

The experimental results listed in Table 10 show the observed kinetic isotope effect on the  $V_{max}/K_m$  ratio,  $^D V/K$ . ( $^D V/K = 0.36, 0.55$  in the presence of n-octylamine. See Table 10 for units.) An observed isotope effect on the  $^D V/K$  term indicates that the commitment to catalysis term is smaller in value than the intrinsic isotope effect.

An observable isotope effect on the  $^D V/K$  term may indicate that substrate adheres weakly to the enzyme prior to a carbon-hydrogen cleavage. This effect may also be due to a difference in the rate of collisions between enzyme and substrate that succeed in product formation.

Theoretical kinetic isotope effects on  $k_{cat}/K_m$  and  $K_m$  - Under the conditions of Scheme 1, if the substrate concentration,  $[S]$  is much smaller than the value of  $K_m$ , then the enzymatic rate is less than  $k_3$ . This condition is due to an abundance of vacant active sites on the enzyme. According to the chapter in Stryer's Biochemistry, entitled: "Introduction to Enzymes" (88), a parameter characterizing the kinetics of an enzyme, under Scheme 1 conditions, is described as equation IX.

$$v_o = (k_3/K_m) [S][E_T] \quad (IX)$$

where:  $[E_T]$  is the total enzyme concentration.

Concluding, that the enzymatic velocity depends on the value of  $k_3/K_m$  and on  $[S]$ . As the substrate concentration approaches saturation the initial rate will approach its maximal rate,  $V_{max}$ .

Stryer explains, that the limit on  $k_3/K_m$  is set by the value of  $k_1$  in the expression:

$$k_3/K_m = (k_3 * k_1)/(k_2 + k_3) \quad (X)$$

Thus, the rate of ES complex formation cannot be faster than the diffusion controlled collisions between an enzyme and substrate.

In a more complex mechanism than illustrated by Scheme 1, the maximal catalytic rate when substrate is saturating is denoted by  $k_{cat}$ . It ( $k_{cat}$ ) is dependent on several rate factors and not on  $k_3$  alone. The  $k_{cat}/K_m$  ratio must also be limited by the value of  $k_1$ . Where,  $k_1$  is the rate at which the enzyme encounters substrate in solution.

Experimental or observed kinetic isotope effects on  $k_{cat}/K_m$  and  $K_m$  -  
Under saturating substrate conditions and the same total enzyme concentrations, the value of the observed isotope effect on  $^D V/K$  represents the isotope effect on the  $k_{cat}/K_m$  ratio. An isotope effect on the  $k_{cat}/K_m$  ratio, but not on  $V_{max}$  ( $^D V$ ), must then indicate that a difference exists between the two substrate's enzyme collision rate. This also means that the rate constant  $k_3$  or  $k_{cat}$  has little effect on the observed isotope effect on  $K_m$ .

In this study, the kinetic isotope effect on  $K_m$  must then be affected only by the  $k_2/k_1$  ratios for each substrate. Thus the value of the isotope effect on  $K_m$  is affected only by the reaction's affinity constant  $K_{aff}$ . In the reaction's forward direction,  $k_1/k_2$ , corresponds to the affinity constant of ES,  $K_{aff}$ . In the reverse direction,  $k_2/k_1$ , corresponds to the dissociation constant of ES,  $K_{diss}$ .

In the absence of an isotope effect on  $V_{max}$ , the observed isotope effect for  $^D V/K$  may be due to the flavin-containing enzyme's higher specificity for the deuterated hydrazine. This difference may also be due to more efficient binding of the substrate to yield an enzyme-substrate complex, [ES].

The deuterium substituted hydrazine had a much lower  $K_m$  value ( $K_m = 0.82, 0.83$  mM with n-octylamine) relative to the protonated hydrazine ( $K_m = 1.70, 1.22$  mM with n-octylamine). If scheme 1 is valid for this reaction, then the deuterated hydrazine shows either a lower tendency to dissociate from the enzyme or a higher affinity for the enzyme than the protonated hydrazine.

Kinetic summary - The observed isotope effects on  $V_{max}$ ,  $^D V$ , and  $V_{max}/K_m$ ,  $^D V/K$ , indicate that the presence of deuterium enhances the formation of the enzyme-substrate complex. The effects observed were directly related to the conditions that affect the substrate encountering the enzyme.

If any of the steps in Figure 44, outlined by Prough (11), occurred after the substrate bound to the enzyme then according to these studies, their reaction rates would not be affected by the presence of deuterium on the substrate.

Figure 44, describes the formation of an azomethanimine and/or a quaternary ammonium intermediate prior to the carbon-hydrogen bond cleavage. If these intermediates in Figure 44 are formed prior to the enzyme binding to substrate or are formed in order to bind to the enzyme, then their formation (the intermediate's) would have been affected by deuterium on the substrate. Deuterium could have stabilized the formation of one of these intermediates through charge delocalization.

However, the relative size of the observed isotope effects (all less than 2) and the effects on the Michaelis-Menton parameters indicates that the carbon-hydrogen bond cleavage does not enter into these studies' observed isotope effects.

Other possible explanations for the observed inverse kinetic effect on  $D_V/K$  may be due to:

1. An alteration in a transition state species prior to enzyme-substrate binding.
2. A change in the substrate's positioning at the enzyme site.

Theoretical analysis of alteration of a transition state species -

1. Hybridization: Hanzlik (85) has shown that a change in hybridization ( $sp^2$  to  $sp^3$ ) is sensitive to a substituent's inductive effect that can be reflected in the reaction's overall rate constant.

Using zero-point energies to demonstrate, the potential energy curve for a C-H ( $sp^2$ ) bond is a relatively shallow parabola and the zero-point energies of C-H and C-D bonds are relatively close. However the potential energy curve for a C-H ( $sp^3$ ) bond is a steep parabola thus placing the zero-point energy of a C-D bond quite a bit lower than a C-H bond. Therefore, the energy of activation for an  $sp^2 \rightarrow sp^3$  change in hybridization is lower for the deuterated than the non-deuterated compound (Hanzlik and Shearer, 1977)(85).

Inverse isotope effects resulting from hybridization changes have been observed in cytochrome P-450 dependent epoxidation of *p*-phenyl styrene and *p*-methylstyrene when deuterium was present on the alpha carbon (Hanzlik and Shearer, 1977)(85). Kaplan and Thornton (1967)(86) also observed this anomaly occurring during the quaternization reaction of N,N-dimethylaniline- $d_6$  and N,N-dimethylaniline in the presence of methyl toluene-sulfonate with an observed inverse isotope effect of ( $k_D/k_H$ ) of 1.13 for the reaction's overall rate constant.

2. Steric effects on transition state: Kaplin and his group explained that the inverse kinetics were a result of steric effects in that the resulting quaternary form has more internal crowding and less freedom of motion relative to the initial reactants. It is believed that the C-D bonds are more rigid than the C-H bonds therefore, less energy is required to change the deuterated form of the starting material to the products than is required to change the protonated reactants.

Steric effects on reactants - H.C. Brown (87) cites steric influences in his discussion as the cause of small inverse secondary isotope effects in the chemical N-demethylation of substituted pyridine compounds.

Ziegler et. al., (1973) (31) also cited that the purified flavin-containing monooxygenase enzyme was sensitive to a substituent's steric effects. N-ethyl amines were oxidized at a slower rate than N-methylamine and secondary N-methylamines are oxidized at 2/3 the rate that tertiary N,N-dimethylamines are oxidized. They stressed that it was a substituent's size rather than the length of its alkyl chain that effected the rate of N-dealkylation.

Under optimal pH and temperature conditions, 1,1-disubstituted hydrazines are N-oxidized by the flavin-containing monooxygenase in the same manner as N,N-disubstituted amines (Hines, 1980)(27) (Prough, 1973)(35). Deuterated methyl groups are by comparison, smaller and denser, with relatively stiffer C-D bonds, compared to their hydrogen analog (Brown, 1966)(87). The literature evidence of increased alkyl chain size effects on reaction rates is classic, thus, deuterated and hydrogen forms should also share this same logic (Brown 1966)(87).

It was of interest to compare the chemical oxidation products of the deuterated and protonated forms of 1,1-dimethylhydrazine to the flavin-containing monooxygenase's oxidation products.

Experimental results: Isotope effects on chemical oxidation products - Normally, chemical oxidation of 1,1-dimethylhydrazine quenched by alkaline solutions ultimately form 1,1,4,4-tetramethyltetrazene. It was important then to examine the resulting chemical oxidation products of both the protonated and the deuterated analog and compare their respective oxidation products.

Both labelled and protonated hydrazine were oxidized using potassium bromate (38) and the resulting solution extracted for organic products. The UV spectrum of the ethyl acetate washings exhibited a broad peak at 280 nm in keeping with literature values of the desired tetrazene (McBride and Kruse, 1957)(40). A 10 ul sample of the organic layer was analysed by HPLC (Waters Assoc., Conn.) for oxidation products. Instrument conditions are listed in the experimental section. The resultant chromatogram showed the presence of unreacted hydrazine and the tetramethyltetrazene. Each was confirmed by standard addition methods. In the event that the oxalate salt was used, oxalic acid was also detected.

Experimental results: Isotope effects on metabolic oxidation products - There exists possibly two pathways for enzymatic oxidation of 1,1-dimethylhydrazine (Prough et. al., 1981)(11). The first consists of a bimolecular degradation of the diazene intermediate that leads to the tetramethyltetrazene. The second path is via an intramolecular degradation of the diazene that leads to an unstable hydrazone, which itself, degrades to formaldehyde and methylhydrazine (Prough, 1981)(11).



Hines (27) has shown, by HPLC analysis, that the only products resulting from the acid quenched purified enzyme oxidation reaction with 1,1-dimethylhydrazine were methylhydrazine and formaldehyde.

Repeating the ethyl acetate extraction procedure and HPLC analysis for both the protonated and deuterated hydrazine substrate yielded unreacted 1,1-dimethylhydrazine, and monomethylhydrazine. No tetramethylnitrazene was detected.

HPLC analysis of the organic layer supports the mechanism that results in the formation of methylhydrazine thus, indicating that a change in metabolic pathway does not occur in the oxidation of deuterated 1,1-dimethylhydrazine from that of the protonated form. However, the amounts of metabolites for these substrates N-dealkylation (formaldehyde and methylhydrazine) were very low, such that any other products formed as a result of a pathway change would probably have been viewed as artifact.

Because prior studies (11, 14 and 27) have found that nitrosamines are not suitable as Ziegler enzyme substrates, no nitrosamine studies were done.

## EXPERIMENTAL RESULTS SUMMARY

Keefer's procedure for deuterium labelling 1,1-dimethylnitrosamine was followed to exchange all the hydrogens for deuterium. The labelled nitrosamine was then reduced to the corresponding hydrazine, 1,1-dimethylhydrazine-d<sub>6</sub>. Possible air oxidation of the reduced product required that the hydrazine be used for all further studies as it's oxalate salt. Purity and proof of the hydrazine salt were done by TLC, HPLC, <sup>1</sup>H-nmr spectrometry, infrared spectrometry, and mass spectrometry.

The results of the purity inspection showed that the deuterated hydrazine was completely exchanged and free of nitrosamine residue.

Metabolism studies using both protonated and deuterated 1,1-dimethylhydrazine and hepatic cytochrome P-450 showed that both forms of the hydrazine rapidly formed a spectral complex exhibiting a Soret maximum at 438 nm when examined by difference absorbance spectroscopy. They are both characteristic of low-spin hemoprotein complexes.

Both complexes were also sensitive to oxygen availability consistent with the ferric to ferrous shift in the heme portion of the cytochrome P-450 (438 nm to 449 nm shift). The fact that both substrates undergo the same reactions required to form the abortive enzyme-metabolite complex may also point that there is no metabolic pathway shift involved for the deuterated substrate as seen in other instances where deuterium has altered pathways.

Cytochrome P-450 binding spectra resulting from unlabeled substrates with larger alkyl chains or ringed groups have given initial rate information however, the rate at which the 1,1-dimethylhydrazine complexes formed are too rapid to measure with the equipment that was available.

From the difference spectra, it appeared that these spectral complexes were the same as those complexes observed when hepatic cytochrome P-450 formed an abortive complex with a metabolite of 1,1-dimethylhydrazine.

An inverse secondary deuterium isotope effect was exhibited for  $K_m$  but not  $V_{max}$  when rate studies were conducted using the hepatic flavin-containing monooxygenase (Ziegler enzyme) to metabolize both protonated and deuterated 1,1-dimethylhydrazine. The findings in the kinetic study indicate that the isotope effect observed was the result of factors that affect the substrate's collisions with enzyme or the enzyme's specificity for the substrate.

Oxidation products of these metabolism studies were monomethylhydrazine and formaldehyde which supports earlier work suggesting that flavin-containing monooxygenase is a primary enzyme for the metabolism of 1,1-dimethylhydrazine. This study, however, can not be used alone to support Prough's mechanism for the oxidation of 1,1-dimethylhydrazine as a substrate of the flavin-containing monooxygenase.

## GLOSSARY OF TERMS

Bathochromic Shifts - A change in a molecule's UV absorption to a longer wavelength or red shift.

Differential Extinction Coefficient - (Hines 1980)(27): To determine an extinction coefficient for the spectral complex, the formation of the carbonyl complex of ferrous cytochrome P-450 was examined in the presence and absence of the metabolite-complex. With NADPH as the source of reducing equivalents, the formation of the carbonyl complex of ferrous cytochrome P-450 was blocked by the metabolite-complex. Assuming a 450 minus 490 nm difference extinction coefficient of  $91 \text{ mM}^{-1}\text{cm}^{-1}$  (Omura and Sato, 1964). the cytochrome P-450 involved in the metabolite-complex can be determined from the difference in the amount of metabolite-complex. Using this method, a 438-510 nm difference extinction coefficient of  $115 \text{ } \pm 18 \text{ mM}^{-1} \text{ cm}^{-1}$  was calculated for the 438 nm-complex formed with N-aminopiperidine. This value is not unlike difference extinction coefficients determined for spectrally similar cytochrome P-450 complexes with nitrogenous ligands such as ethyl isocyanide ( $d\epsilon = 114 \text{ mM}^{-1} \text{ cm}^{-1}$ ) (Griffin and Peterson, 1971) or nitric oxide ( $d\epsilon = 116 \text{ mM}^{-1} \text{ cm}^{-1}$ ) (O'Keefe et al., 1978). It is important to note, that this calculation assumes that in the control experiment all of the cytochrome P-450 that was capable of forming the metabolite-complex was reduced by NADPH via cytochrome P-450 reductase and binds carbon monoxide. This assumption is most likely justifiable since both processes require reduction of cytochrome P-450. In the presence of sodium dithionite, all of the cytochrome P-450 was recovered as the carbonyl complex. However, this reducing agent apparently had direct effect since addition without carbon monoxide also results in the slow decay of the 438 nm-complex.

Gas Chromatography - Purity analysis was done by a gas chromatography because of its reproducibility, selectivity and sensitivity. The strongly basic liquid phase 10% Carbowax 20M/2% KOH on 80/100 mesh Chromosorb W AW, was required to reduce the possibility of the nitrosamine adsorbing indefinitely onto the support material in the packed column. This liquid phase has been used to separate several nitrosamine species including 1,1-dimethylnitrosamine from 1,1-dipropylnitrosamine (Supelco).

Hyperchromic Effect - An increase in a molecule's absorption or band intensity.

I.U. of Catalase - One unit will decompose 1.0 umole of  $\text{H}_2\text{O}_2$  per minute at pH 7.0 at  $25^\circ\text{C}$  while the  $\text{H}_2\text{O}_2$  concentration falls from 10.3 to 9.2 umoles per ml of reaction mix. The rate of disappearance of  $\text{H}_2\text{O}_2$  is followed by observing the rate of decrease in absorbance at 240 nm.

I.U. of Glucose Oxidase - One unit will oxidize 1.0 umole of beta-D-glucose to D-gluconic acid and  $H_2O_2$  per minute at pH 5.1 at 35°C.

I.U. of Isocitrate Dehydrogenase - one unit will convert 1.0 umole of isocitrate to alpha-ketoglutarate per minute at pH 7.4 at 37°C.

Methylene Chloride - Curtin and co-workers (82) used methylene chloride as part of a solvent mixture to solublize esters for lithium aluminum hydride directed reductions. Other type of impurities from the starting material would be removed during final clean-up following the reduction stage.

Soret Absorbances - Typify cytochromes in their reduced states. The Soret bands; alpha, beta, and gamma, (usually the largest), are three distinct absorption bands in the visable range with specific values for a particular cytochrome system.

Spin, Low - Refers to a complex involved with transition metals and their ligands whose total valence electron book keeping indicates all valence electrons are spin paired.

Spin, High - Refers to a metal-ligand complex whose valence electrons are not spin paired.

Ter-bi Kinetic Mechanism - The sequential ordered ter-bi mechanism discussed is in reference to the enzymatic reaction involving the three substrates oxygen, NADPH and the chemical substrate going to form a terenary complex. The bi portion of the mechanism involves the release of the oxidized substrate and  $NADP^{+}$ .

## REFERENCES

- 1 Estabrook, R.W., (1971), Cytochrome P-450 - Its function in the oxidative metabolism of drugs, Chap. 38. pp. 264-282, in Concepts in Biochemical Pharmacology, Part 2, ed. Brodie, B.B., and Gillette, J.R., Springer-Verlag, Berlin.
- 2 Omura, T. and Sato, R. (1964a). The CO-binding pigment of liver microsomes. Evidence for its hemoprotein nature. J. Biol. Chem. 239, 2370-2378.
- 3 Omura, T. and Sato, R. (1964b). The CO-binding pigment of liver microsomes. Solubilization, Purification and properties. J. Biol. Chem. 239, 2379-2385.
- 4 Estabrook, R.W., Cooper, D.Y., Rosenthal, O. (1963). The light reversible CO inhibition of the Steriod C21-hydroxylase system of the adrenal cortex. Biochem. Z. 388, 741-755.
- 5 Cooper, D.Y., Levin, W., Narasimhulu, S., Rosenthal, O. and Estabrook, R.W. (1965). Photochemical action spectrum of the terminal oxidase of mixed function oxidase systems, Science 147, 400-402.
- 6 Masters, B.S.S., Yasukochi, Y., Okita, R.T., Parkhill, L.L., Taniguchi, H. and Dees, J.H. (1980). Laurate hydroxylation and drug metabolism in human and pig liver and kidney microsomes and in reconstituted systems from pig liver and kidney. In Microsomes, Drug Oxidations and Chemical Carcinogenesis (Coon, M.J., Conney, A.H., Estabrook, R.W., Gelboin, H.V., Gillette, J.R. and O'Brien, P.J., eds.) Vol. II, pp. 709-720, Academic Press, New York.
- 7 Harding, B.W., Wong, S.H. and Nelson, D.H. (1964). CO-combining substance in rat adrenal, Biochim. Biophys. Acta., 92, 415-417.
- 8 Sato, R., (1978). A short history of cytochrome P-450, in Cytochrome P-450. (Sato, R., and Omura, T., eds.) pp. 23-46, Kidansha Ltd., Tokyo and Academic Press, Inc., New York.
- 9 Masters, B.S.S., Kamin, H., Gibson, Q.H. And Williams, C.H. (1965). Studies on the mechanism of microsomal triphosphopyridine nucleotide-cytochrome c-reductase, J. Biol. Chem., 240, 921-931.
- 10 Peterson, H.A., White, R.E., Yasukochi, Y., Coomes, M.L., O'Keefe, D.H., Ebel, R.E., Masters, B.S.S., Ballou, D.P. and Coon, H.J. (1977). Evidence that purified liver microsomal cytochrome P-450 is a one electron acceptor, J. Biol. Chem., 252, 4431-4434.

- 11 Prough, R.A., Freeman, P.C., and Hines, R.N., (1981). The Oxidation of Hydrazine Derivatives Catalyzed by the Purified Liver Microsomal FAD-Containing Monooxygenase, J. Biol. Chem., 259, 9, pp 4178-4184.
- 12 Mitani, F. and Horie, S., (1969). Studies on P-450. IV, The spin state of P-450 solubilized from bovine adrenocortical mitochondria. J. Biochem. (Tokyo) 66, 139-149.
- 13 Jeffcoate, C.R.E., and Gaylor, J.L. (1969). Ligand interactions with hemoprotein P-450 II. Influence of phenobarbital and methylcholanthrene induction processes on P-450 spectra. Biochem. 8, 3464-3472.
- 14 Ullrich, V. and Schnabel, K.H. (1973) Formation and binding of carbanions by cytochrome P-450 of liver microsomes. Drug Metabolism and Disposition, in J. Pharm. Exp. Therap. 1, 176-182.
- 15 Hamilton, G.A., (1974), Chemical models and mechanisms for oxygenases, in Molecular Mechanisms of Oxygen Activation, ed. Hayaishi, O., Chap. 10, pp. 405-451, Academic Press, N.Y.
- 16 Ernester, L. and Orrenius, S. (1965). Substrate-induced synthesis of the hydroxylating enzyme system of liver microsomes. Fed. Proc. 24, 1190-1199.
- 17 Remmer, H. (1970). The role of the liver in drug metabolism, Amer. J. Med., 49, 617-628.
- 18 Wiebel, F.J., Leutz, J.C., Diamond, L., and Gelboin, H.V., (1971). Aryl hydrocarbon (Benzo[a]pyrene) hydroxylase in microsomes from rat tissues: Differential inhibition and stimulation by benzoflavones and organic solvents. Arch. Biochem. Biophys. 144, 78-86.
- 19 Lowry, O.H., Rosebrough, N.J., Farr, A.L. and Randall, R.J., (1951), Protein measurement with the Folin Phenol Reagent, J. Biol. Chem., 193, 265-275.
- 20 Imai, Y. And Sato, R. (1966). Evidence for two forms of P-450 hemoprotein in microsomal membranes. Biochem. Biophys. Res. Commu. 23, 5-11.
- 21 Imai, Y. and Sato, R. (1967). Anomalous spectral interactions of reduced P-450 with ethyl isocyanide and some other lipophilic ligands. J. Biochem. (Tokyo) 63, 270-273.
- 22 Ichikawa, Y. and Yamano, T. (1968). The electron spin resonance and absorption spectra of microsomal cytochrome P-450 and its isocyanide complexes. Biochim. Biophys. Acta. 153, 753-765.
- 23 Nishibayashi, H., Omura, T. and Sato, R. (1966). The binding of ethyl isocyanide by hepatic microsomal hemoprotein. Biochim. Biophys. Acta. 118, 651-654.

- 24 Schenkman, J.B., Remmer, H. and Estabrook, R.W., (1967). Spectral studies of drug interaction with hepatic microsomal cytochrome. Mol. Pharmacol. 3, 113-123.
- 25 Remmer, H., Greim, H., Schenkman, J.B. and Estabrook, R.W. (1967). Methods for the elevation of hepatic microsomal mixed function oxidase levels and cytochrome P-450, in Methods in Enzymology, (Estabrook, R.W. and Pullman, M.E., eds.), Vol. 10, pp. 703-708, Academic Press, Inc., New York.
- 26 Mansuey, D., Battioni, J.P., Chottard, J.C. and Ullrich, V. (1979), Preparation of a prophyrin-iron-carbene model for the cytochrome P-450 complexes obtained upon metabolic oxidation of the insecticide synergists of the 1,3-benzodioxole series. J. Amer. Chem. Soc., 100, 3971-3973.
- 27 Hines, R.N., (1980), The interaction of 1,1-disubstituted hydrazines with drug metabolizing enzymes, Thesis Archive, The University of Texas Health Science Center at Dallas, Dallas, Texas.
- 28 Werringloer, J. and Estabrook, R.W., (1978). The characterization of product adducts of liver microsomal cytochrome P-450 and their use as probes for the heterogeneity of cytochrome P-450 as modified by the induction of drug metabolism, in The Induction of Drug Metabolism (Estabrook, R.W. and Lindenlaub, E., eds.) pp. 269-307, F.L. Schattauer Verlag, Stuttgart-New York.
- 29 Mansuey, D., Beayne, P., Chottard, J.C., Bartoli, J.f. and Gans, P. (1976), The nature of the "455 nm absorbing complex" formed during the cytochrome P-450 dependent oxidative metabolism of amphetamine, Biochem. Pharmacol., 25, 609-612.
- 30 Mansuey, D., Gans, P., Chottard, J.S. and Bartoli, J.F., (1977), Nitrosoalkanes as Fe(II) ligands in the 455 nm-absorbing cytochrome P-450 complexes formed from nitroalkanes in reducing conditions, Eur. J. Biochem., 76, 607-615.
- 31 Baker, J.R., Struempier, A. and Chaykin, S., (1963). Biochem. Biophys. Acta., 71, 58.
- 32 Ziegler, D.M. and Petit, F.H., (1964). Biochem. Biophys. Res. Comm., 15, 188
- 33 Ziegler, D.M., Mitchell, C.H., and Jollow, D., (1969) in Microsomes and Drug Oxidation, (J.R. Gillette, A.H. Conney, G.J. Cosmides, R.W. Estabrook, J.R. Fout, and G.J. Manning, eds.), p 173, Academic Press, NY
- 34 Ziegler, D.M., (1980). Microsomal flavin-containing monooxygenases: Oxygenation of nucleophilic nitrogen and sulfur compounds, in Enzymatic Basis of Detoxication (Jakoby, W.B., ed.) Vol. 1 pp. 201-227. Academic Press, Inc., New York.



- 35 Prough, R.A., (1973), The N-oxidation of alkylhydrazines catalyzed by the microsomal mixed-function amine oxidase, Arch. Biochem. Biophys., 158, 442-444.
- 36 Poulsen, L.L., Hyslop, R.M. and Ziegler, D.M., (1974), S-Oxidation of thioureylenes catalyzed by a microsomal flavoprotein mixed-function oxidase, Biochem. Pharmacol., 23, 343-352.
- 37 Ziegler, D.M. and Mitchell, C.H. (1972). Microsomal Oxidase IV: Properties of a mixed-function amine oxidase isolated from pig liver micromsomes. Arch. Biochem. Biophys. 150, 116-125.
- 38 Poulsen, L.L. and Ziegler, D.M., (1979), The liver microsomal FAD-containing monooxygenase. J. Biol. Chem. 254, 6449-6455.
- 39 Smith, P.A.S., (1965), The Chemistry of Open-Chain Organic Nitrogen Compounds. Vol. I, p. 9 and Vol. II, 119-210. W.A. Benjamin, Inc., New York.
- 40 McBride, W.R., and Kruse, J.W., (1957), Alkylhydrazines. I. Formation of a new diazo-like species by the oxidation of 1,1-dialkylhydrazines in solution, J. Amer. Chem. Soc., 79, 572-567.
- 41 Lemal, D.M., (1970), Aminonitrenes (1,1-diazenes), in Nitrenes, (Lwowski, W. ed.) Chapter 10, pp. 345-403, Interscience Publishers, New York.
- 42 McBride, W.R. and Bens, E.M., (1958), Alkylhydrazines. III. Dimerization of certain substituted 1,1-dialkyldiazenes to tetraalkyltetrazines, J. Amer. Chem. Soc., 81, 5546-5550.
- 43 McKennis, H. Jr., Weatherby, J.G. and Witkin, L.B., (1955), Studies on the Excretion of hydrazine and metabolites, J. Pharm. Exp. Therap., 114, 385-390.
- 44 Yard, A.S., and McKennis, H., (1955), Effect of structure on the ability of hydrazino compounds to produce fatty livers, J. Pharm. Exp. Therap., 114, 391-397.
- 45 El Masiri, A.M., Smith, J.N. and Williams, R.T. (1958). Studies on the detoxification 75. Further observations on the metabolism of hydroxides of amomatic acids. Biochem. J. 68, 587-592.
- 46 Pinkerton, M.K., Hagan, E.A., Badk, K.C., (1967), Distribution and excretion of <sup>14</sup>C-monomethylhydrazine, Toxicol. Appl. Pharmacol., 10, 401-402.
- 47 Dost, F.N., Reed, D.J. and Wang, C.H., (1966), The metabolic fate of monomethylhydrazine and unsymmetrical dimethylhydrazine, Biochem. Pharm., 15, 1325-1332.
- 48 Prough, R.A., Wittkop, J.A. and Reed, D.J., (1969), Evidence for the hepatic metabolism of some monoalkylhydrazines, Arch. Biochem. Biophys., 131, 369-373.

- 49 Wittkop, J.A., Prough, R.A. and Reed, D.J., (1969). Oxidative demethylation of N-methylhydrazines by rat liver microsomes, Arch. Biochem. Biophys., 134, 308-315.
- 50 Back, K.C., Pinkerton, M.D., Cooper, A.B. and Thomas, A.A. (1963) Absorption, distribution and excretion of 1,1-dimethylhydrazine and (UDMH). Toxicol. Appl. Pharmacol., 5, 401-413.
- 51 Silverstein, R.M., Bassler, G.C. and Morrill, T.C., (1981) Spectrophotometric Identification of Organic Compounds, 4th ed., John Wiley and Sons, New York.
- 52 Lyle, R.E., Saavedra, J.E., Lyle, G.G, Barton, R., Yoder, S. and Jacobson, M.K., (1979) Stereochemical effects on N-Nitrosamines Chemistry, in N-Nitrosamines, pp 39-55.
- 53 Michejda, C.J., Kroeger-Koepke, M.B., Koepke, S.R. and Kupper, R.J., (1979). Oxidative activation of N-Nitrosamines: Model compounds, in N-Nitrosamines, pp. 77-89.
- 54 Magee, P.N. ed., (1982), in The Banbury Report 12: Nitrosamine and Human Cancer, Cold Spring Harbor Laboratory, pp 1-599, New York.
- 55 McWeeny, D.J., (1983). Nitrosamines in Beverages, Food Chemistry, 11, 273-287.
- 56 Keefer, L.K., Fodor, C.H., (1970), Facile hydrogen isotope exchange as evidence for an alpha-nitrosoamino carbanion, J. Amer. Chem. Soc., 92, 5747-48.
- 57 Magee, P.N. and Barnes, J.M., (1967), Carcinogenic Nitroso Compounds, Adv. Cancer Res., 10, 167.
- 58 Arcos, F.C., Davies, D.L., Brown, C.E.L., and Argos, M.F. (1977). Repressable and Inducible Enzymic Forms of Dimethylnitrosamine-Demethylase, Z. Krebsforsch., 89, 181.
- 59 Appel, K.E., Ruf, H.H., Mahr, B., Schwarz, M. Rickart, R., and Kunz, W., (1979). Binding of Nitrosamines to Cytochrome P-450 of Liver Microsomes, Chem. Biol. Inter., 28, 17-33
- 60 Kroeger-Koepke, M.B. and Michejeda, C.J., (1979). Evidence for several demethylase enzymes in the oxidation of dimethylnitrosamine and phenylmethylnitrosamine by rat liver fractions, Cancer Res., 39, 1587-1591.
- 61 Potter, D.W. and Reed, D.J. (1982). Denitrosation of Carcinostatic Nitrosoureas by Purified NADPH Cytochrome P-450 Reductase and Rat Liver Microsomes to yield Nitric Oxide under Anerobic Conditions, Arch. Biochem. Biophys., 216, 1, June pp 158-169.
- 62 Ebel, R.E., O'Keefe, D.H. and Peterson, J.A., (1975). Nitric oxide complexes of cytochrome P-450, FEBS Lett., 55, 198-201.

- 63 O'Keefe, D.H., Ebel, R.E. and Peterson, J.A. (1978). Studies of the oxygen binding site of cytochrome P-450, J. Biol. Chem., 253, 3509-3516.
- 64 Urey, H.C., Brickwedde, F.G., and Murphy, G.M., (1932) Phys. Rev., 39, 164.
- 65 Biegeleisen, J., and Mayer, M.G., (1947). J. Chem. Phys., 15, 261.
- 66 Katz, J.J., and Crespi, H.L., (1971). Isotope effects in Biological Systems, in Isotope Effects In Chemical Reactions, ACS Monograph 167, (Collins, C.J. and Bowman, N.S.,) Van Nostrand Reinhold Co., New York.
- 67 Harris, J.M. and Wamser, C.C., (1976), in Fundamentals of Organic Reaction Mechanisms, John Wiley and Son, New York, New York.
- 68 Fry, A. (1964) Isotope Effect Studies of Elimination Reactions, Pure Applied Chem. 8, 409.
- 69 Collins, C.J. and Bowman, N.S., ed.,(1971). Isotope effects in Biological Systems, in Isotope Effects In Chemical Reactions, ACS Monograph 167, Van Nostrand Reinhold Co., New York.
- 70 Richards, J.H. (1970), Kinetic isotope effects in enzymic reactions, In The Enzymes, (Boyer, P.D., ed.), 3rd ed., 2, pp. 321-333.
- 71 Horning, M.G., Nowlin, J., Thenot, J.P. and Bouwasma, O.J., (1979) Effect of deuterium substitution on the rate of caffeine metabolism, in Stable Isot., Proc. Int. Conf., 3rd 1978, 379-84, (eds., Klein, E.R., Klein, P.D. Academic, New York, NY).
- 72 Miwa, G.T., Garland, W.A., Hodshon, B.J., Lu, A.Y.H. and Northrup, D.B., (1980) Kinetic isotope effects in cytochrome P-450-catalyzed oxidation reactions. Intermolecular and intramolecular deuterium isotope effects during the N-demethylation of N,N-dimethylphenterimine, J. Biol. Chem., 255, (13), 6049-54.
- 73 Lu, A.Y., Miwa, G.T., West, S.B., Hodshon, N.J., Garland, W.A. (1980) Kinetic isotope effects in cytochrome P-450-catalyzed oxidation reactions. II. Interactions of cytochrome P-450 with substrates and NADPH-cytochrome c reductase, Adv. Exp. Med. Biol., 132, (Alcohol Aldehyde Metab. Syst. - 4), 95-108.
- 74 Miwa, G.T., Zweig, J.D., Walsh, J.S.A. and Lu, A.Y.H., (1980), Kinetic isotope effects in cytochrome P-450-catalyzed oxidation reactions. II. Substrate-cytochrome P-450 interactions, in Microsomes, Drug Oxid. Chem. Carcinog., (Int. Symp. Microsomes Drug Oxid.), 4th, 1979, (eds. Coon, M.J., Conney, A.H., Estabrook, R.W.), Academic, New York, NY, 363-366.
- 75 Keefer, L.K., Lijinsky, W. and Humberto, G., (1973), Deuterium Isotope Effect on the Carcinogenicity of Dimethylnitrosamine in Rat Liver, J. Natl. Cancer Inst., 51, 299-302.

- 76 Challis, B.C. and Challis, J.A. (1982), N-Nitrosamines and N-nitrosimines, in The Chemistry of Amino, Nitroso and Nitro Compounds and Their Derivatives, Part 2, Supplement F, (ed. Patai, S., John Wiley and Son, New York, pg. 1177.
- 77 Fieser, L.F. and Fieser, M., (1967), Reagents for Organic Synthesis, Vol. 1, Wiley, New York.
- 77 Scheuler, F.W. and Hanna, C., (1951), A Synthesis of Unsymmetrical Dimethyl Hydrazine using Lithium Aluminum Hydride, J. Amer. Chem. Soc., 77, 4996.
- 78 Registry of Mass Spectral Data, Vol. I, (1974) (eds. Stenhagen, E., Abramson, S. and Mc Lafferty, F.W.), John Wiley and Sons, New York.
- 79 The Aldrich Library of Infrared Spectra, 3 ed., (1981), (ed. Pouchert, C.J.) Aldrich Chemical Co., Milwaukee, Wis.
- 80 The Aldrich Library of NMR, Vol. I, 2 ed., (1983), (ed. Pouchert, C.J.) Aldrich Chemical Co., Milwaukee, Wis.
- 81 Vogel's Textbook of Practical Organic Chemistry including Qualitative Organic Analysis, 4 ed., (eds. Furniss, B.S., Hannaford, A.J., Rogers, V., Smith, P.W.G. and Tatchell, A.R.), Longman Press, New York.
- 82 Curtin, D.Y., Kampmeier, J.A. and Farmer, M.L., (1965), J. Amer. Chem. Soc., 87, 874.
- 83 Lehninger, A.L., Enzymes: kinetics and inhibition, Biochemistry, 2 ed., Worth Publishers, Inc, New York, pp. 183-216.
- 84 Tynes, R.E. and Hodgson, E., (1985), Magnitude of Involvement of the Mammalian Flavin-Containing Monooxygenase in the Microsomal Oxidation of Pesticides, J. Agric. Food Chem. 33, 471-479.
- 85 Hanzlik, R.P. and Shearer, G.O., (1977), Biochem. Pharmac., 27, 1441-1444.
- 86 Kaplan, E.D. and Thornton, R.E., (1967), J. Amer. Chem. Soc., 87, 161.
- 87 Brown, H.C. and Mc Donald, G.J., (1966) Secondary isotope effects in the reaction of methyl-d<sub>3</sub>-pyridines with alkyl iodides. Evidence for a smaller steric requirement of methyl-d<sub>3</sub> over the methyl-d<sub>0</sub> group, J. Amer. Chem. Soc., 88, 2514-2519.
- 88 Stryer, L., Introduction To Enzymes, Biochemistry, 2nd ed., W.H. Freeman and Co., San Francisco, CA, pp. 103-135.